# BODY SEGMENT INERTIAL PARAMETERS OF TODDLERS

by

Erika Jackson

A thesis submitted to the Department of Mechanical and Materials Engineering

In conformity with the requirements for the degree of Master of Applied Science

Queen’s University

Kingston, Ontario, Canada

June, 2017

# Abstract

Body segment inertial parameters (BSIPs) are required to study human kinetics and to model the human form. The purpose of this study was to determine the BSIPs in toddlers using the photogrammetric method. Twelve male and twelve female toddlers (1.5-3years) were photographed in two planes, front and side, with reflective markers placed at the joint centres. The subjects were also weighed and had their height measured. Jensen's elliptical model was used to segment the images and zone the segments in 3mm thick slices. The segment masses, centre of mass (COM) locations and radii of gyration (ROGs) about the three principal axes were calculated and normalized in a percent form.

Segment mass proportion of the head was found to decrease as the child ages while the mass proportion of the thigh increases. The trunk's mass proportion increased with body mass index. These trends follow those found in the literature. The COM locations of segments were compared to the literature. The COM location of the head moves distally as the child ages. The COMs of the thigh and shank move proximally as muscle mass is developed. ROGs were highly variable due to posture variability from a population who found the photogrammetric protocol difficult to follow. To minimize positional errors, all subjects were analyzed together. The arm, forearm, thigh and shank were found to be similar to the literature while the hand and foot differed due to protocol difficulties. The ROGs of the head, neck and trunk could not be compared to the literature due to segmenting differences. The estimated total body mass was compared to the measured mass using a scale. The average error was 1.7% (SD=2.9%).

Despite some challenges and limitations of working with toddlers, the study was able to collect BSIPs of toddlers and provide data for a frequently overlooked population. The results of this study provide important data for those studying the biomechanics of toddlers or developing models of toddlers.

## Acknowledgements

Dr. Genevieve Dumas, thank you for being a fantastic supervisor. You were always extremely helpful and have provided guidance and support when I needed it. Thanks to my lab mates as well who were always willing to provide help and advice. Spending time with all of you was always enjoyable (which is why I think our lab meetings were so long).

Thanks to everyone in Rm 323 (even Matt who ran away) for keeping me company when I wasn't feeling productive. Thank you, Jan Sneep, for all the invigorating conversations and occasional life advice.

Paldies and thanks to Mama and Dad for continually being supportive, listening to my frustrations and always eager to help whenever possible.

Special thanks to Ali and Jess who were always happy to have a cup of tea with me. Those moments are greatly appreciated and allowed me to forget any troubles (or just listened to me complain about them).

Thanks to my subjects and their parents who consistently provided a new and exciting data collection experience. Without the help of the parents, I would not have been able to collect any data.

And thanks to you, the actual reader of this, because it means you have taken the time to read my thesis!

# Table of Contents

# List of Figures

# List of Tables

# List of Abbreviations

BMI- Body mass index

BSIP- Body segment inertial parameter

COM- Centre of mass

MOI- Moment of Inertia

NP-COM- Non-projected centre of mass

P-COM- Projected centre of mass

ROG- Radius of Gyration

# Chapter 1

# Introduction

## 1.1 Introduction

Body segment inertial parameters (BSIPs) and mass distribution of the human body have been used practically since the $19^{th}$ century. These data were mostly used for military infantry soldiers carrying equipment and rifle and evaluating new packs to carry the equipment (Braune and Fischer 1889 as cited by Clauser, McConville, & Young, 1969). The importance of these data increased as technology advanced. Common examples are ejection seats in aircrafts, dynamics crash tests for vehicles and simulating other hazardous environments. These tests demanded the development of dummies comparable to the human body.

Smrcka (2017) discusses the history of dummies and some limitations in modeling the human form. Early dummies had limited biofidelity and the internal instrumentation was limited. These dummies have greatly progressed through the years and are able to more accurately mimic the human body. Modern crash test dummies attempt to simulate spinal responses, internal organ impact and brain trauma along with each segment's movement and impact. Humanetics' (Humanetics Innovative Solutions Inc 2017) adult dummy has features such as steel ribs with polymer based damping material to simulate human chest force-deflection characteristics and the femur and tibia are instrumented to predict bone fractures and ligament injury. Having accurate BSIPs allows for realistic modeling of the human form.

BSIPS are also an important part of studying human kinetics. Rao et al. (Rao et al. 2006) compared six common BSIP estimation models and joint kinetics during walking were determined using a bottom-up inverse dynamic approach. The study found the BSIP models had deviations ranging from 9.73% to 60%. This caused the peak values for the hip joint flexion/extension moment to have a maximum variation of 20.11%. The authors emphasize the importance of having accurate BSIP estimates for kinetic analysis.

BSIPs for toddlers can be used for the applications mentioned above as well as developing a toddler automaton to evaluate the risk for those working with toddlers. Low back pain and shoulder/neck pain are common problems among child-care workers. Back problems are commonly seen in workers who frequently lift, bend or stoop, squat, and carry loads. These tasks are considered normal when caring for young children. It has been recommended to evaluate the physical demands of child-care workers (Ono et al. 2002; Owen 1994). For evidence based recommendations to be formed, repeated kinetic and kinematic trials must be done to measure the stresses on the daycare workers during work activities. Having a living child involved in these data collections is both impractical and unethical. To have repeated measures on the daycare school worker, the toddler's motions must also be repeatable. An alternative to a living child is a toddler automaton. A critical factor of a toddler automaton is that it needs to have the weight and feel of a real toddler.

There have been ample amounts of anthropometric measurements done on adults but the data for children is lacking and is negligible for toddlers. Toddler BSIPs are needed for kinetic studies of toddlers and the modeling of toddlers. As toddler safety in car seats is of utmost importance, it is critical to have BSIPs for toddlers to produce accurate simulations. By collecting and developing a database of toddler BSIPs, more applicable body characteristics can be used for the above applications.

## 1.2 Objectives

The first objective of this study is to adjust the photogrammetric method for calculating BSIPs in toddlers aged 1.5-3 years. The main objective of this study is to determine the BSIPs of toddlers. The BSIPs of interest in this study are mass, centre of mass location and radius of gyration. The final objective was to determine the limitations associated with this method for this population as the young subjects had difficulty following the protocol.

### 1.3 Thesis Outline

This thesis is written in the traditional thesis format. Chapter 2 is a review of BSIPs and the methods of collection and the limited data on child BSIPs. In Chapter 3, the collection protocol is explained and the data analysis is discussed. Chapter 4 presents the mass proportions, centre of mass locations and radii of gyration of a 17 segment body model of 24 toddlers (1.5-3years). Chapter 5 provides an interpretation of results, comparison with the literature and discusses the limitations of the methodology. Conclusions and future work are presented in Chapter 6.

# Chapter 2

# Literature Review

## 2.1 Body Segment Inertial Parameters

The kinetic analysis of movement measures the influence of different forces and moments acting on body segments. The human body is represented as a linked segment system and each link has specific body segment inertial parameters (BSIPs). These parameters include mass, location of centre of mass (COM), moments of inertia (MOI) and radii of gyration (ROG). The movement of a segment depends on the segment's BSIPs and the external forces acting on it. Therefore, it is crucial to know the mass, location of COM, and the inertial tensor of each segment. Without these parameters, it is impossible to simulate or optimize human movement whether using direct dynamics or inverse dynamics (Reid & Jensen 1990). When studying kinetics, it is important to note, the accuracy of the kinetic analysis depends on the accuracy of the BSIPs.

COM of a segment is an important variable in biomechanical analysis of movements because it represents the point at which the force of gravity is applied. Mass distribution and COM vary between subjects and rely on the subject's build. It cannot be assumed that the COM of an underweight subject would be consistent with an overweight subject. Drillis et al. (1966) states that the greatest error in measuring BSIPs is due to variations in body build. Different researchers using the same technique on different subject pools have reported different BSIPS on the same body segments. Somatotyping, classifying the body on size and composition, is used to categorize subjects based on body type. The body types are often classified as endomorph, ectomorph, and mesomorph. With a somatotype and general anthropometrics, parameter coefficients can be used for other subjects matching body types to provide a more accurate representation of BSIPs.

Human subjects are difficult to measure because of the variation between humans and the properties of segments depend on the measurement methodology. Some clear examples of these are the density of the chest depends on whether the subject has inhaled or exhaled and the centre of mass of the hand greatly depends on the position of the fingers.

Contini et al. (1963) recommend multiple measurements for each body segment and for the mean and standard deviation be reported. If the standard deviation of a particular segment is too high, the mean should not be considered a good representative. When looking at segment length and mass, the measurements are typically normalized by using the relative length and mass of the whole body. Normalizing the data in this manner is accepted as the basis for the proportions of various segments (Drillis et al. 1963).

Reid and Jensen (1990) note the major methodologies for measuring or estimating BSIPs are direct measurement, immersion, reaction change, photogrammetry, mathematical modelling and imaging. In the last few years, video capture and light scanner have also been used to measure BSIPs. When reading below, it is important to note that there is not a universally accepted protocol for measuring BSIPs. Some of the variation in data is due to methodology while other variation is from the various populations.

## 2.2 Cadavers

Historically, the mass of body segments was measured by multiplying the volumes by the density of the whole body with the assumption of homogeneous density. Cadaver studies allow for the body to be physically separated and each segment to be analysed independently. This allows for measurements of segmental mass, density, COM and MOI which cannot be done on a living subject. Cadaver studies also provide the opportunity to measure the accuracy of indirect measurements used on living subjects.

Harless (1860) was one of the earliest cadaver studies which consisted of segmenting two male cadavers into 15 segments (as cited in Drillis et al., 1966). Individual segments were weighed and COM was found using a balance platform. There were problems with the protocol as the subjects were decapitated prisoners with unknown blood loss but it was the start of a new method of analysis BSIPs.

Braune and Fischer (1889) collected data from 3 muscular male cadavers to represent the average German soldier (as cited in Reid & Jensen, 1990). The segments were weighed and the COM was found by driving thin metal rods at right angles to each cardinal plane and the segment was suspended. The equilibrium was found along each middle rod and the intersection of the three equilibriums was considered the COM. Braune and Fischer used a compound pendulum to measure the MOI. Their cadavers were frozen to reduce the blood loss experienced by Harless (1860).

Dempster (1955) measured mass, density, location of COM and mass MOI on eight male cadavers who were above 50 years old and below average height and weight of the male population. Dempster placed the joints in mid flexion for segmentation so the mass of each joint was properly allocated to each segment. Each segment was weighed and the COMs were located using a balance plate. MOI was determined using a compound pendulum (Figure 1). The volume of each segment was measured using the immersion method. Dempster determined the volume of the cadaver segments by immersing the segment in a tank of water and measuring the weight of the immersed part (Figure 1). The difference between the weight in air and the weight in water represented the weight of water displaced and the volume equivalent was used for the segment's volume. Reid and Jensen (1990) note that Dempster's study is considered one of the most comprehensive cadaver studies.

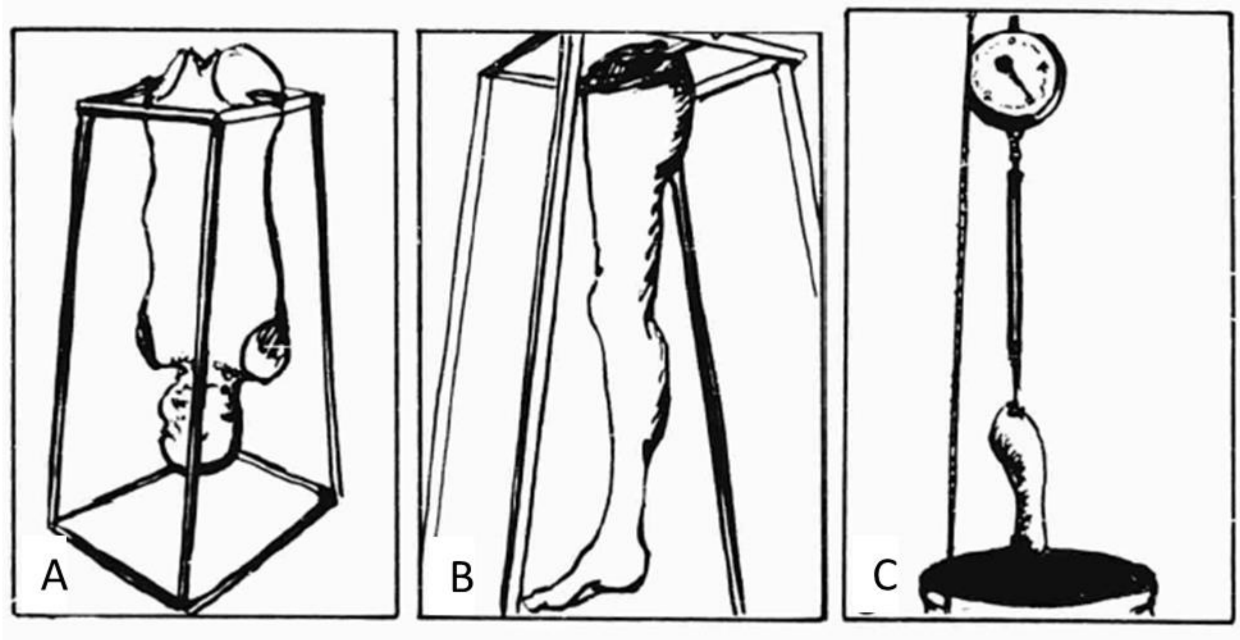


**Figure 1: Dempster's procedures associated with cadaver dismemberment. A- Trunk suspended on a knife edge to determine MOI. B- Leg suspended on a knife edge to determine MOI. C- Arm suspended from a scale for water imersion to determine mass (Image from Dempster**, **1955)).**

Clauser et al. (1969) collected BSIPs from 13 preserved male cadavers with an average age of 49.3 years. The cadaver sample was both shorter and lighter than the military and civilian working databases. The density of the preservation solution was close to the average density of an adult male. Each segment was weighed and the COM locations were found using a balance table. After the COM was located in one axis, the table was tilted and the COM was found along the second axis. Repeated trials found the maximum variation between COM measurements to be within +/- 3mm. The volume was measured using water displacement. Depending on the segment, the displaced water was measured to determine the volume or the difference between the weight in air and the weight in water. MOIs were not measured.

Chandler et al. (1975) investigated 6 preserved male cadavers using similar methods to Clauser et al. (1969) with the addition of MOI measurements. The subjects were frozen to form a rigid body to minimize fluid loss during segmentation and to measure MOI. MOI was measured using a Styrofoam holders and each segment was swung in six axes (Figure 2).

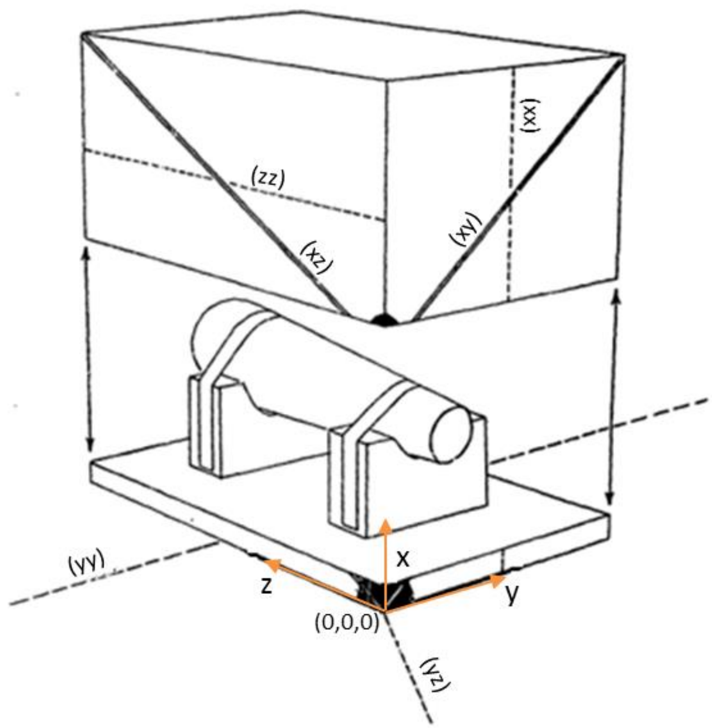


**Figure 2: Specimen holder with top and measurement-axis system. The six swing axes are indicated with a two letter designation. (Image adjusted from Chandler, 1975)**

Differences between segmentation and measuring procedures restrict the reliability of combining multiple cadaver studies to increase population sizes. A major disadvantage in cadaver studies is the small sample size with a narrow population scope. Majority of cadaver studies use elderly Caucasian males, most of which are shorter and lighter than average, which provide poor representations of males of different size and ethnicity, females, younger adults and children. Although these data is not truly representative, it is still used for other populations due to the difficulty in conducting cadaver studies. Another disadvantage is that cadavers do not exactly mimic the living human form. There is some blood loss and the MOI found in frozen cadavers does not precisely model living movement. Lephart et al. (2014) studied the BSIPs of cadavers to determine the applicability of cadaver studies for living subjects. The study found significant differences between body types and significant differences between frozen densities and thawed densities. They suggest thawed densities should be used in analysis of movement as they are more comparable to analyses in vivo and BSIPs from cadaver data should only be used for matching somatypes. The cost is another limitation in undertaking cadaver studies. It is expensive and time consuming so large sample sizes are impractical. There are also ethical implications such as cadaver studies on young populations.

## 2.3 Living Subjects

### 2.3.1 Immersion Method

The immersion technique can be applied on both cadavers and living subjects. The immersion method is used to determine the volume of the segment by measuring the volume of water displaced by the segment. It can determine the total segment volume or any portion of it using a step-by-step sequence.  With cadaver studies, the mass of the segment can be measured and the density of the individual segment is determined. With living subjects, the segment can be immersed and average density from literature can be used to estimate the segment's mass. COM of the segment can be estimated using the immersion technique by reimmersion of half the displaced volume. MOIs are estimated using the step-by-step sequence and displacing small equal volumes of fluid and measuring the distance from the centre of each volume to a reference axis. When measuring living subjects, Dempster (1955) had the subjects place the segment into tanks of water filled to the brim. As the segment was placed into the water, the overflow was collected. The water was weighed and the comparable volume of displaced water was measured. Contini et al. (1963) used the immersion method by placing the subject's segment into an empty tank and filling it to successive predetermined levels at two-centimeter increments. The authors state the volume of the whole body can also be measured this way but great accuracy cannot be expected. Air in the lungs becomes a large factor when measuring the volume of the chest.

A major limitation of the water immersion technique is measuring with precision on living subjects. The segmentation planes are difficult to identify correctly along the immersion line. The segments should closely fit the immersion tubes and it is often difficult for the subject to hold steady during the measurements (Reid & Jensen 1990). Holding segments steady is particularly difficult in specific populations. Young and old populations, as well as populations with neuromuscular problems, would find it difficult to remain motionless during the collection. These errors are compounded when measuring partial volumes along the segment.

### 2.3.2 Quick Release Method

This method is used to determine the MOIs of a segment in a living body. It uses Newton's Law for rotation by moving a segment at a known acceleration by applying a known force at a given distance and calculating the moment of inertia. The segment is placed so the proximal joint does not move. The distal end of the segment has a cord attached. The subject pulls the cord and the force is measured. The cord is cut and the segment accelerates. By measuring the instantaneous acceleration, the MOI about the proximal end can be calculated (Drillis et al. 1963). This technique was used by Bouisset and Pertuzon (1969) to measure the MOIs of the forearm and hand for 11 subjects about the transverse elbow axis. The experimental set-up can be seen in Figure 3. A major limitation of the quick release method is the difficulties in isolating segments and their axes of motion. Another limitation is the BSIPs measured by the quick release method are limited to the MOIs and are affected by the muscle activity in the segment.

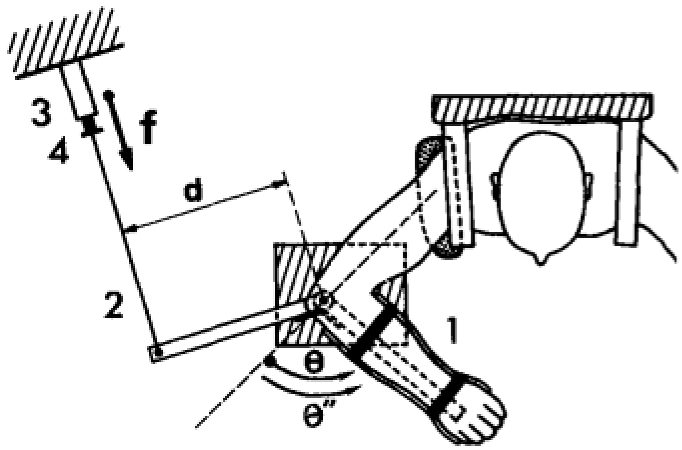


**Figure 3: Quick release set-up for measuring the MOI of the lower arm. (Image from Goubel & Pertuzon, 1973)**

### 2.3.3 Mathematical and Geometric Modeling

Mathematical and geometric modeling represents each segment or component of each segment as geometric shapes with known density. The complexity of these models has increased since they were developed, trying to more accurately model the human shape. Shapes used to model the body are frustrums of right circular cones, elliptical cylinders, spheres, ellipsoids and rectangular parallelepipeds (Whitsett 1963). Hanavan (1964) used 15 geometric shapes (Figure 4) based on the individual's anthropometry. Segment mass was estimated using segment densities from Dempster (Dempster 1955) and regression equations from Barter (1957). Rodrigue and Gagnon (1984) studied the validity of Hanavan's model for the forearm and found Hanavan's method predicted the COM location with errors ranging from 1-14.6%. Rodrigue and Gagnon suggest the Hanavan model should be redefined as the model's forearm shape does not adequately represent the segment. Hatze (1980) used 242 anthropometric measures and divided the body into 17 segments (Figure 4). The study used segment densities from Dempster (1955). Anthropometric measurements were taken on four subjects (two male, one female and one 12 year old boy).

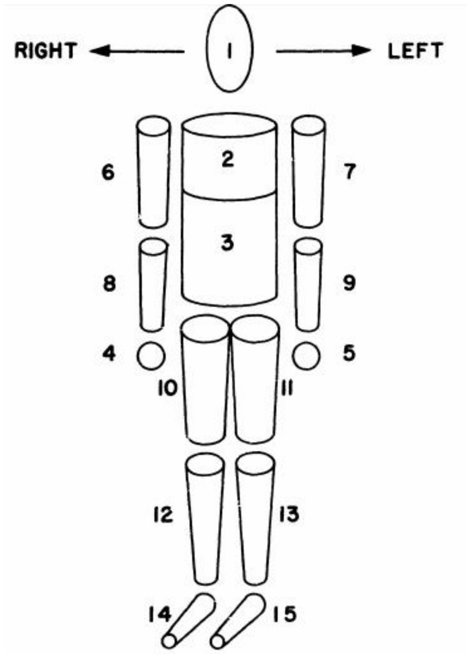

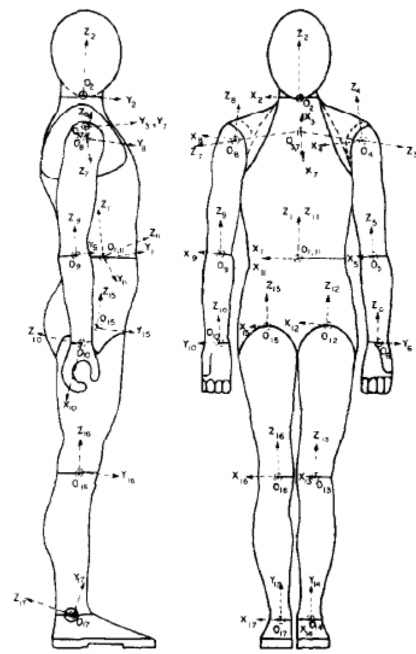

**Figure 4: Left: Segment shapes for the mathematical model by Hanavan (Image from Hanavan, 1964) Right: 17-segment anthropomorphic model by Hatze (Image from Hatze, 1980)**

A limitation to these mathematical/geometric models is they are developed for adults and cannot be applied for toddlers. Segment shapes and body proportions are different between adults and toddlers and the mathematical/geometric models cannot be simply scaled to represent toddlers. Toddler specific equations would be required and are not currently available.

### 2.3.4 Medical Imaging

Medical imaging provides the ability to measure segment mass and mass distribution in each segment. Tissues are differentiated and specific tissue densities are used. Medical imaging techniques include gamma-ray scanning, computed tomography (CT), dual energy X-ray absorptiometry (DEXA) and magnetic resonance imaging (MRI).

Gamma scanning techniques use the principle that a tissue's ability to absorb or attenuate gamma rays is proportional to the density of the tissue. This allows for the differentiation of fat, muscle and bone in the segment. Zatsiorski and Seluynov (1985) developed a gamma ray scanning protocol for measuring BSIPs in humans. They estimated segment mass, COM location and principal MOIs of 100 adult men and 15 adult women.  Although these data have been available, cadaver data of elderly males is still preferred even when estimating the BSIPs of healthy young subjects. de Leva (1996) reasons that this is likely because Zatsiorsky's group used body landmarks near the joints as reference points for locating segment centre of mass (COM). Some of these points were notably distant from the joint centre. As subjects flex their joints, the distance between the bony landmark and the segment's COM changes. de Leva suggested an adjustment which uses joint centers for reference rather than bony landmarks. Reid and Jensen (1990) note that the gamma radiation technique is rarely used due to the difficulty in getting the methodology approved because of the inherent dangers from radiation.

Reid (1984) used CT to examine the trunk segment of two male and two female subjects. Scans were performed at 1-cm intervals to measure dimension of the trunk, estimate COM location and mass. Zhu et al. (1986) measured the accuracy and precision of CT and MRI area measurements. Images phantoms were more common in MRI and had more grey level variation. The authors recommend MRI area measurements should be interpreted with caution.  Pearsall et al. (1996) used CT imaging to determine COM location and MOIs about the COM of the trunk for two males and two females. The CT scans were collected at 1-cm intervals. The study found variations in BSIPs between the four subjects but the values were within those found in previous studies (Figure 5).

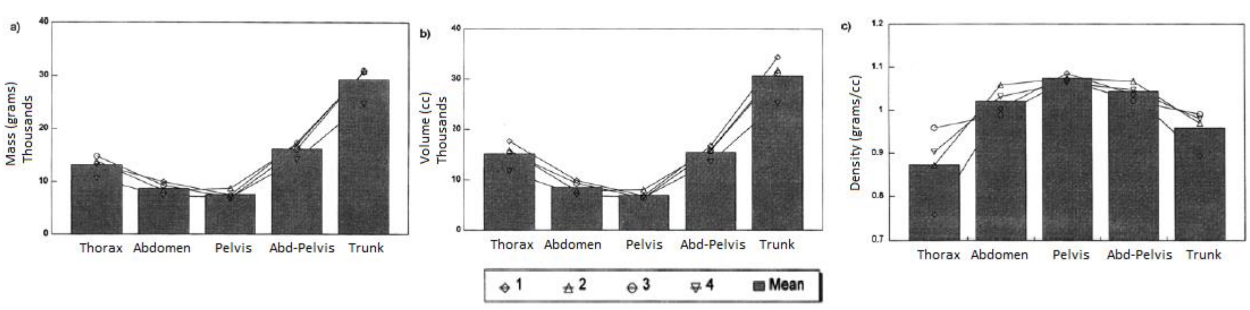


**Figure 5:  Mass, volume and density of the trunk (Image adjusted from Pearsall et al., 1996)**

Durkin et al. (2002) used DEXA to estimate the whole body mass of 11 males. Their study also scanned a plastic cylinder and human cadaver leg to measure the error in determining mass, length, COM location and MOI about the COM. The whole body mass had an error of -1.05% ± 1.32% for the human subjects. With the exception of MOIs, BSIP errors in the cylinder and cadaver leg were under 3.2% compared to the pendulum method. When comparing to geometric calculation, the error in MOI was 2.62%. The authors concluded that DEXA is a simple and accurate way to measure BSIPs in living humans. Sandoz et al. (2010) used biplanar X-rays to determine subject specific masses and 3D location of COM in six children and six adults. Low dose X-rays were used to minimize radiation. Tissue densities from the literature of adult males were used to define the masses. The mean error between the estimated and measured total body mass was 2.6%. The children were aged 9-13 and the x-rays were made on medical prescription for the children.

Mungiole and Martin (1990) studied the feasibility of using MRI for estimating BSIPs. They compared MRI-based BSIP estimates of the lower leg of 12 adult male distance runners with those based on other estimation techniques. The study used an MRI slice thickness of 4mm and a series of cross-sectional images were taken at 2.5cm apart along the longitudinal axes of rotation. They found the MRI estimated leg mass and MOI about the transverse axis through COM varied considerably from the various mathematical models. This could be due to different muscle distribution for healthy runners and older cadavers. COM locations were consistent across methods. Mungiole and Martin also looked at the tissue distribution along the longitudinal axis of the lower leg. Their study compared this density distribution to the assumption of uniform density and found a variation in segment density of only 2.3%.

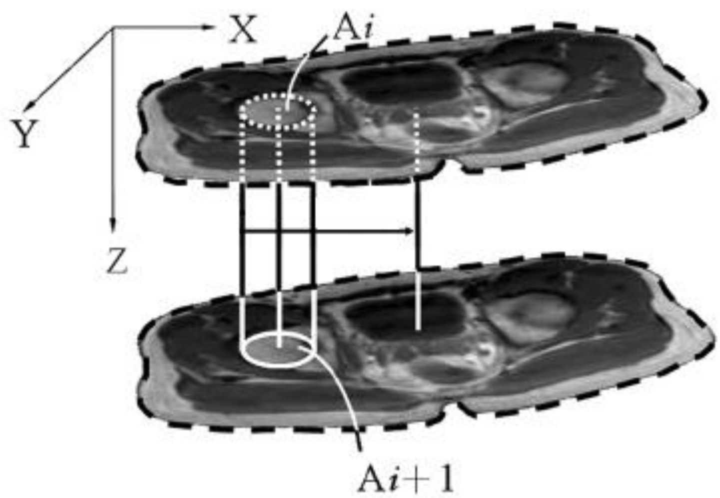


**Figure 6: Diagram of separating the tissue from two adjacent MRI scans (Image from Ho, Shiang, Lee, & Cheng, 2013)**

Ho et al. (2013) estimated BSIPs of 50 young Chinese men using MRI (Figure 6). The study found slight differences in percent body mass of segments and percent COM location compared with other cadaver-based and *in vivo* studies. The differences are attributed to a different population and discrepancies in segment boundaries.

The major limitations of medical imaging are the cost and availability as well as exposure to radiation for some of the imaging methods. Medical imaging is usually limited to medically necessary procedure for young subjects who are at higher risk from radiation and may struggle with the logistics of MRI scans.

### 2.3.5 Photogrammetry Method

The photogrammetric method is able to determine the volume of body segments using two perpendicular photographs. The images are scaled using reference measurements of known length in the plane of the subject in both images. The body is then digitally segmented and the elliptical method is used. Each segment can be broken down in two directions into many sections of equal height and each slice is assumed to be elliptical. The diameters of each slice are measured and the volume of the slice is calculated. The volume of the segment is calculated by summing the volumes of each slice. This method also allows for the calculation of COM locations and MOIs. The accuracy of the volume relies on the slice thickness and how similar the slice is to the elliptical cylinder it is being represented by.

Weinbach (1938) was the first study to use the photogrammetry/elliptical method. Front and side photos were taken of males aged 3.5, 25 and 26 and females aged 2 and 23 and elliptical horizontal sections were taken along the body. Weinbach presented volume contour maps which showed the cross sectional area of the subjects along the longitudinal axis of the body.

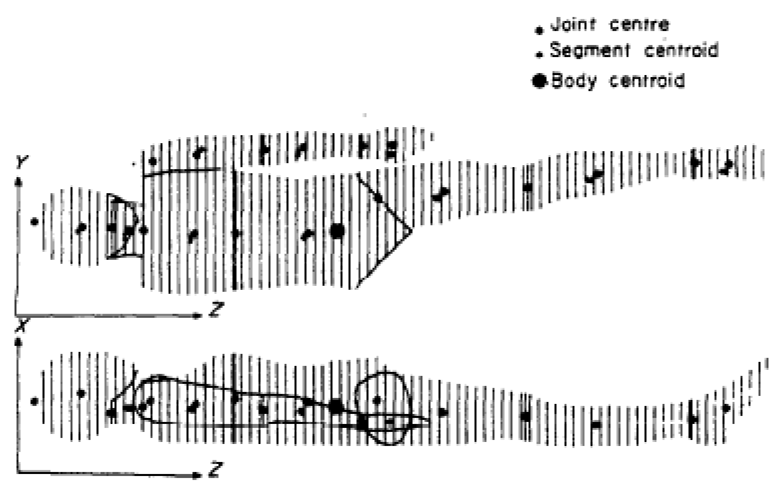


**Figure 7: Elliptically sectioned body** (Jensen 1978)

Jensen (Jensen 1978) further developed the photogrammetric method and compared three body types. Using two photographs, the subjects were sectioned in elliptical zones 2cm thick (Figure 7). A comparison between body types was made on three boys. Jensen found differences in the BSIPs across the body types. Although the endomorph and mesomorph had similar total body masses, for some segments the masses for the endomorph were substantially greater than the mesomorph.

The error in the photogrammetric method is often measured by comparing the sum of the estimated segment masses and the measured total body mass. Jensen (1989) reported an average error of -0.87% (SD = 2.63%, n=89). Yokoi et al. (1986) reported a similar error of 1.65%

(n=255). Yokoi et al. also measured the body's COM for various postures using a reaction board. They found the standard errors for COM location to be 1.64-3.0% (n=29). Ackland et al.(1988) compared the photogrammetric/elliptical zone estimates of mass and transverse MOI to CT scans of one subject's leg. The study found a mass difference of 3% and a 2.7% difference in transverse MOI. Wicke et al. (2009) adjusted Jensen (1978) model to provide gender-specific density profile and use sectioned ellipses for the trunk segment at the shoulder and hip segmentation lines. When comparing the sectioned ellipse and entire ellipses, the sectioned ellipses significantly (P<0.01) reduced the error in cross-sectional area. The adjusted model was compared to the Jensen's model as well as other accepted models and DEXA which was considered the gold standard. The study consisted of 25 females and 24 males from a university population. The adjusted model had BSIP errors within 6.0% and the other models had higher average errors 10-50%.

As technology has improved, higher quality images and reduction in elliptical slice thickness have improved the accuracy in the measurement of the segment's volume.

## 2.4 Child Data

Toddler and child data cannot be scaled down from adult data as the segment proportions and shapes are significantly different. This is clearly visible in Figure 8. The growth of the human body has been greatly studied (Centers for Disease Control and Prevention 2001) with growth charts available to parents to compare their child's growth to the average healthy population. Although these data are helpful to parents, they have limited use in the field of biomechanics. Other than some measurement of segment lengths and largest circumference of some segments, there is no segment specific inertia data from these studies. Studies looking at BSIPs in children and toddlers have been limited.

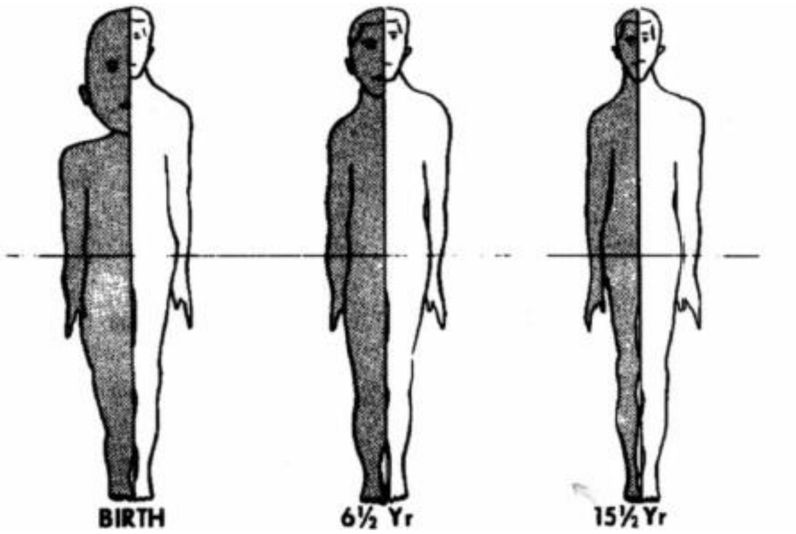


**Figure 8: Developmental change in body proportions as seen in direct comparison between the adult and the newborn, child and adolescent** (Huelke 1998)

The photogrammetric method has been used for children to measure the changes in BSIPs as the children age. Jensen performed a longitudinal study looking at 12 boys aged 4, 6, 9 and 12 across 3 years (Jensen 1986a; Jensen 1986b) and 9 years (Jensen 1989). A total of 88 annual observations were made. The studies showed different rates of mass/volume growth for different segments. The COM location moved more proximally in the limbs as the subjects aged and Jensen attributed this to muscle mass development. Using data from the elliptical model, segment mass and principal MOIs have been predicted (Jensen and Wilson 1988 as cited by Reid & Jensen 1990) using a curvilinear regression presented by Yeadon and Morlock  (1989) and the anthropometric parameters reported by Hanavan(1964). The parameters could be predicted with common variance ($R^2$) of at least 0.8 with the exception of the head and foot. With minimal error, the extrapolation beyond ages 4-20 could be done. These equations were able to account for 84-94% of the variance across these age groups.

Yokoi et al. (1986) also used the elliptical zone method to study Japanese children. 255 children aged 3-15 years were classified into 18 groups based on sex, age and body type. The younger age groups (3-5, 6-8) combined male and female as there were not significant differences in BSIPs at that age. The study found that the sex differences in BSIPs develop during the secondary growth pattern after 9 years old. The study's results found the same trends as Jensen (Jensen 1986a; Jensen 1989). The changes of percent total mass of the head decreased with age while the percent body mass of the thigh and shank increased. The COM location of the limbs moved closer to the proximal end and the COM of the head moved downwards to the midpoint between both tragions. They propose this is due to the head changing shape from spherical to ellipsoidal. Huelke (1998) discusses growth trends of children without going into detail of BSIPs. The trends they discuss parallel those found by Jensen and Yokoi et al. (Figure 9 and Figure 10).

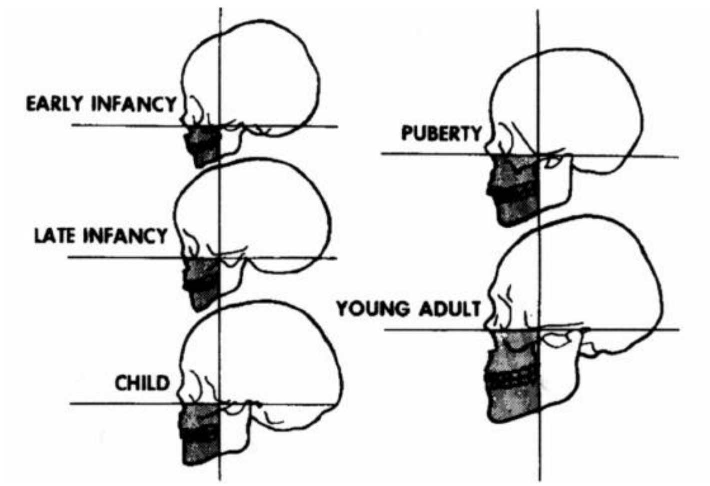


**Figure 9: Changes in head shape with age** (Huelke 1998)

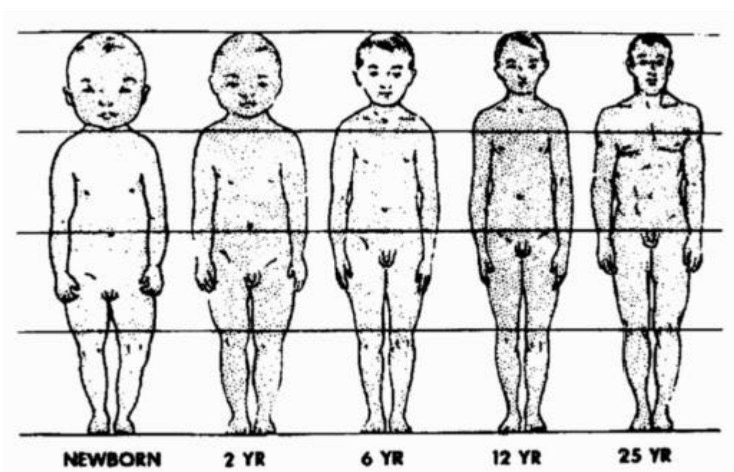


**Figure 10: The proportional changes in body segment with age** (Huelke 1998)

Yokoi et al. (1986) also found differences in the ROGs (relative to segment length) in the longitudinal axis of the torso, upper arm and thigh. The longitudinal ROGs of these segments was larger in the overweight children.

Ackland et al. (1988) measured BSIPs of adolescent males (average age=13.7 years) as they aged (Figure 11). They developed predictive equations for BSIP with growth which accounted for 84% of the variance in the leg, thigh, lower trunk and upper trunk. These predictive equations were slightly different than those found by Jensen (1986a) and Yokoi et al. (1986) and the authors suggest this is due to the differences in the protocol and the use of chronological age without accounting for maturation variance.

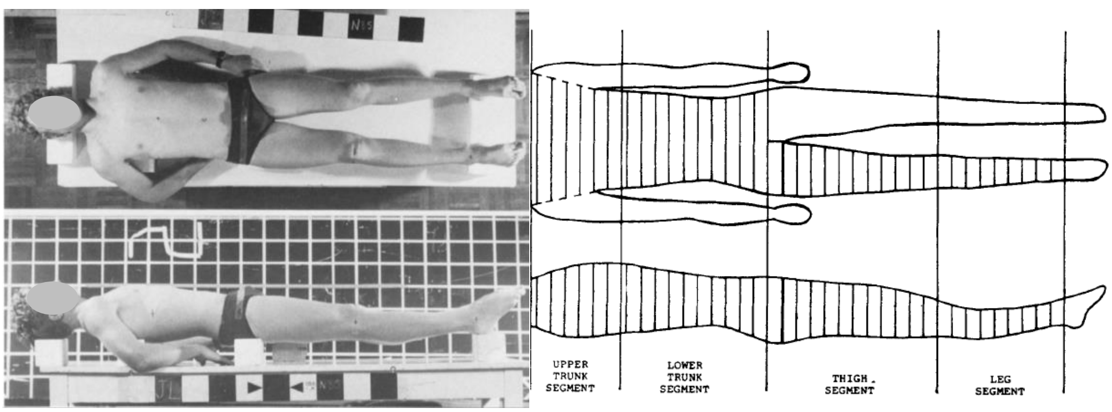


**Figure 11: Photographic set-up and sectioned body(Ackland, Blanksby, et al. 1988)**

Bauer et al. (2007) compared the regression equations developed by Jensen based on 12 boys and MRI estimated BSIPs in 10 girls aged 9. The study compared the BSIPs of the left thigh and shank and kinematics and kinetics were collected for 10 walking trials. Hip and knee moments and powers were compared using the BSIPs from the two methods. The study found significant differences (P<0.01) in the BSIPs between the two methods but determined the differences in kinetics were not meaningful. The authors state that BSIPs estimated using Jensen's regression equations are suitable for girls as well as the boy population it was developed for.

The photogrammetric method has been used for children due to its ease of use and minimal risk. Regression equations for ageing have been developed to estimate BSIPs in subjects outside the age group measured but no BSIP measurements could be found for ages younger than three.

### 2.5 Summary

The importance of accurate BSIPs is well documented in the literature. Early BSIP data were determined using cadavers which were limited to elderly males. Measurement techniques evolved to measuring volumes in living subjects while using data such as segment densities from the cadaver studies. Medical imaging further developed BSIP measurements by making it possible to measure specific tissue volumes in each segment in living subjects. The BSIPs in adult males has been thoroughly studied. Other populations such as women and children have been under represented. From the current literature, BSIPs for toddlers can be estimated using regression equations from older children. Many anthropometric and growth studies have been done for toddler populations but comprehensive BSIP studies have not focused on toddlers.

Limitations for many of these BSIP measuring techniques for toddlers are the complexity of collection, equipment costs or radiation exposure. The photogrammetric method allows for BSIP measurements for highly specific populations (pregnant women, children, etc.) as it is simple, fast and is safe for at risk populations. The photogrammetric method has been used for children as young as 3 years old. As the toddler population finds it difficult to follow the photogrammetric protocol, some adjustments have been made which are discussed in Chapter 3.

# Chapter 3

# Methods

## 3.1 Introduction

The purpose of this study was to measure the range of body segment inertial parameters (BSIPs) of toddler males and females and to adjust the photogrammetric method to collect the data for this age group. The experimental set-up is discussed and the methods and results of protocol testing are evaluated in this section. This protocol testing was used to determine the camera placement for the subject collections and experimental adjustments to make collection easier with toddlers. The photogrammetric elliptical model was used to determine the BSIPs of toddlers and these data were compared to other child inertial parameters and growth trends.

## 3.2 Experimental Set-up

A bathmat with footprints was placed to indicate where the participant was to stand. The angled platform commonly used in the photogrammetric method was omitted due to difficulties in balancing for the age group being collected. Reflective markers were placed on the ground as the horizontal scale measures. These reference points were placed in the frontal and sagittal planes of the subject. The markers were placed a metre apart with the 50cm mark coinciding with the centre of the subject. This set-up can be seen in Figure 12.

Two metre sticks were hung from the ceiling along their long axis for use as vertical scale measures. Pieces of reflective tape were placed at the ends of the metre sticks to help identify the scaling reference points during image digitization. As the subjects were shorter than one metre, the 50 cm mark could not be aligned with the midpoint of the body. Therefore, the metres were a few centimetres off the ground to have them as low as possible without touching the ground. The first metre stick was hung behind the subject in the subject's midsagittal plane. The second metre stick was hung to the left of the subject in the frontal plane. The vertical scale measures can be seen in Figure 13.

Two digital cameras (Fujifilm Finepix AX 600), with lens specifications of 33-165mm F/ 3.3-5.9/ 8-14.4, were placed orthogonally to take images of the frontal and sagittal planes of the subject. The cameras were placed on tripods 65cm above the ground. This height provided clear images with the subject in the centre of the image and was an accessible height for the operator. Levels were used to ensure the camera was parallel to the ground. The cameras' modes were set to 'Auto' (Automatic mode setting according to shooting conditions). The captured image size was 4608x2440 at 16 mega pixels. The cameras were placed 4 metres from the subject. The choice of this distance is discussed in Section 3.3.

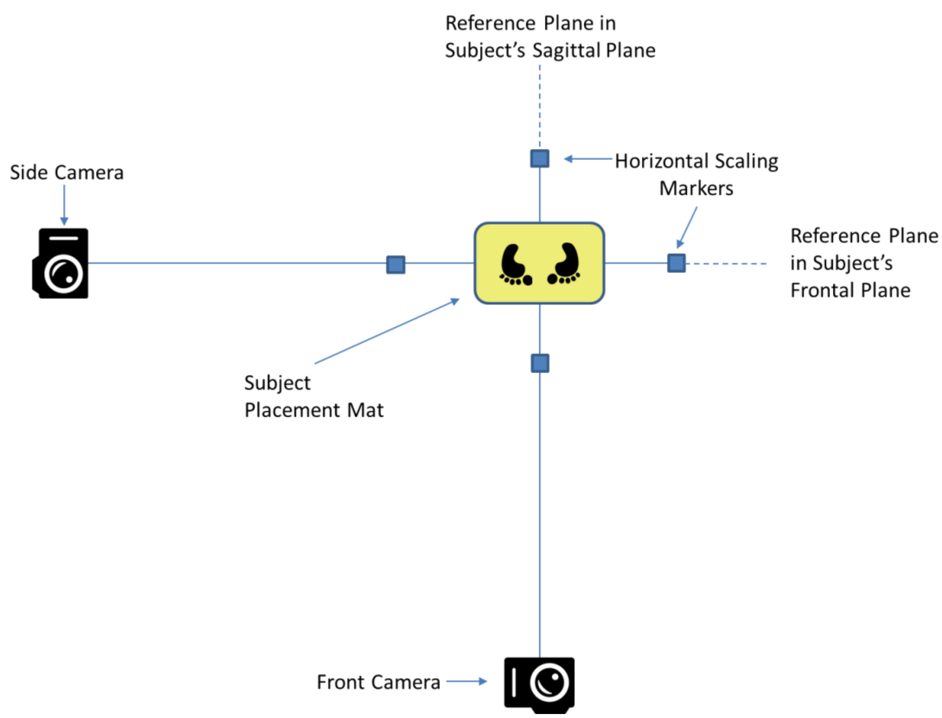


**Figure 12: Experimental set-up with cameras, horizontal reference markers and subject placement mat. Image is not to scale**

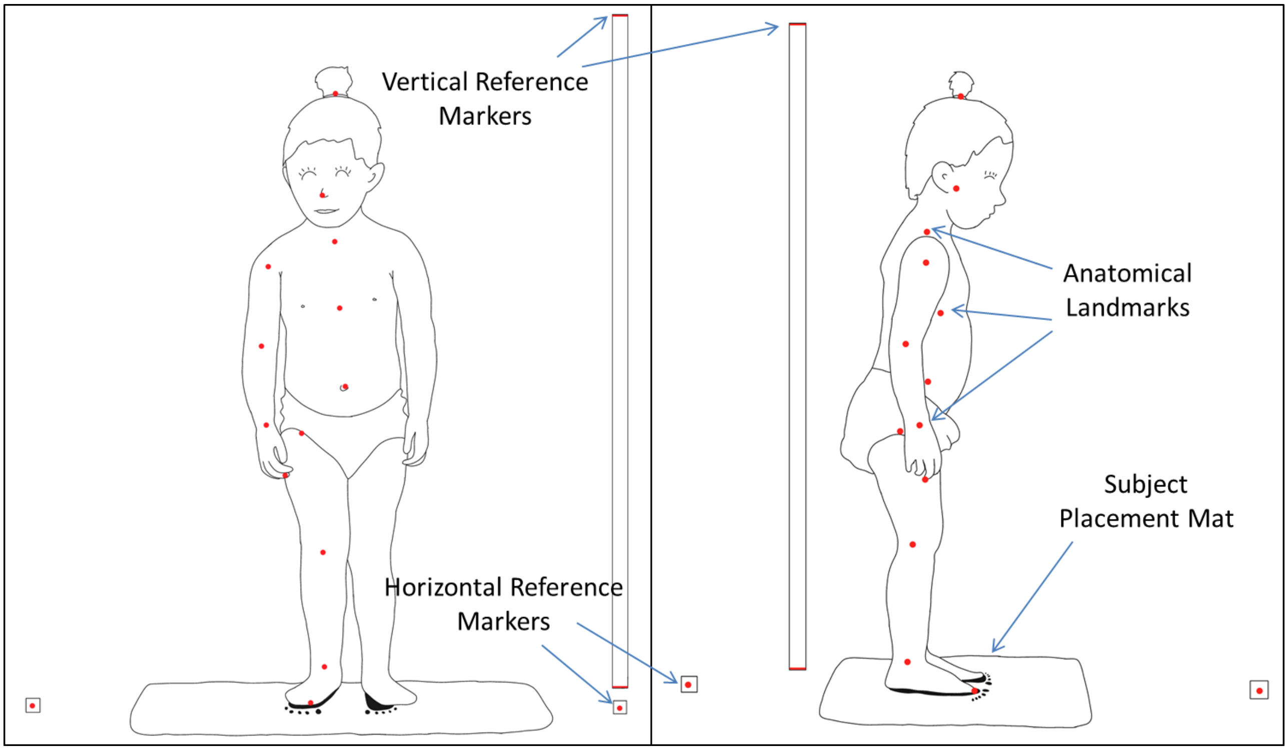


**Figure 13: Experimental set-up with image scaling reference markers and anatomical markers. Image is not to scale**

The subjects were asked to stand on the indicated footprints facing the front camera. This camera was usually operated by the parents who were able to get maximum cooperation from the subject. The ideal subject position is with the feet slightly apart so the outline of the inner thighs was visible and the feet pointing straight ahead. The chin is elevated so both front and back C1 and C7 markers were aligned and the head looking forward so both ears were visible to the front camera. The arms are down by the sides with a gap between the arm and trunk. The hands should be pronated with the fingers held together. The hands should not be cupped and the fingers should be extended. As this ideal subject placement was too difficult for many of the subjects, compromises were made. The placement of standing on the footprints was prioritized while the head angle and hand position were not stressed when the subject was having difficulties.

### 3.2.1 Anatomical Land Marking

Anatomical landmarks were determined by palpation. The accuracy of palpation varied between subjects as not all toddlers enjoy being poked by a stranger. The landmarks noted in Table 1 were indicated using reflective tape (NuVue Safety Tape) in 1 cm squares. The trunk was segmented in three parts, upper trunk, abdomen and pelvis. An apex marker for the top of the head was used for some subjects but was often removed by many of the subjects. As the top of the head was easily visible in both images, if subjects removed the apex marker, it was not replaced. The marker placed on the tip of the finger was also often removed by the subject and was not replaced because the finger's tip could easily be identified in the images.

**Table 1: Reflective markers were placed on anatomical landmarks to indicate joint centres. Markers are placed on the front and right side of the body at each joint centre.**

| | **Proximal** | **Distal** |
|---|---|---|
| **Head** | Apex (Top point of the head) | C1 |
| **Neck** | C1 | C7 |
| **Upper Trunk** | C7 | Xiphoid Process |
| **Abdomen** | Xiphoid Process | L4/L5 (Just below Umbilicus) |
| **Pelvis** | L4/L5 (Just below Umbilicus) | Pubis |
| **Upper Arm** | Acromion | Epicondyle of the Humerus |
| **Forearm** | Epicondyle of the Humerus | Styloid Process |
| **Hand** | Styloid Process | Finger Tip |
| **Thigh** | Greater Trochanter | Femoral Condyle |
| **Shank** | Femoral Condyle | Malleolus |
| **Foot** | Malleolus | Toe Tip |

A table of the palpation protocol can be found in Appendix B but high accuracy palpation was impossible as toddlers do not like to be touched by strangers. Another difficulty was the subjects would often remove the markers as they were being placed so speed was also a major factor.

### 3.2.2 Image Processing

The photogrammetric method developed by Jensen (1978) was used. *SlicerProject* software written by McIlwain et al. (2002) uses front and side images of the participants and the user's segmentation to determine the subject's volume using Jensen's elliptical cylinder model (ECM). The raw photos are loaded into the Slicer program. The images are scaled and the anatomical landmarks are selected. Segments are outlined and a slice thickness of 3mm was used to section each segment. Raw and process photos can be seen in Figure 14. The inertial data are then exported into a CSV file. Details of the Slicer program can be found in Appendix C.

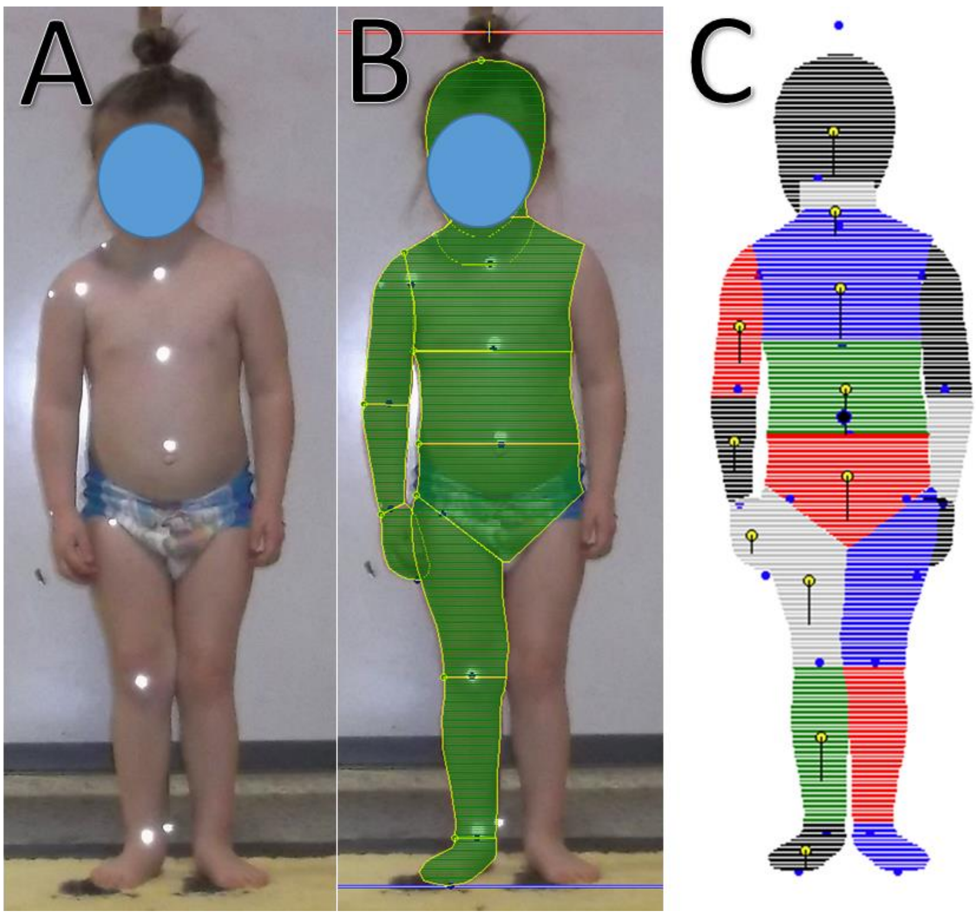


**Figure 14: A: Raw photo. B: Digitized image. C. Elliptical Slices with right and left side symmetry.**

### 3.2.3 Segmentation

The body was divided into 17 segments. The palpated bony landmarks used for indicating the joint centres (Table 1) are used to establish the segmentation planes. The segmentation boundaries can be seen in Figure 15. A segmentation protocol similar to those used by Dempster (1955) and Clauser et al. (1969) was used to have relevant density values for each segment. The adjustments done by Jensen (1978) were used to allow for relevant comparisons to the literature.

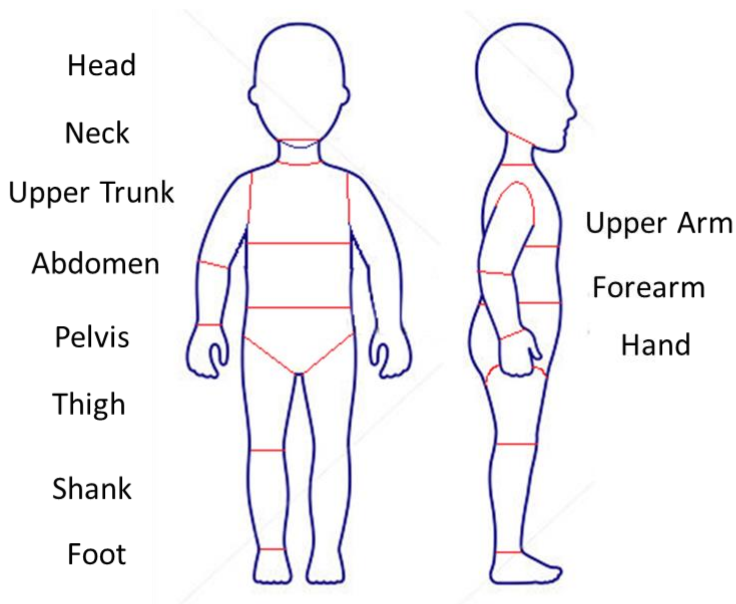


**Figure 15: Segmentation boundaries**

### 3.2.4 BSIP Calculations

Each segment length was determined from the digitized coordinates of the proximal and distal joint centres. The Slicer program divided across the x-y plane in 3mm thick elliptical slices with the exception of the most proximal and distal zones of each segment. For these zones, a slice thickness of less than 3mm was used to match the size of the segment's contour. Each slice was assumed to be elliptical with the major and minor axes fitting the segment's shape and the centroid of each zone was found. The volume, moments of inertia (MOI) and radii of gyration (ROG) of each zone were calculated using the standard formulas for elliptical plates.

Specific details of the elliptical mathematical model are described elsewhere (Jensen 1978). A general overview of BSIP calculations is discussed and any deviations from Jensen's method are explained.

The zone volumes were summed across each segment to calculate the segment's volume. Clauser et al.'s (1969) segment density values were used to calculate segment mass. Clauser's trunk was measured as a single segment so for a 3 segment trunk model, Dempster's (1955) two segment trunk densities were used for the upper and lower trunk. The abdomen and pelvis both use the lower trunk density. Segment density values can be found in Table 2.

**Table 2: Segment densities from the literature used for calculating segment mass**

| Segment | Density (kg/m$^3$) | Reference |
|---|---|---|
| Head and Neck | 1070 | (Clauser et al. 1969) |
| Upper Trunk | 920 | (Dempster 1955) |
| Abdomen and Pelvis | 1010 | |
| Upper Arm | 1060 | (Clauser et al. 1969) |
| Forearm | 1100 | |
| Hand | 1110 | |
| Thigh | 1040 | |
| Shank and Foot | 1080 | |

The centre of mass (COM) is commonly described as a percent distance of the total length. This is often calculated along the long axis of the segment although the COM often does not lie directly on the long axis between the segment's proximal and distal joint centres. As segments are commonly modeled as a line with the segment mass located at the COM location, it is important to know where this COM point would be projected on the line between the two joint centres. In a custom Matlab script, the COM location was orthogonally projected on the line between the proximal and distal joint centres. The distance between the proximal joint centre and the projected COM was divided by the segment length to give the COM location as a percent of the total segment length.

The MOI with respect to the COM was calculated and by using the parallel axis theorem, the MOIs with respect to the proximal and distal ends were determined. As some subjects were unable to maintain the desired position for the photographs, segments with the improper posture were excluded from the analysis. To normalize the MOIs across subjects, the radii of gyration (ROGs) were divided by the segment length.

The BSIPs calculated using the elliptical mathematical model are mass, centre of mass location, moments of inertia and radii of gyration. Segment masses are expressed as a percentage of total body mass and the COM was projected onto the line between the proximal and distal joint centres and expressed as a percent of the total length of the segment from the proximal joint centre. The ROGs are expressed as a percentage of segment length.

## 3.3 Camera Placement

The photogrammetric method takes two orthogonal photos from the front and side of the subject. The two photographs portray a 3D body in two 2D images in the frontal and sagittal planes. The photos are scaled using horizontal and vertical reference points.

Perspective distortion occurs when a 2D photo is taken of a 3D object. Different camera placements, and therefore difference focal lengths, cause different perspective distortion. The photogrammetric method assumes the subject is on the reference plane but the subject is three dimensional and has volume which extends past the plane. The goal is to maximize the image size while minimizing perspective distortion. By minimizing the perspective distortion, the volume measured by the photogrammetric method will be more accurate.

### 3.3.1 Photogrammetric Method

To determine the ideal camera placement which minimizes this distortion while maximizing image quality and size, photographs of a toddler sized doll were taken at various distances. Five distances, 0.5m apart between 2.5m and 4.5m, were compared to one another and to a true volume measured by a 3D scanner. A toddler sized doll was used as the subject held by a frame with minimal interference in the image (Figure 16). The full doll was digitized and segmented according to the photogrammetric segmentation protocol and the volume of the detachable leg was compared. If there was a trend in perspective distortion and error, the distance which provided the most accurate volume would be used for the human participant protocol

Each image was digitized and segmented three times and averaged to ensure the volume differences were due to position and not image processing. The five distances were compared using a one-way analysis of variance.

**Figure 16: Toddler sized doll with plastic support frame**

### 3.3.2 3D Scanner

The toddler doll's leg was removed. Distinguishing marks were placed around the leg to improve scanning accuracy (Figure 17). An Artec Eva light scanner was used to scan the doll's leg by an experienced user. It was considered a closed (watertight) part. The scan was exported as a stl file and opened in Magics program (Version 18) and the total volume was determined. The Artec Eva processes two million points per second with a 0.1mm accuracy. The 3D scan volume was considered the gold standard and the volumes obtained at the various camera positions were compared to the 3D scanner result to determine the error associated with each position.

**Figure 17: Image of the doll's removable leg with distinguishing marks to improve the 3D scanner's accuracy**

### 3.3.3 Results and Discussion

The 3D scanner measured the doll's leg volume to be 1027cm$^3$. This value was used as the reference to measure the error in the photogrammetric method due to camera positions. Images were digitized 3 times for each camera distance and averaged.

There were no significant differences between camera placement means as determined by a one-way ANOVA ($p = 0.96$). The average volume for each distance is in Figure 18 with the 3D scanner volume.

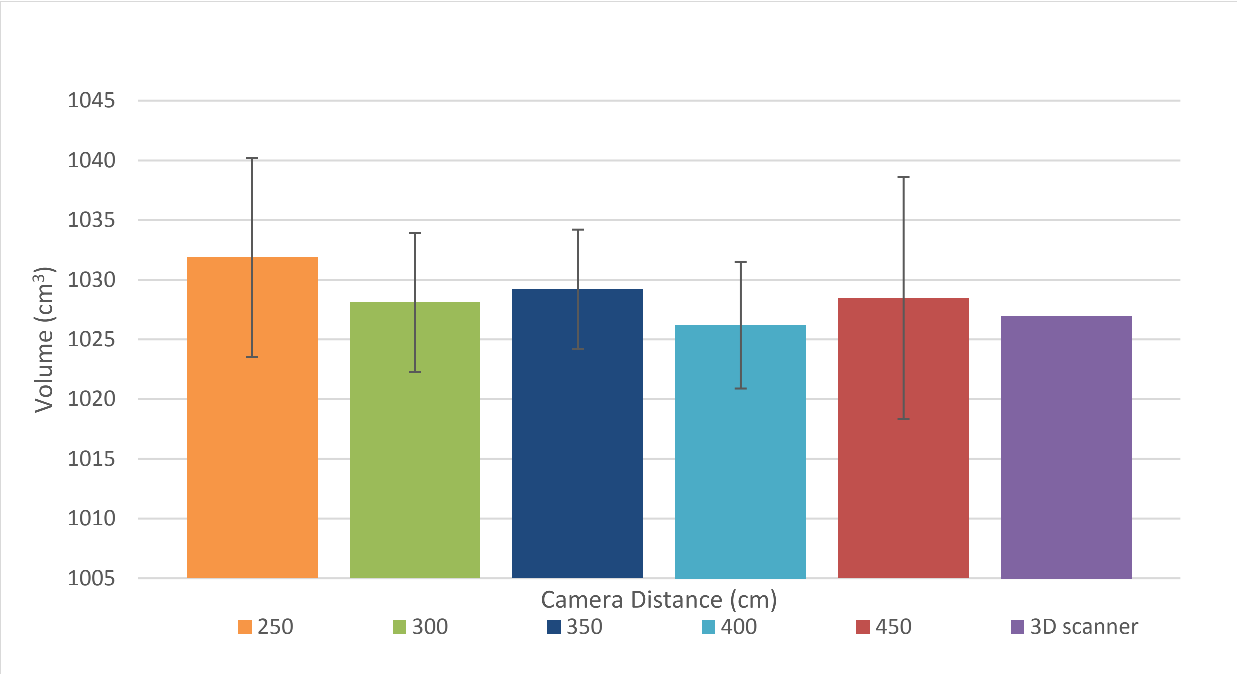


**Figure 18: Average doll leg volume for each camera distance using the photogrammetric method compared to the 3D scanner volume. Error bars are standard deviations for 3 measurements.**

The percent difference between each camera distance's average volume and the 3D scan volume can be seen in Figure 19. The photogrammetric method overestimated the leg volume compared to the 3D scanner with the exception of 400cm. The average volumes resulted in differences of less than 0.5%. The maximum differences of single images were 1.4% overestimation at 2.5m and 4.5m and 1.1% underestimation at 4.5m. All other images had a volume difference of below 1%.

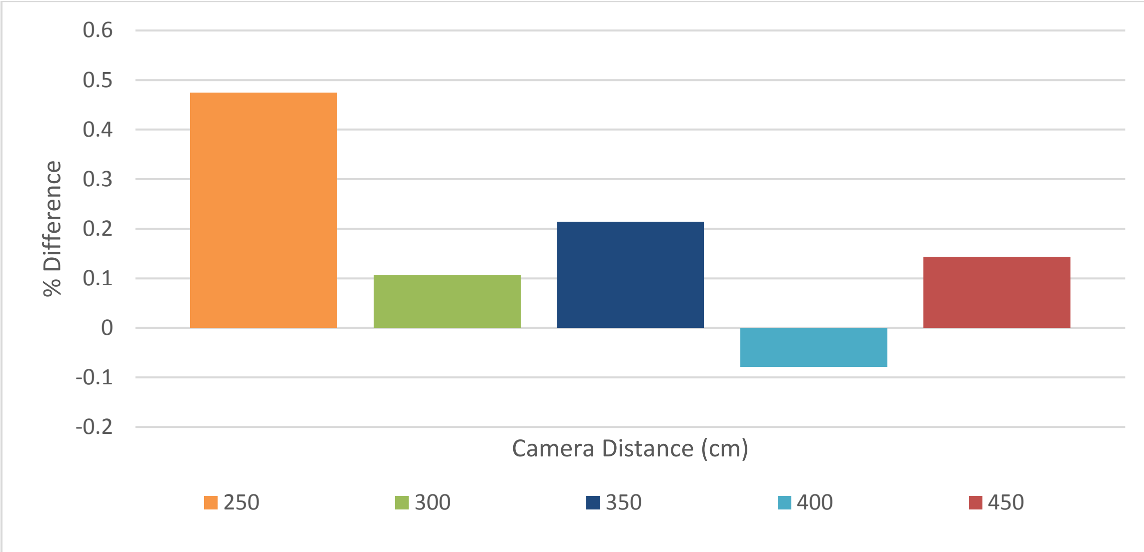


**Figure 19: Percent Difference from the 3D scanner for the average volume at each camera distance using the photogrammetric method.**

The average volumes for each camera distance showed no significant differences. The error due to photo digitizing and leg segmentation was greater than any error caused by camera placement. The most critical aspect to getting accurate volume measurements was the scaling of the photo. Small changes in the points selected for the reference metres resulted in bigger differences in the volume output than individual points while segmenting the leg.

To minimize this variance, the smallest pieces of reflective tape were used on the reference metres to get the most accurate measurement when digitizing the photos. The differences can be seen in Figure 20

**Figure 20: Reducing the size of the reflective markers from the left picture to right picture to minimize errors while digitizing images.**

### 3.4 Subjects

Subjects were recruited from daycares throughout Kingston by use of posters and through Queen's University community by word of mouth and e-mail recruitment. Before the collection started, the subject's parent/guardian went through the letter of information and signed the consent form approved by Queen's University Ethics Board (Appendix A). The participants were asked to wear minimal clothing for the collection and any clothing should be form fitting to be able to easily identify the shape of the body without added volume. The parent/guardian decided at the beginning of collection how much clothing the child was comfortable in. For the participants wearing diapers, a dry diaper was requested at the beginning of collection to minimize volume associated with a full diaper. The inclusion criterion was toddlers aged 18 months – 3 years who are able to stand. A total of 12 male and 12 female participants were collected. The sexes were evenly split in the subgroups <2, 2-2.5, and >2.5. The subject characteristics can be seen in Table 3. Individual subject characteristics can be seen in Appendix D.

**Table 3: Subject characteristics. Values are averages (standard deviations)**

| | Age (years) | Height (cm) | Mass (kg) | BMI |
|---|---|---|---|---|
| **Male (n=12)** | 2.25(0.52) | 89.4 (5.7) | 13.1 (1.5) | 16.3 (1.5) |
| **Female (n=12)** | 2.28 (0.40) | 88.8 (5.9) | 13.2 (2.4) | 16.7 (1.5) |
| **Total (n= 24)** | 2.27 (0.46) | 89.1 (5.8) | 13.1 (2.0) | 16.5 (1.5) |

## 3.5 Statistical Analysis

To determine if significant differences exist between genders, the subjects were divided into two groups and two-tailed t-tests were run for every dependent variable (segment mass, COM and ROG) in their percent form. The significance level was selected to be $p<0.05$.

As each age group was too close to each other, less than a month separating some subjects in one group from another, one-way analysis of variance was excluded. Age trends were found for segment mass proportions and the least squares regression line was determined. The correlation between variables was also evaluated. Least squares regression lines and correlations were also found for mass proportion and body mass index.

A Bland Altman plot was used to identify if there was a bias in determining the total body mass between the photogrammetric method and the medical scale. 95% limits of agreement are calculated by using the mean and the standard deviation of the differences between the two measurements.

## 3.6 Accuracy and Comparison to Literature

The accuracy of using the photogrammetric method for toddlers was indicated by comparing measured total mass with the computed total mass. During the collection process, subjects are weighed on a medical scale (Detecto Physician Scale). This mass is compared to that calculated using the elliptical model. The percent error was calculated for each subject. The percent error is a common method in evaluating the accuracy of a model (Jensen 1978; Yokoi et al. 1986; Finch 1985; Kudzia 2015).

To review and validate the BSIPs collected in this study, the mass, COM, MOI and ROG are compared to the literature. Since there is minimal data for this age group, most data is compared to the aging trends found by Yokoi et al. (1986). Yokoi et al.'s subject group was older (3-15 years) and Japanese but still provides an appropriate comparison using the growth trends for both male and females. Comparisons are also made with Jensen (1986, 1989) which reports BSIPs of males aged 4-20 years.

A literature comparison is used to assess the accuracy of the data as there is not another practical method available to measure BSIPs in toddlers. This literature comparison provides a check on the estimated BSIPs for toddlers with pre-established BSIP growth trends. When obvious divergences occurred, further inspection of the data was done to determine why there would be differences. Body morphology and subject positioning was often a cause for differences.

### 3.7 Subject Placement Error

After collection of some participants, it was noticed that not all subjects were able to remain still on the designated footprints and moved slightly out of plane of the cameras and reference measurements. These photos were retaken attempting to get better images but in the cases where no ideal photo was taken, the subject was standing a few centimetres out of plane.

To measure the error due to the subject's placement, the toddler sized doll was used. The doll was placed in nine positions: Centre, and -15, -7.5, 7.5 and 15cm off centre for each the side and front camera (Figure 21). The doll was placed using a doll support frame (Figure 22). Images were taken for each position and the leg volumes were measured using the photogrammetric method. The volume of the leg for each position was compared to the 3D scanner volume.

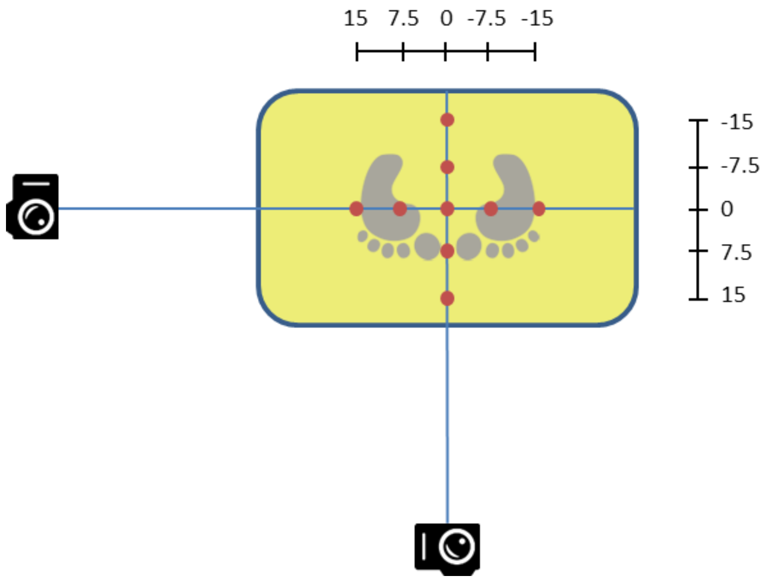


**Figure 21: Red circles indicate the subject placements for the toddler sized doll to measure error when the subject is off the reference plane. Position values are cm off centre towards the front and side camera. Image is not to scale.**

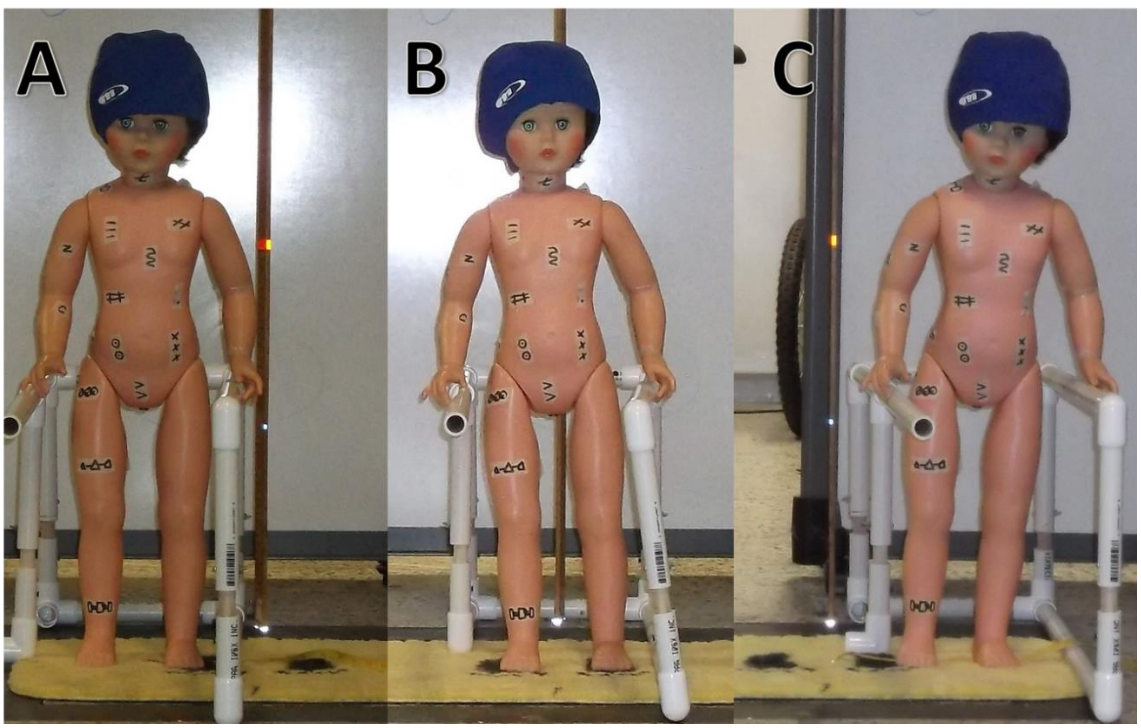


**Figure 22: Doll images for A: 15cm to the right, B: centre, C: -15cm to the right camera**

# Chapter 4

# Results

## 4.1 Introduction

The BSIPs of 12 male and 12 female toddlers (1.5-3years) are presented in this section. The BSIPs this study focuses on are segment masses, COM locations and ROGs. When enough data are available, sex, age and BMI effects on BSIPS are compared. Due to high variability in measurements and a small sample size, comparisons are limited within the data collected and some trends are only established when compared to the literature.

## 4.2 Segment Mass

Segment masses were normalized using the total body mass estimated using the elliptical method. The data discussed are the mass proportion as a percent of total mass and the changes in this distribution based on sex, age and body type.

### 4.2.1 Sex Differences

Table 4 shows the average segment mass as a percent of total body mass for males and females and the comparison between sexes. The thigh was the only segment whose mass had significant differences between sexes ($p = 0.02$). The head mass difference was approaching significance ($p = 0.07$). Females had larger thigh mass proportions while males had larger head mass proportions. The neck, hand and foot had the highest variability in mass proportion relative to the segment's size for both sexes.

**Table 4: Segment mass proportions for males and females and sex differences in segment mass. Mass values are averages (standard deviations).**

| Segment | Mass (% total) Male (n=12) | Mass (% total) Female (n=12) | p Value |
|---|---|---|---|
| **Head** | 18.61 (1.46) | 17.33 (1.57) | 0.07 |
| **Neck** | 1.68 (0.28) | 1.66 (0.31) | 0.89 |
| **Trunk** | 46.49 (1.53) | 45.98 (1.52) | 0.52 |
| **Upper Arm** | 2.22 (0.34) | 2.31 (0.34) | 0.13 |
| **Forearm** | 1.68 (0.16) | 1.61 (0.18) | 0.29 |
| **Hand** | 0.84 (0.25) | 0.94 (0.28) | 0.33 |
| **Thigh** | 6.24 (0.52) | 7.08 (0.95) | 0.02 |
| **Shank** | 3.97 (0.30) | 3.99 (0.19) | 0.86 |
| **Foot** | 1.67 (0.35) | 1.58 (0.28) | 0.47 |

### 4.2.2 Age Trends

Trends in mass proportion with age of the trunk, head and thigh for males and females combined are shown in Figure 23 and the linear regression equations for all segments can be found in Table 5. The head shows a decrease in mass proportion as the child ages with a moderate correlation (-0.54). The thigh's mass proportion increased with age and had a weak correlation (0.38). The upper arm had a slight increase in mass proportion with age and had a moderate correlation (0.46). The trunk's mass proportion showed no trend with age. Regression equations for males and females can be found in Appendix F.

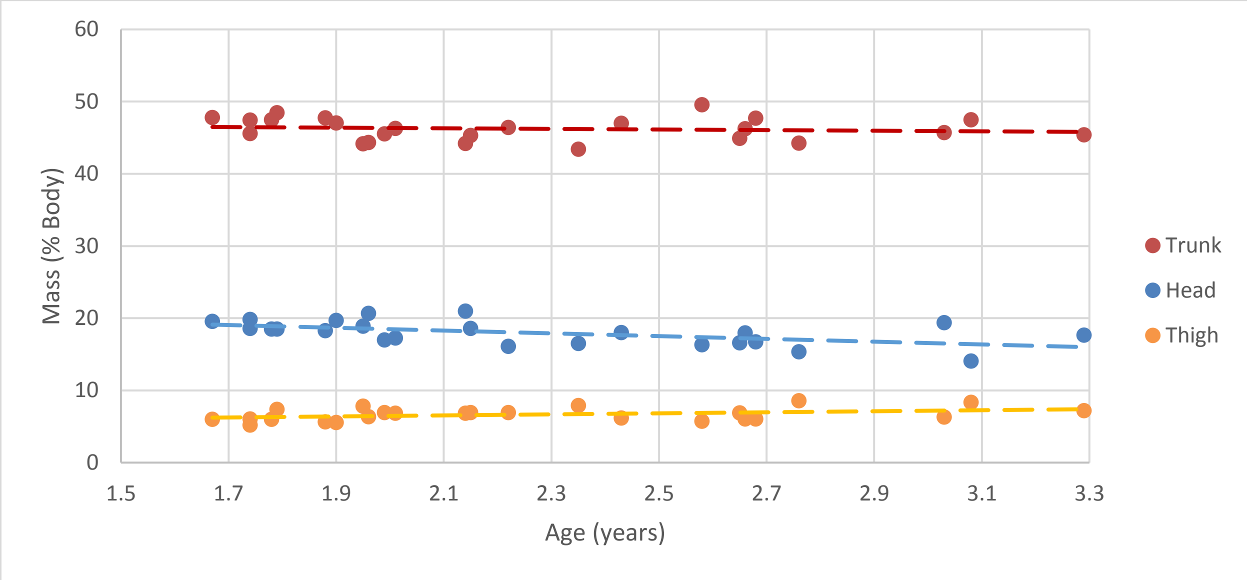


**Figure 23: Trunk, head and thigh mass proportion variation with age for males and females combined**

**Table 5: Mass proportion and age linear regression coefficients for males and females combined. %mass = age (a) + b**

| Segment | a | b | $R^2$ | Correlation |
|---|---|---|---|---|
| **Head** | -1.9204 | 22.321 | 0.29 | -0.54 |
| **Neck** | -0.0932 | 1.879 | 0.02 | -0.14 |
| **Upper Trunk** | 0.8415 | 11.486 | 0.10 | 0.31 |
| **Abdomen** | -0.784 | 19.371 | 0.05 | -0.21 |
| **Pelvis** | -0.4769 | 16.331 | 0.02 | -0.15 |
| **Trunk** | -0.4195 | 47.188 | 0.02 | -0.13 |
| **Upper Arm** | 0.3428 | 1.4884 | 0.21 | 0.46 |
| **Forearm** | 0.0152 | 1.6107 | 0.001 | 0.04 |
| **Hand** | -0.0666 | 1.0416 | 0.01 | -0.11 |
| **Thigh** | 0.7183 | 5.0317 | 0.15 | 0.38 |
| **Shank** | 0.1834 | 3.5615 | 0.12 | 0.34 |
| **Foot** | 0.0234 | 1.572 | 0.001 | 0.03 |

### 4.2.3 BMI Trends

Mass proportions of all segments were compared to the body mass index (BMI) of the subjects to establish mass trends based on body type. The trends in mass proportion of the trunk, head and thigh is shown in Figure 24 and linear regression equation for all segments can be found in Table 6. The only segment which changed based on BMI was the trunk. The trunk's mass proportion increased with a weak correlation (0.36). Sex specific regression equations for mass proportion and BMI can be found in Appendix F.

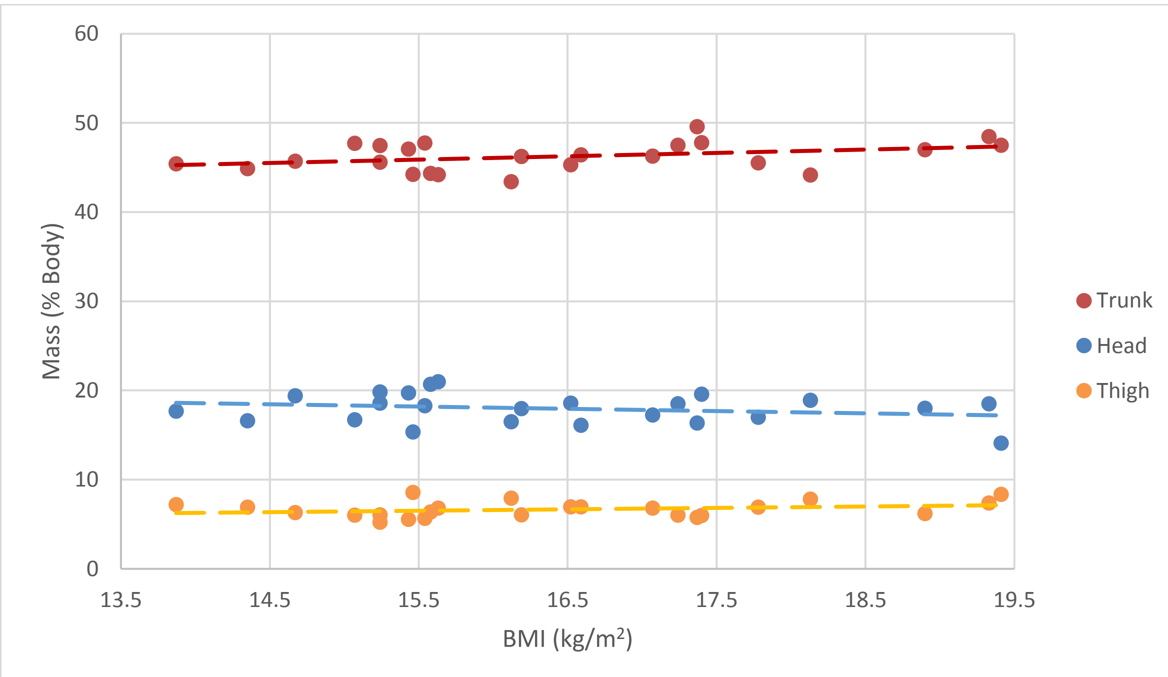


**Figure 24: Trunk, head and thigh mass proportions variation with BMI for males and females combined.**

**Table 6: Mass proportion and BMI linear regression coefficients for males and females combined. %mass = BMI (a) + b.**

| Segment | a | b | $R^2$ | Correlation |
|---|---|---|---|---|
| **Head** | -0.2546 | 22.147 | 0.05 | -0.23 |
| **Neck** | -0.0855 | 3.0724 | 0.19 | -0.43 |
| **Upper Trunk** | -0.1097 | 15.196 | 0.02 | -0.13 |
| **Abdomen** | 0.3216 | 12.311 | 0.08 | 0.29 |
| **Pelvis** | 0.1638 | 12.559 | 0.03 | 0.16 |
| **Trunk** | 0.3757 | 40.066 | 0.13 | 0.36 |
| **Upper Arm** | 0.0115 | 2.0764 | 0.002 | 0.05 |
| **Forearm** | -0.0323 | 2.1753 | 0.08 | -0.28 |
| **Hand** | -0.0733 | 2.0946 | 0.16 | -0.40 |
| **Thigh** | 0.1586 | 4.0569 | 0.07 | 0.27 |
| **Shank** | -0.0674 | 5.0845 | 0.16 | -0.41 |
| **Foot** | -0.0149 | 1.8696 | 0.005 | -0.07 |

## 4.3 Centre of Mass

The centre of mass (COM) was calculated in two ways. Non-projected centre of mass (NP-COM) is the distance of the COM to the proximal joint centre divided by the segment length. The projected centre of mass (P-COM) is the point where the COM would orthogonally be projected along the line between the proximal and distal joint centres. This orthogonally projected COM is calculated because body segments are often modeled as a straight line between joint centres with the segment mass located at the percent distance from the proximal end reported by the literature. As the COM rarely falls directly on the line between joint centres, this COM position is not properly represented. By calculating the P-COM, a more representative COM location is found for when the segment is simplified to a line.

There were significant differences between NP-COM and P-COM for all the segments ($p<0.001$) with the exception of the forearm ($p=0.069$) (Table 7). Large differences between the two methods are seen in the pelvis and foot.

**Table 7: Comparison between non-projected COM and projected COM locations. COM is expressed as a percent of the segment length from the proximal end. Values are averages (standard deviation). n=24**

| | Non-Projected COM (% Segment Length) | Projected COM (% Segment Length) | Difference (% Segment Length) | p Value |
|---|---|---|---|---|
| **Head** | 72.92 (3.97) | 72.37 (3.78) | 0.55 | <0.001 |
| **Neck** | 74.81 (4.89) | 73.81 (4.49) | 1.00 | <0.001 |
| **Upper Trunk** | 54.67 (1.11) | 53.84 (1.30) | 0.83 | <0.001 |
| **Abdomen** | 51.62 (1.67) | 50.93 (1.26) | 0.69 | <0.001 |
| **Pelvis** | 48.10 (4.88) | 36.58 (4.28) | 11.53 | <0.001 |
| **Upper Arm** | 51.05 (3.07) | 50.70 (3.07) | 0.36 | <0.001 |
| **Forearm** | 43.73 (1.51) | 43.26 (1.19) | 0.46 | 0.069 |
| **Hand** | 42.26 (5.18) | 41.47 (5.55) | 0.79 | <0.001 |
| **Thigh** | 50.59 (2.26) | 50.25 (2.23) | 0.34 | <0.001 |
| **Shank** | 44.24 (1.47) | 43.95 (1.59) | 0.29 | <0.001 |
| **Foot** | 32.62 (2.72) | 28.18 (3.55) | 4.44 | <0.001 |

### 4.3.1 Sex Differences

The COM locations were compared between males and females in Table 8. No significant differences were found between sexes ($p>0.05$). The upper arm and forearm differences were approaching significance ($p=0.09$ and $p=0.08$ respectively) with males having a more distal COM.

**Table 8: Sex differences in segment COM. COM is expressed as a percent of the segment length from the proximal end. Projected COM values are averages (stand deviations).**

| | COM Male (n=12) (% segment length) | COM Female (n=12) (% segment length) | p Value |
|---|---|---|---|
| **Head** | 71.81 (3.72) | 72.93 (3.47) | 0.53 |
| **Neck** | 74.93 (4.65) | 72.69 (3.64) | 0.27 |
| **Upper Trunk** | 53.45 (1.32) | 54.24 (1.03) | 0.17 |
| **Abdomen** | 51.07(1.44) | 50.80 (0.89) | 0.59 |
| **Pelvis** | 36.92 (4.63) | 36.22 (3.47) | 0.70 |
| **Upper Arm** | 51.83 (2.74) | 49.57 (2.75) | 0.09 |
| **Forearm** | 43.71 (1.18) | 42.81 (0.92) | 0.08 |
| **Hand** | 42.35 (5.86) | 40.60 (4.60) | 0.56 |
| **Thigh** | 51. 06 (2.36) | 49.44 (1.55) | 0.11 |
| **Shank** | 43.56 (1.76) | 44.33 (1.14) | 0.22 |
| **Foot** | 27.26 (3.49) | 29.11 (3.08) | 0.22 |

### 4.3.2 Age Trends

No age trends could be determined from the data in this study. There was too much variation in subjects so that all correlations between P-COM and age were weak. The strongest correlation was for the head (-0.37) with an $R^2$ value of 0.14. Due to the small sample size with high variability, the data had to be compared with literature to establish any trends with age (Section 5.4.1).

## 4.4 Radius of Gyration

The radius of gyration (ROG) has extreme variability across age and sex and was greatly affected by the position of the subject. For this reason, differences in age and sex were not identifiable and all subjects were grouped together to minimize positional effects. Some segments were excluded due to incorrect positioning observed in the photos. Small positional differences in individual segments should not greatly affect the average. ROG averages are shown in Table 9.

**Table 9: Summary of ROGs with respect to the COM in the three body axes. Values are averages (standard deviations). Sample size is shown for each segment.**

| | ROG Ant/Post (% segment length) | ROG Transverse (% segment length) | ROG Longitudinal (% segment length) |
|---|---|---|---|
| **Head** (n=24) | 36.72 (2.67) | 38.62 (2.81) | 33.67 (3.03) |
| **Neck** (n=23) | 30.79 (3.02) | 29.80 (2.54) | 36.45 (3.85) |
| **Upper Trunk** (n=24) | 46.37 (2.83) | 39.68 (2.17) | 46.66 (4.81) |
| **Abdomen** (n=23) | 46.82 (3.25) | 43.91 (2.85) | 50.77 (5.31) |
| **Pelvis** (n=23) | 45.70 (4.81) | 46.52 (4.56) | 43.73 (5.04) |
| **Upper Arm** (n=24) | 30.24 (1.27) | 31.21 (1.27) | 14.01 (1.17) |
| **Forearm** (n=20) | 28.40 (0.53) | 31.22 (1.27) | 13.41 (1.17) |
| **Hand** (n=20) | 24.49 (1.90) | 26.76 (0.43) | 19.33 (1.73) |
| **Thigh** (n=24) | 29.56 (1.21) | 30.37 (1.28) | 18.20 (1.72) |
| **Shank** (n=24) | 28.63 (0.74) | 28.90 (0.70) | 13.21 (1.32) |
| **Foot** (n=24) | 30.11 (2.18) | 27.56 (2.53) | 17.33 (2.10) |

## 5.5 Results Summary

Age and BMI trends were established for mass proportions of the head, thigh and trunk. Some gender differences were seen in the mass proportion of the thigh and head. No significant differences were found between the sexes for COM location. COM was too variable for the small sample size so age trends could not be establish. All subjects were grouped together for the analysis of ROG to minimize the subject's posture effects. A summary of the results can be seen in Table 10: Means and standard deviations of BSIPs in males and females.

**Table 10: Means and standard deviations of BSIPs in males and females. Mass is percent body mass, COM is percent segment length from the proximal end and ROGs with respect to COM are percent segment length.**

| Segment | Males Average age = 2.25 years (n=12) | | | | | Females Average age = 2.28 years (n=12) | | | | |
|---|---|---|---|---|---|---|---|---|---|---|
| | | | Radius of Gyration | | | | | Radius of Gyration | | |
| | Mass | COM | A/P | TVS | LONG | Mass | COM | A/P | TVS | LONG |
| **Head** | 18.6 (1.4) | 71.8 (3.7) | 37.3 (2.4) | 39.3 (2.8) | 33.7 (2.6) | 17.3 (1.5) | 72.9 (3.5) | 36.1 (2.8) | 37.9 (2.8) | 33.7 (3.4) |
| **Neck** | 1.7 (0.3) | 74.9 (4.7) | 29.9 (2.1) | 29.4 (1.8) | 36.5 (2.1) | 1.7 (0.3) | 72.7 (3.6) | 31.6 (3.5) | 30.2 (3.1) | 36.4 (4.9) |
| **Up-Trunk** | 13.9 (1.3) | 53.4 (1.3) | 45.5 (2.5) | 39.3 (2.3) | 45.4 (4.1) | 12.9 (0.8) | 54.2 (1.0) | 47.2 (2.9) | 40.0 (2.1) | 47.8 (5.1) |
| **Abdomen** | 17.3 (1.8) | 51.1 (1.4) | 47.4 (4.0) | 44.7 (3.1) | 51.6 (6.0) | 17.9 (1.4) | 50.8 (0.9) | 46.3 (2.3) | 43.2 (2.4) | 50.0 (4.5) |
| **Pelvis** | 15.3 (1.2) | 36.9 (4.6) | 46.2 (6.0) | 45.9 (4.2) | 44.5 (6.2) | 15.2 (1.7) | 36.2 (3.5) | 45.2 (3.2) | 47.1 (5.0) | 43.0 (3.6) |
| **Upper Arm** | 2.2 (0.3) | 51.8 (2.7) | 30.2 (1.3) | 31.2 (1.4) | 14.1 (1.4) | 2.3 (0.3) | 49.6 (2.7) | 30.3 (1.1) | 31.2 (1.2) | 14.0 (0.8) |
| **Forearm** | 1.7 (0.2) | 43.7 (1.2) | 28.8 (0.3) | 29.0 (0.4) | 13.6 (1.3) | 1.6 (0.2) | 42.8 (0.9) | 28.1 (0.5) | 28.6 (0.4) | 13.3 (1.0) |
| **Hand** | 0.8 (0.2) | 42.3 (5.9) | 24.5 (2.2) | 26.0 (2.4) | 18.4 (1.5) | 0.9 (0.3) | 40.6 (4.6) | 26.5 (0.7) | 26.6 (0.9) | 20.2 (1.5) |
| **Thigh** | 6.2 (0.5) | 51.1 (2.4) | 29.6 (1.3) | 30.4 (1.4) | 18.4 (1.8) | 7.1 (0.9) | 49.4 (1.6) | 29.6 (1.1) | 30.3 (1.2) | 18.0 (1.6) |
| **Shank** | 4.0 (0.3) | 43.6 (1.8) | 28.4 (0.8) | 28.6 (0.7) | 13.2 (1.4) | 4.0 (0.2) | 44.3 (1.1) | 28.9 (0.6) | 29.2 (0.6) | 13.2 (1.2) |
| **Foot** | 1.7 (0.3) | 27.3 (3.5) | 30.5 (1.9) | 27.4 (2.2) | 17.9 (2.1) | 1.6 (0.3) | 29.1 (3.1) | 29.7 (2.4) | 27.7 (2.9) | 16.7 (1.9) |

# Chapter 5

# Discussion

## 5.1 Introduction

The first portion of the discussion includes the interpretation of results and the comparison with the literature. When compared to the literature, if differences arise, potential causes for the dissimilarity are discussed. The second part of the discussion explores the limitations of the methodology. These include limitations of using the photogrammetric and elliptical methods and the challenges with working with toddlers.

## 5.2 Total Body Mass

Using the Slicer software, the mass of each segment was estimated. As it is impossible to weigh individual segments with a scale for validation, the sum of estimated segments was compared to the total body mass measured by a medical scale for each subject. The error in total body mass estimation was 1.7% (SD = 2.9%). The photogrammetric method overestimated the mass 75% of the time. Appendix G shows the individual body mass errors and potential factors for the error such as subject placement, body posture, clothing, and diapers. The errors found in this study were similar to the errors reported by Jensen (1989) -0.82% (SD= 2.63%) and Yokoi et al. (1986) 1.65 % who studied children, as well as Finch (1985) 0.77% (SD = 0.29%) and Kudzia (2015) 0.45% (SD = 0.78) who studied adults.

A Bland Altman plot was used to evaluate the bias between mean differences of the estimated total body mass calculated using the photogrammetric and a weigh scale (Figure 25). The mean difference of 0.225kg indicates the photogrammetric method has a bias of overestimating the total body mass. The photogrammetric method measures total body mass with a difference within -0.34kg and 0.79kg with 95% confidence.  There is no evidence of proportional bias as the change in average mass does not show a trend in the difference between methods.

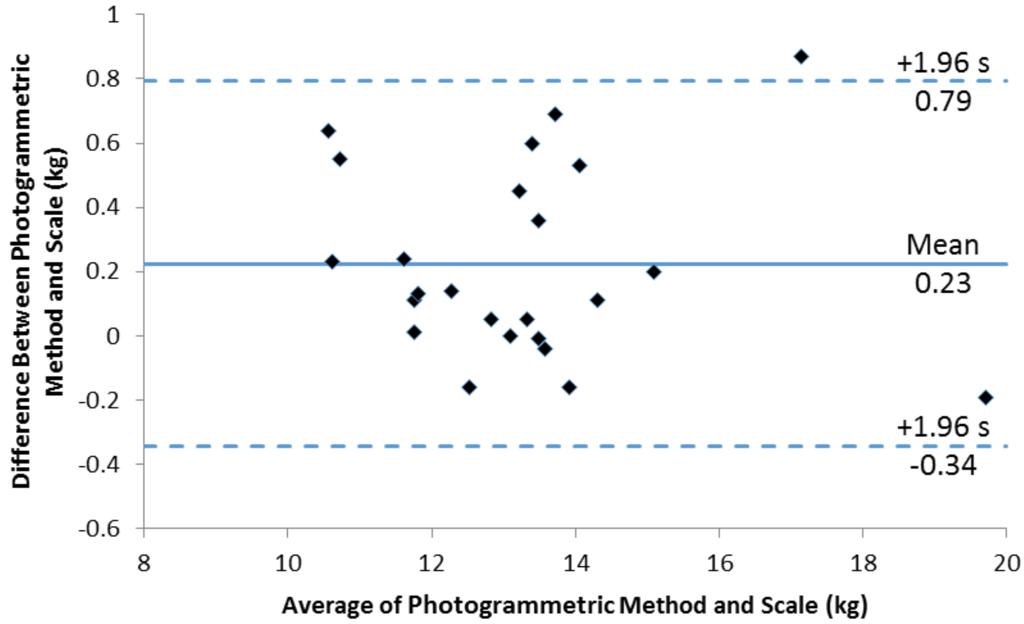


**Figure 25: Bland Altman plot comparing the difference between the Photogrammetric Method and a weigh scale in measuring total body mass. Limits of agreement (doted line) from -1.96s to +1.96s are shown.**

One factor for discrepancy in total body mass is the use of adult cadaver density values when calculating segment mass. The difference between these densities is unknown as there is no available segment density data for toddlers. Bone densities and tissue distribution in toddlers are likely different than adults but specific density differences for segments are unknown.

The volume of the pelvis was affected by subjects wearing a diaper. Although most of the diaper volume was able to be identified as separate from the subject, the outline of the subject's pelvis was not clearly defined. Five subjects were collected without a diaper but no comparison between subjects with and without diapers was made as the size of the diaper was influenced by the age of the subject but did vary based on the parent's preference.

Five subjects had difficulty standing still and the best image set included some motion. For most cases, the arms were moving which causes errors in the arms volume estimation. Another factor in trunk volume estimation is the placement of the arm. For some subjects, the arm was in a position which hid the outline of the subject's back. This can be seen in Figure 26.

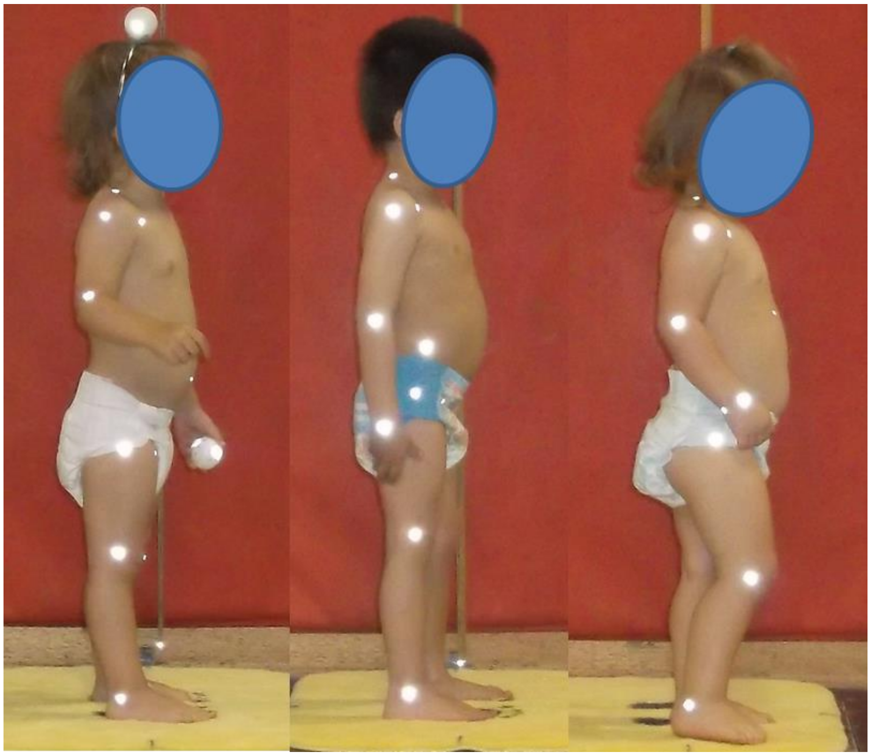

**Figure 26: Three subjects with their arms placed in a way that covers the outline of the back**

Most subjects that had error above 2% had a combination of affecting factors such as poor subject placement and body posture, wearing clothing, or had movement in the arm or head. Variation in diapers (cloth vs. disposable) also caused difficulties in consistently contouring the pelvis.

## 5.3 Segment Mass

The neck, hand and foot had the highest variability in mass. As these segments have the smallest mass, small changes in mass result in large variations in the estimated mass. The foot is the segment most affected by subject's position which is discussed in Section 5.6.2. The hand is highly influenced by its posture. Separation between fingers or the subject holding an item causes errors in the mass estimation. Having the subject hold a small item was used to occupy the subject so he or she would stand in the reference plane long enough for a photo even though it was a known cause of error (Figure 27). The neck segmentation had variation based on the head's position. Although these segments had the highest variability and causes of error, they have minimal impact to the total body mass as the segments are substantially smaller than the head, trunk, arms and legs.

**Figure 27: Hand positioning of the subject causing error in BSIP measurements.**

Trends in segment mass proportion with age and BMI were determined and linear regression equations were calculated (Table 5 and Table 6). The trunk's mass proportion had a weak trend of increasing with BMI and age trends are discussed in Section 5.3.2. The linear regression equations calculated for age and BMI had low $R^2$ values which is expected when analyzing a high variability measurement such as human anthropometrics. The $R^2$ values for Jensen's polynomial regression equations for age (Jensen 1989) ranged from 0.14 for the trunk to 0.76 for the head.

### 5.3.1 Sex Differences

When comparing the mass distribution in the segments across sexes, the thigh was the only segment whose mass reached significance (Table 4). Yokoi et al.(1986) stated that sex differences are minor until adolescence when the secondary sex characteristics develop. Snyder et al. (1977) also found that segment proportions have minimal sex differences until age fourteen (n=4127). This large sample size indicates that for subjects under 14, there is likely no significant differences between segments due to sex. In this study, the significant result for the thigh was likely due to segmentation differences. The diaper often interfered with the hip segmentation which may have resulted in some thigh mass being incorrectly included in the trunk segment. The significant difference in thigh mass could be due to the segmentation difficulty as the trunk was different between sexes although not significantly. The average thigh mass was greater in males while the average trunk mass was greater in females.

Differences between sexes in the head's mass proportion were approaching significance with males having proportionally larger heads. This could be indicative of a true trend as the head circumference of infant boys has been reported to be larger than girls (Centers for Disease Control and Prevention 2001). The Centre for Disease Control and Prevention (CDC) reports head circumference for a 50$^{th}$ percentile 3 year old boy to be 49.7cm and 3 year old girl to be 48.7cm. This circumference difference was consistent from birth to age of 3 when the measurements were stopped. Although the head was not found to be significantly larger with boys, the trend was noted.

### 5.3.2 Age Trends

The head, arm and thigh indicated trends of changing based on age (Table 5). The other segments either had no change based on age or too much variability to determine if there was a trend. As the child ages, the mass proportion of the head decreases and the mass proportion of the thigh increases (Figure 23). This trend is well documented in studies evaluating child BSIPs (Huelke 1998; Jensen 1986a; Jensen 1989; Yokoi et al. 1986). Figure 28 shows the change in mass proportions of the head and thigh for ages 1.5-9 using data from this study and Yokoi et al.

(1986). When directly compared to the changes in mass proportions by Yokoi et al., the data from this study is in agreement with previous study.

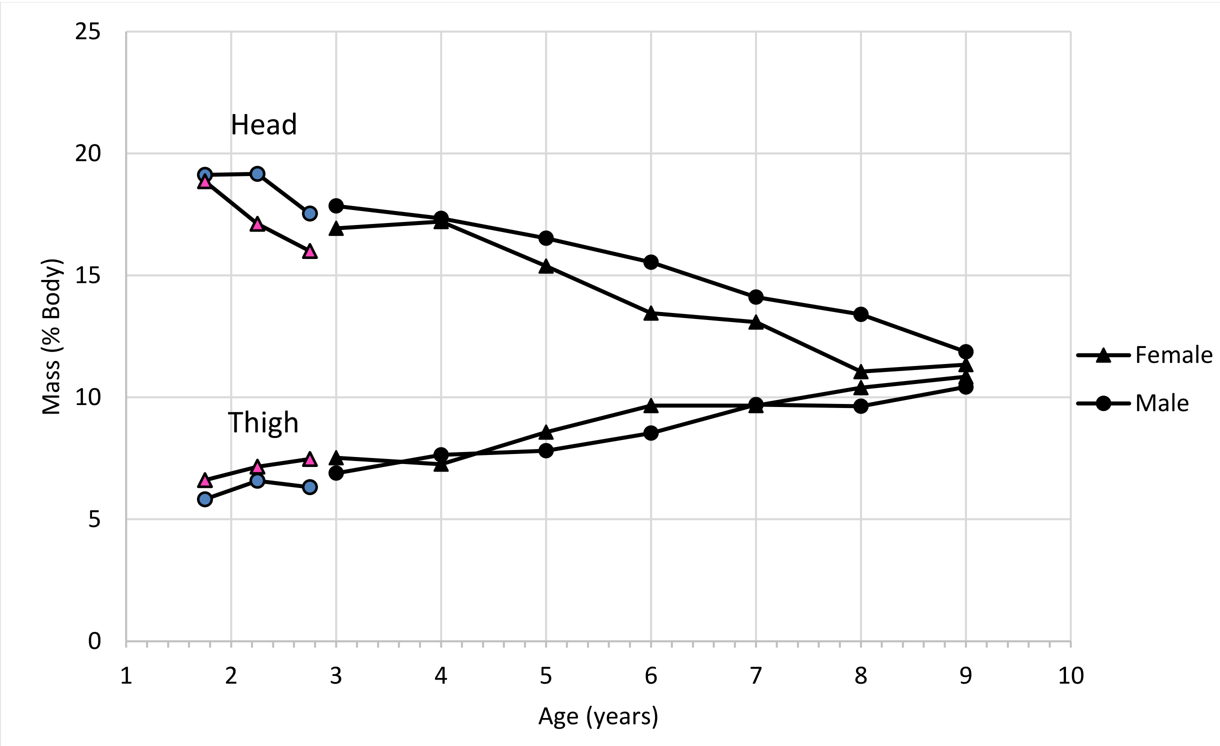


**Figure 28: Changes in mass proportions of the head and thigh in males and females with aging. Coloured data on the left is from the current study (n=4 for each data point). Black data on the right is from Yokoi et al. (1986) (female n =74, male n =81).**

Jensen developed age based regression equations for determining the mass proportion of segments. The average age from this study, 2.27 years, was inputted in both Jensen's linear (1986a) and polynomial (1989) equations. These regression equations were developed using male child and adolescent populations .The average segment mass proportion from all subjects (n=24) is compared to the values calculated by the regression equations and the average of the normal body mass group of 3-5 year olds measured by Yokoi et al. (1986). This comparison can be seen in Figure 29.

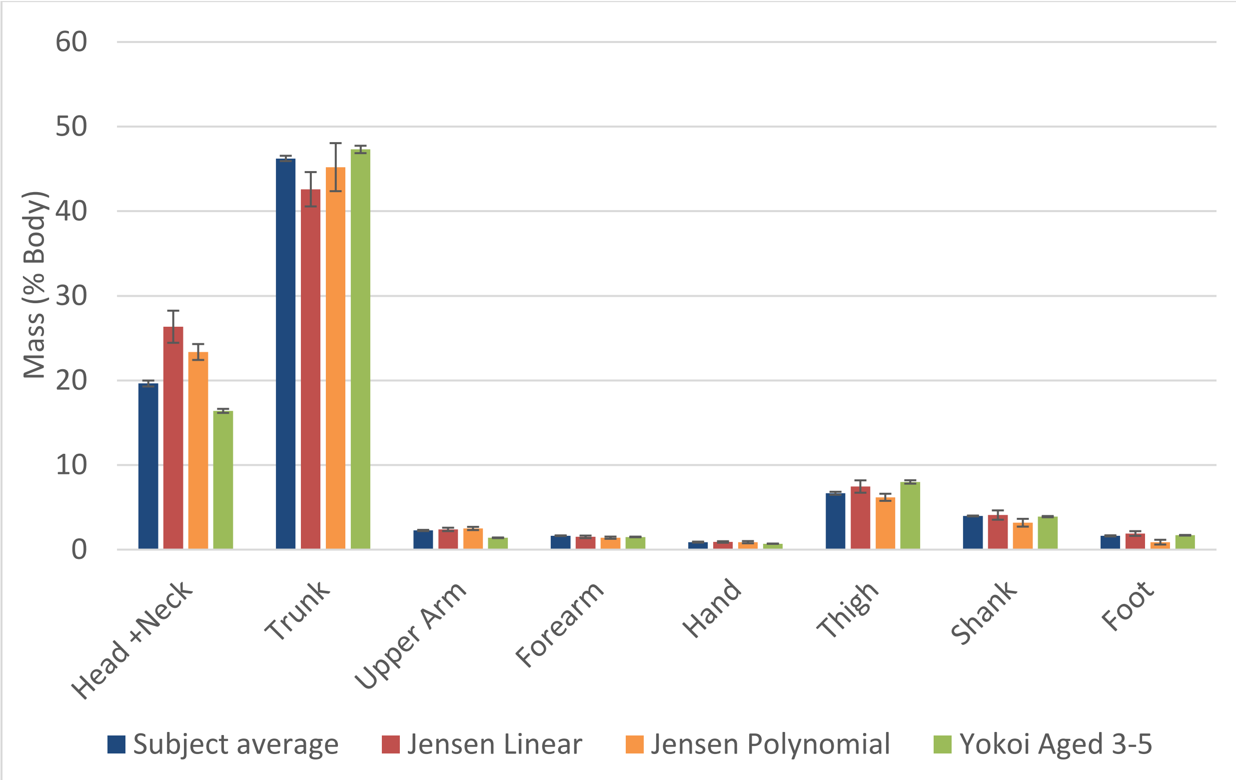


**Figure 29: Mass proportions of the segments from this study compared to those calculated using Jensen's linear (1986a) and polynomial (1989) regression equations and those found by Yokoi et al. (1986) for ages 3-5 (n=30). Error bars are standard error.**

The average segment mass proportions matched Jensen's regression equations and Yokoi et al.'s 3-5 year old averages. The head and neck was the only segment which had a noticeable difference from the calculated values using Jensen's equations. However, the head's mass proportion was similar to those found by Yokoi et al. This could mean that Jensen's regression equations are not accurate for the mass proportions of the head for those less than 4 years old.

### 5.4 Centre of Mass

The centre of mass (COM) is expressed below in two different ways, non-projected COM (NP-COM) and projected COM (P-COM). The NP-COM uses the point where the COM is located while the P-COM is where on the line between proximal and distal joint centres, the centre of mass is projected.

The comparison between the NP-COM and P-COM (Table 7) showed significant differences between the segments with the exception of the forearm. This is due to an even distribution of mass along the long axis of the segment. Although there were significant differences between NP-COM and P-COM, the differences were very small for most segments (<1% of segment length). Two segments were greatly affected by orthogonally projecting the COM location, the pelvis and foot. The COM location of the pelvis depends on the size of the subject's buttocks. As the rear size increases, the farther the COM location moves from the line between joint centres. Any extra diaper mass would influence the COM location. The foot's COM is affected by the shape of the foot. The proximal joint centre is at the ankle and the distal joint centre is the tip of the longest toe. This results in very little mass on the top of the segment's line. The uneven distribution of the mass creates greater difference between NP-COM and P-COM.

The hand had variability in posture as some segments were in fists, some with fingers separated and a few with the hand close to the ideal position (Figure 27). As there were not enough in any group to allow a true comparison, they are grouped together in the results. Therefore, for the hand there is considerable error in COM location.

The NP-COMs and P-COMs were compared to those calculated using Jensen's regression equations (1986, 1989) and those found by Yokoi et al. (1986) (Figure 30). The foot and upper arm had the greatest differences between this study and the literature. Previous studies have had the subjects stand on an angled platform which redistributes the mass along the line of the foot. As toddlers are not stable enough to stand on the angled platform, there will be inherent differences in foot COM location. The foot was also the most problematic in segmentation when the subject stood off the plane which affected the BSIP calculations. The COM location of the foot is likely inaccurate due to this as it is also substantially different from Jensen's equations and Yokoi et al.'s data. The COM location of the arm from this study is more proximal than Yokoi et al.'s but more distal than in Jensen's equations. This could mean that Jensen's equations cannot accurately predict ages below 4. Another potential difference between this study and the literature could be due to segmentation differences and joint centre identifications. Although efforts were made to use consistent segmentation protocols, segmentation at the shoulder was difficult to keep uniform.

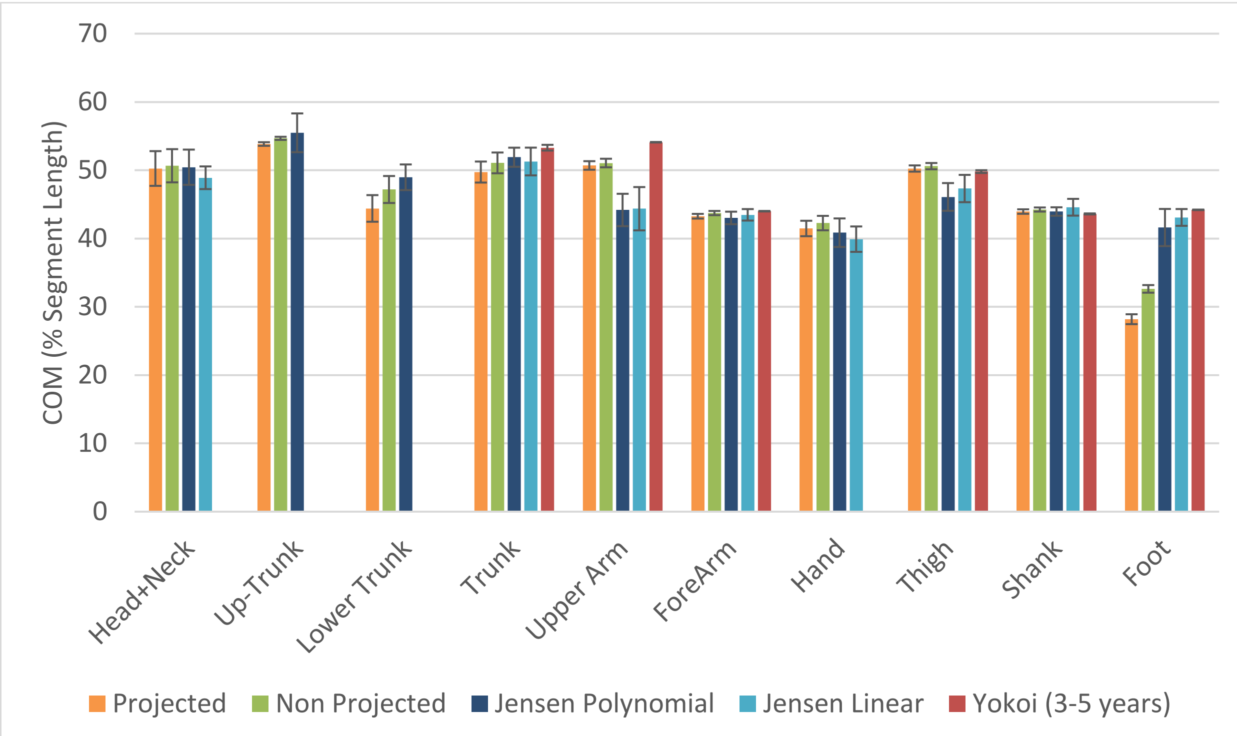


**Figure 30: Average projected COM locations and non-projected COM locations from proximal end for this study compared to the calculated COM locations using Jensen's polynomial (1989) and linear (1986a) regression equations and those measured by Yokoi et al. (1986) for ages 3-5. Error bars are standard error. Missing data is due to different segmentation in the literature.**

### 5.4.1 Age Trends

The age trends in COM location for the head, thigh and shank were compared to those found by Yokoi et al.(1986) in Figure 31. The data from this study shows variability with no direct trends but when used in conjunction with Yokoi et al.'s data, general trends can be established. As the child ages, the head's COM location moves distally. Huelke (1998) shows how the skull shape changes with the mass of the head moving distally (Figure 9).

As the subject moves from crawling to walking, more muscle mass is developed in the legs. This moves the mass proximally as the child ages. The COM of the thigh from this study follows the same trend as Yokoi et al.'s data. The COM of the shank also follows the trend in Yokoi et al.'s data but with more variability. With both the thigh and shank, muscle mass is being developed, moving the COM proximally.

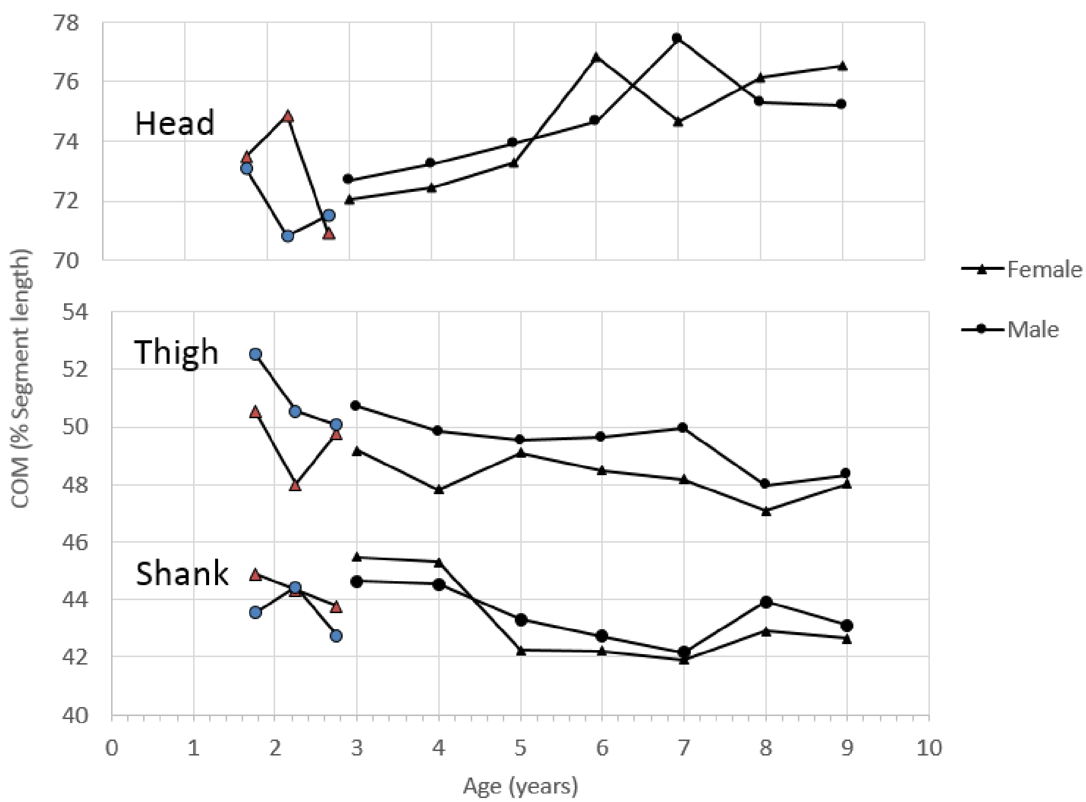


**Figure 31: Changes in COM location from the proximal end of the head, thigh and shank in males and females with aging. Coloured data on the left is from the current study (n=4 for each data point). Black data on the right is from Yokoi et al. (1986) (female n =74, male n =81).**

## 5.5 Radius of Gyration

The radii of gyration (ROGs) of all subjects in 3-axes are shown in Table 9. A few subjects were excluded due to postural errors. The most commonly affected segments were the hand and forearm. This was usually due to a bent elbow causing the axis of the segments to change in the global reference. As the amount of change indeterminate, the values were excluded. Some cases with minimal posture differences were included and all sexes and ages were pooled to minimize error due to posture.

The average ROGs about the transverse axis from this study were compared to those calculated using Jensen's polynomial regression equations (1989) using the average subject age and Yokoi et al.(1986) averages for children ages 3-5 years (Figure 32).

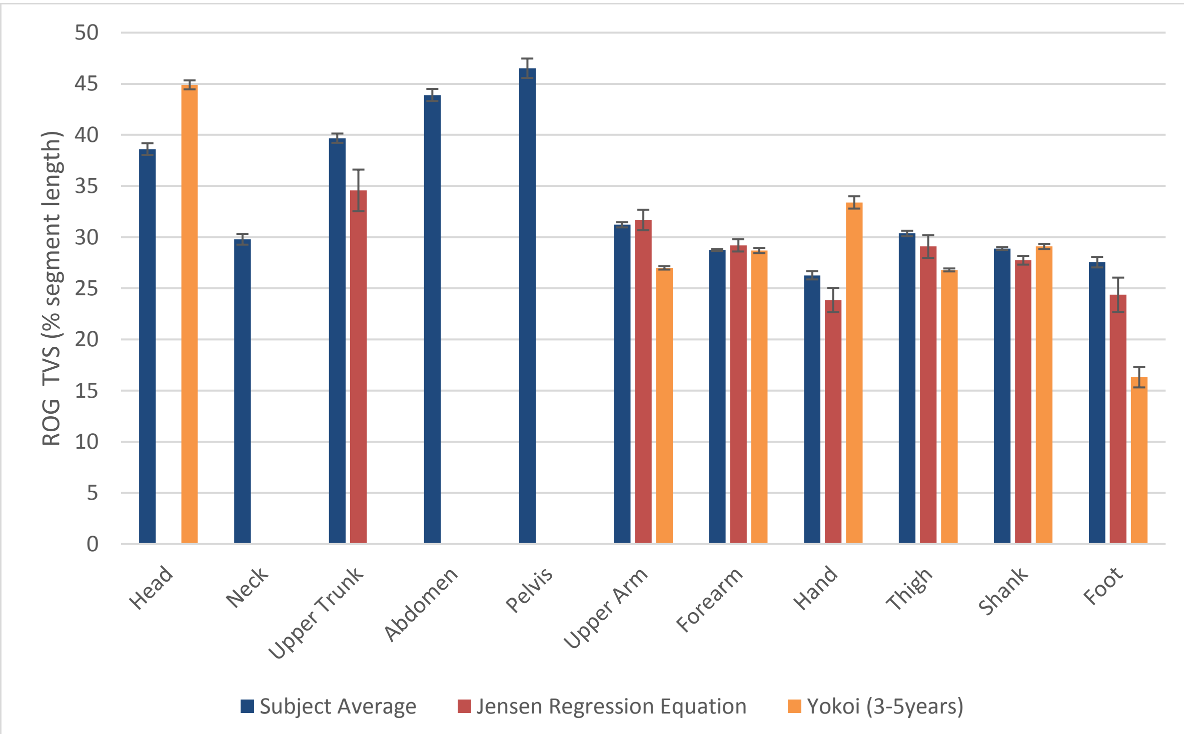


**Figure 32: Average ROG values with respect to COM in the transverse axis from this study compared to the calculated ROG using Jensen's polynomial (1989) regression equations and those measured by Yokoi et al. (1986) for ages 3-5. Error bars are standard error.**

For most segments, the ROGs about the transverse axis in this study were similar to those calculated using Jensen's regression equations (1989) and the data by Yokoi et al.(1986). The transverse ROGs of the hand and foot are likely different due to posture differences. As mentioned before, the hand was in a range of positions (Figure 27) and the lowest priority segment for getting in the correct position. These different postures create an unreliable ROG value. There are also notable differences between the value calculated using Jensen's equation and Yokoi et al.'s data. This shows that the hand has high variability and is sensitive to postural differences. The foot is affected by the same factor. Whether the subject is standing on an inclined platform or not, the segment's ROG axes will be affected.

## 5.6 Limitations

The photogrammetric method was chosen due to the simplicity of its collection process. With many 3D scanning set-ups, the subject must stand motionless for the collection which would not have been possible for the subjects under 2.5 years. Some of the participants between 2.5-3 years were able to understand and follow the protocol. As discussed, medical imaging was not feasible due to radiation exposure, cost, and again, the ability for the participant to understand and follow the protocol. Although the photogrammetric method has a simple collection process, it was still challenging to use this method with toddlers. The errors and challenges of using the photogrammetric with toddlers is discussed below.

### 5.6.1 Methodological Errors

The main disadvantage with photogrammetric elliptical method of measuring BSIPs is the uncertainty of segment densities. The density values used in this study are from adult cadavers as child segment densities are unknown. This assumes constant density and universal tissue development rates. Toddlers should be expected to have different density values than adults as well as the different volume changes measured in this study.

Errors are also caused by modeling the segments using elliptical slices. This assumption causes errors in segments such as the hands and feet which do not closely resemble an ellipse. This error is minimized by having thinner slices. This protocol used 3mm slices compared to the 2cm slices used by Jensen (1978) as computer processing has improved. However, even with the thinner slices, elliptical cylinders can still only provide an approximation of the segment shape. The trunk is usually underestimated as the shoulder and hip segmentation causes gaps when modeled by an ellipse (Wicke et al. 2009).

### 5.6.2 Subject Placement Errors

The majority of subjects stood in the correct position. Four subjects stood slightly off centre (Figure 33A) and five subjects stood noticeably off centre (Figure 33B).

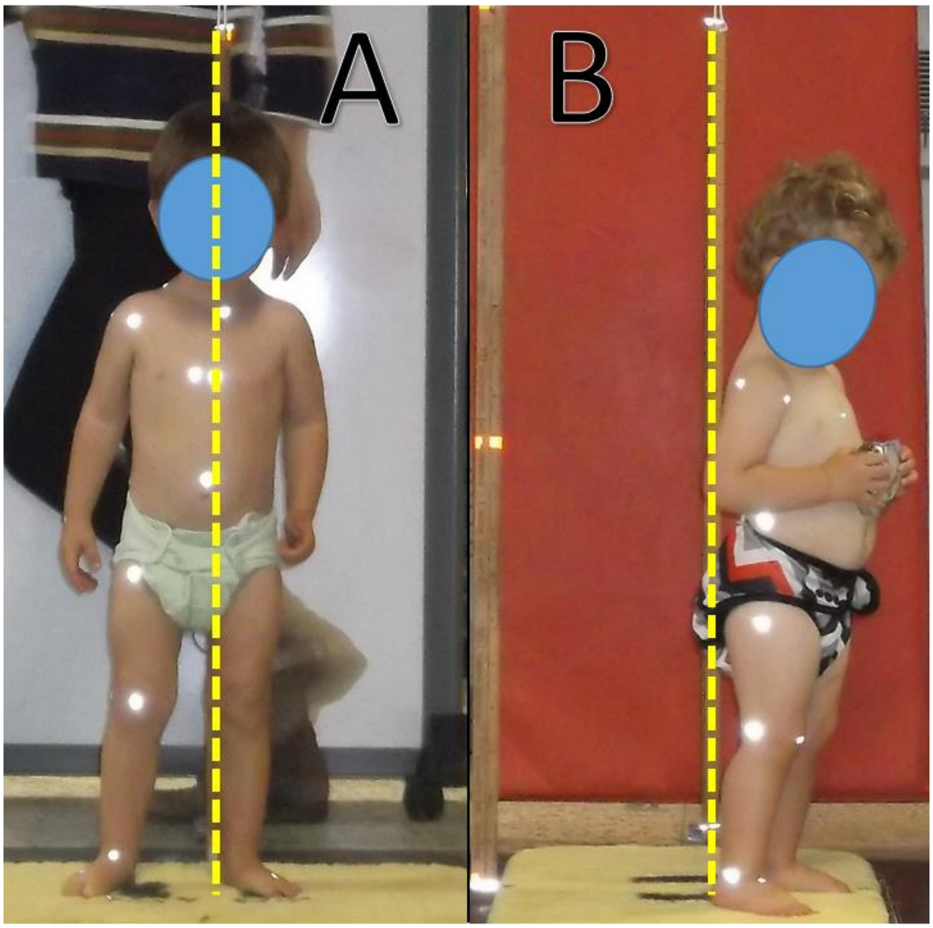


**Figure 33: A: Subject standing slightly off centre towards side camera. B: Subject standing noticeably off centre with the majority of the body in front of the reference metre.**

To determine the range of error caused by the subject's position, a toddler sized doll was used to replicate the subject's positions. The doll's leg volume was compared at 9 different positions (Figure 34). As expected, the volume of the leg was overestimated as it was moved towards the camera and underestimated as it was moved away. The doll's leg experienced more error when moved relative to the front camera than the side camera (Figure 35).

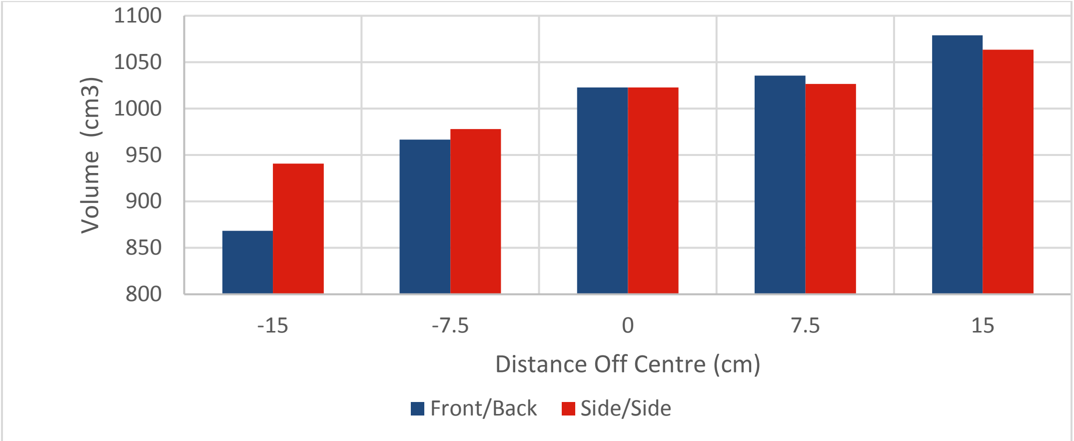


**Figure 34: Subject placement comparison of the measured volume of the doll's leg using the photogrammetric method. The doll was moved either towards (+) or away from (-) the front or side camera.**

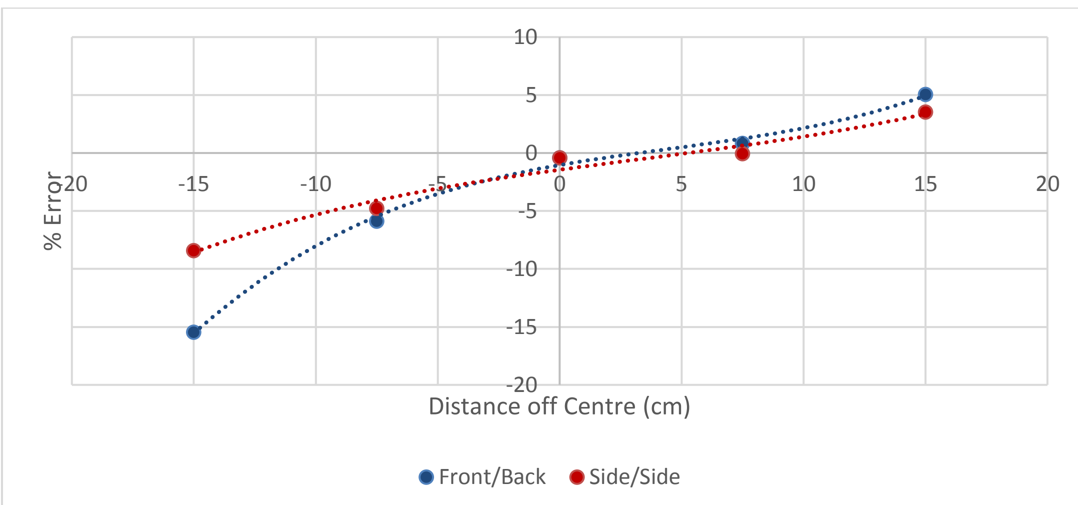


**Figure 35: Percent error in leg volume relative to the doll's placement off the camera and reference scaling plane. The error in leg volume is compared to the 3D scan volume of the doll's removable leg. Positive values are moving towards the camera and negative values are moving away from the camera.**

The errors in volume were greater when the subject stood farther from the camera than closer. This is because gaps were created between segments increasing the error in volume. The front and side images are matched using the apex marker and the scaling of each photo. As the distance in the image from the apex increases, the discrepancy between the two photos increases. When the improperly scaled photo is with the subject standing closer to the camera, the segment outlines are used from the smaller and correctly scaled photo. When the subject stands farther from the camera, the segment outlines are taken from the smaller, incorrectly scaled image resulting in higher error. The gap between segments is most noticeable in the ankle and the bottom of the foot being omitted as the foot is the farther segment from the apex. An example of an ankle gap and missing foot can be seen in Figure 36 when the doll was placed 15cm behind the scaling plane. A comparison of the digitized leg volume 15cm behind and in front of the camera plane can be seen in Figure 37. The ankle and the majority of the foot are missing from the segmented leg at 15cm back. The ankle can be seen to be segmented lower at 15cm forward but with no ankle gap and minimal loss of toe volume.

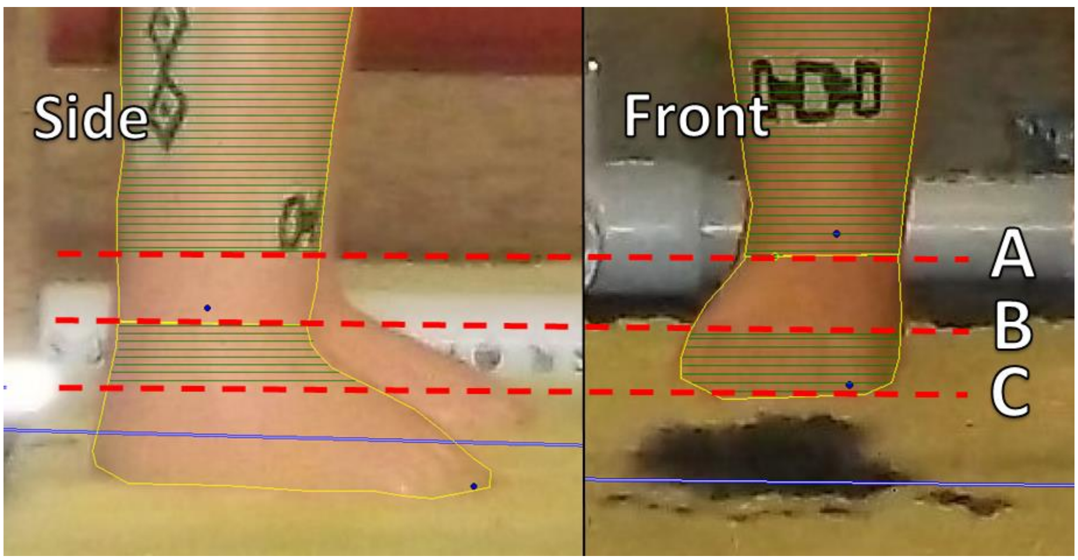


**Figure 36: Ankle gap and missing foot occurs when the subject stands off the reference plane. Line A indicates the front image's ankle, Line B indicates the side image's ankle and line C is the bottom of the front image's foot. The area between A and B is lost mass at the ankle and the area below C is missing mass from the foot.**

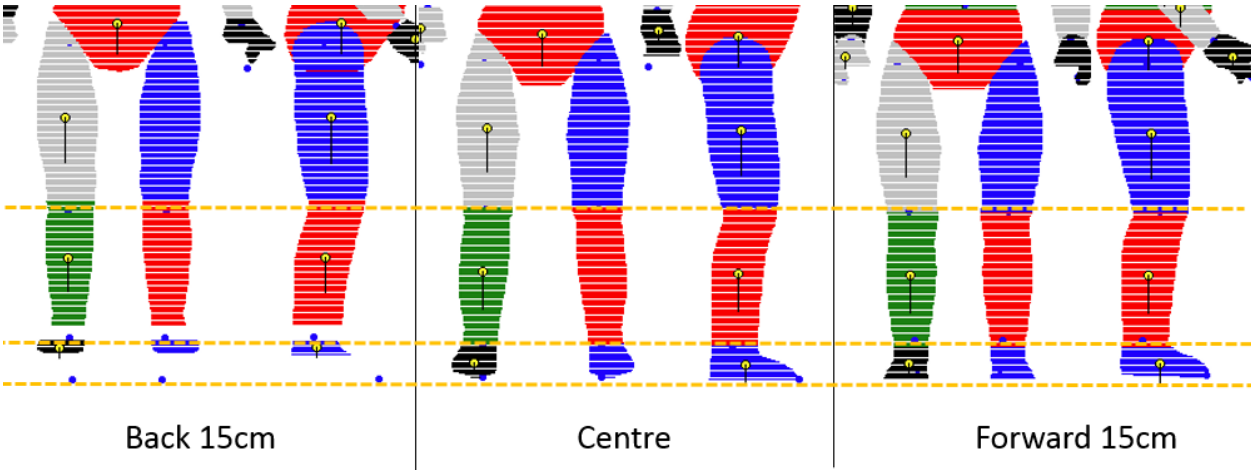


**Figure 37: Digitized images of the doll's leg placed at different distances from the front camera. A gap at the ankle and loss of foot volume is apparent when the subject is farther from the camera. This ankle gap and foot discrepancy is not present when the subject is standing closer to the camera**

The subject placement tests with the doll show that the estimated mass is affected by location of the subject. Nine of the subjects stood off centre and the comparison between the measured mass and estimated mass is shown in Table 11. The errors in mass tend to follow the same trends discussed above with more variation. This is because other factors such as body posture (arm placement, trunk rotation, etc.), diapers and clothing also affected the estimated mass. The three subjects with the highest total body mass error were not affected by the subject placement. For this reason, the estimated mass of each segment cannot be scaled in a consistent manner to try to adjust for the subject's standing location.

**Table 11: The approximate distances each subject stood off centre with the difference in the estimated mass calculation and the directly measured total mass.**

| | Measured Mass (kg) | Estimated Mass (kg) | % Difference | Direction Off Centre | Approximate Distance Off Centre (cm) |
|---|---|---|---|---|---|
| B04 | 12.60 | 12.44 | -1.28 | Side | -5 |
| G02 | 14.00 | 13.84 | -1.17 | Front | -2.5 |
| G11 | 13.50 | 13.49 | -0.10 | Front | -5 |
| B01 | 11.75 | 11.76 | 0.07 | Side | 2.5 |
| B05 | 12.80 | 12.85 | 0.41 | Front | 5 |
| B09 | 11.70 | 11.81 | 0.90 | Front | -2.5 |
| B06 | 12.20 | 12.34 | 1.19 | Side | 2.5 |
| B03 | 10.50 | 10.73 | 2.23 | Front | 5 |
| G06 | 13.10 | 13.70 | 4.57 | Side | 7.5 |

### 5.6.3 Challenges of Working with Toddlers

As discussed in the subject placement section, some subjects shifted during the data collection and were no longer centred. This caused the body to be closer or farther from the camera than the photo's scaling references. The footprints on the ground were helpful for the older subjects to get positioned but many subjects wandered on the mat. For many subjects, there was a compromise between the subject's position on the mat and the anatomical position the subject was standing in. Palpation and marker placement were also challenging with toddlers. For most subjects, placing markers first on the parent resulted in a more cooperative child and allowed the reflective markers to be placed on the skin. However, palpation to identify bony landmarks made most children uncomfortable and "best guesses" had to be made. Another challenge with markers was the quick removal of markers as the child wanted to stick them on different parts of their body or their parent's. Additional reflective stickers were given to the children to preoccupy them as well as ordinary picture stickers that the child could enjoy.

Many subjects had problems with their hands. The younger subjects (<2) had trouble keeping their hands in the anatomical position and moved their arms continuously. This resulted in some images having the elbows bent and the hands closer to the front camera. This caused segmentation difficulties as well as misalignment of the segment's axes.

During photo processing, the body segments are sliced in the vertical axis of the image. The slices are 3mm thick elliptical cylinders trying to best capture the segment's volume. The foot has little vertical length and therefore few slices. Jensen (1986; 1989) and other studies deal with this by having the subjects stand on an angled surface. This keeps the foot more vertical allowing for more slices along the foot. Many of the toddlers in this study struggled to stand in place on the subject placement mat with indicated footprints. These subjects would not have been able to stand upright while standing on an angled platform.

Despite all the difficulties with working with toddlers, it was also very enjoyable. From "designing superhero costumes" to having two friends compete to have better poses in the picture, it was always entertaining during data collection. The parents were certainly very helpful and they were truly appreciated. They were able to work with their children to make them as cooperative a possible.

# Chapter 6

# Conclusion

## 6.1 Summary of Results

The objective of the study was to measure the BSIPs of toddlers between the ages 1.5-3 years. To collect this data, the photogrammetric, elliptical method (Jensen 1978) was adjusted to be applicable to toddlers. The angled platform was replaced by a flat mat with footprints and the camera placement was adjusted to 4m as it provided a clear image and was a comfortable distance from the subject. Subjects were asked to wear minimal or tight clothing with the exception of the diaper. After experiencing complications with the subjects standing in the proper position, an additional objective was formed to measure the subject placement error. Nine different positions were compared where the subject stood centre, 7.5 and 15cm closer and farther from both the side and front cameras. 12 male and 12 female toddlers were recruited from the Kingston community. The results for estimated total body mass using the photogrammetric method were compared to the measured mass of each subject using a scale. The average error in total body mass was 1.7% (SD = 2.9%). This overestimation could be due to segment density differences between adult cadavers and toddlers. As density values of toddler segments are unavailable, this error is unavoidable.

Segment masses followed the trends established in the literature (Jensen 1986a; Jensen 1989; Yokoi et al. 1986). The mass proportion of the head decreases with age while the mass proportion of the thigh increases.

The COM location of segments also followed the trends discussed in the literature. As the child ages, the head's COM moves distally as the head shape changes. The COMs of the thigh and shank move proximally as more muscle is developed.

The ROG had more variability because the segment axes depended on the subject's position relative to the global axis. To minimize positional errors, all subjects were grouped together in the analysis. For this reason, age trends could not be found within the subjects of this study but when compared to the literature, similar values were found for the arm, forearm, thigh and shank. The hand and foot had measurement difficulties due to the subjects having problems with the protocol. The ROG for the head, neck and trunk could not be compared to the literature due to differing segmentation protocols.

When measuring the error due to the subject placement, higher volume measurement error was found when the subject stood farther from the camera in comparison to closer to the camera. When the subject stood 15cm back from centre and 15cm in front of centre relative to the front camera, the leg volume had an error of 15.5% and 5.0% respectively. This was due to a gap being formed at the ankle and part of the foot not accounted for when the subject stood behind the scaling reference.

Although there were challenges with working with toddlers, BSIPs of 24 toddlers were determined. The study of adult male BSIPs has been well documented in the literature but most other populations have limited or negligible data. The data in this study fills the void of BSIPs for a population that had previously been looked over. The data from this study followed the trends found in the literature from child populations. The agreement in BSIP trends with the literature reinforces the validity of the data.

## 6.2 Future Work

The two main points for future work are to increase the population size and reduce the errors encountered with this method. Like most studies, a larger sample size would strengthen the results found in the study and allow for more comparisons. A larger population size would increase the ability to establish age trends for COM and ROG and would better determine significant differences between sexes. As ROG was highly variable, a larger sample size would allow for more groups and differences for age and sex to be evaluated.

One error which was unavoidable in this study was that the segment density values were from adult cadavers. As this is not representative of the population, the segment masses were affected. To improve the BSIPs collected using volume measurement methods, more accurate segment density values are needed. Medically prescribed imaging could be used to collect toddler segment densities similar to the study done by Sandoz et al. (Sandoz et al. 2010) with children aged 9-13. Other than imaging with medical prescriptions, developments in density collection protocol must be made to ethically collect accurate toddler segment densities.

Another error encountered in this study was the subjects' difficulty in standing in the correct position. A volume collection system that does not require a scaling reference and can be collected instantaneously would be able to eliminate the subject placement error.

Future applications of toddler BSIPs range from the design of dynamic crash test dummies to kinetic gait studies of toddlers. For example, The Spine Biomechanics Lab at Queen's University is currently developing a toddler automaton to be used in daycare studies. The BSIPs determined in this study were used to create a realistic robotic toddler. These data can also be applied in simulations for clinical applications such as toddler concussion testing. For these applications and more, the BSIPs determined in this study provide data which help bridge the gap in current BSIP literature.

# References


Ackland, T.R., Blanksby, B.A. & Bloomfield, J., 1988. Inertial characteristics of adolescent male body segments. *Journal of Biomechanics*, 21(4), pp.319–327.

Ackland, T.R., Henson, P.W. & Bailey, D.A., 1988. The Uniform Density Assumption: Its Effect Upon the Estimation of Body Segment Inertial Parameters. *International Journal of Sport Biomechanics*, 4, pp.146–155.

Barter, J.T., 1957. Estimation of the mass of body segments. *Wright Air Development Center, Air Research and Development Command, United States Air Force, Wright-Patterson Air Force Base, Ohio*.

Bauer, J.J. et al., 2007. MRI-derived body segment parameters of children differ from age-based estimates derived using photogrammetry. *Journal of Biomechanics*, 40, pp.2904–2910.

Bouisset, S. & Pertuzon, E., 1969. Experimental determination of the moment of inertia of limb segments. In *Biomechanics. Karger Publishers*. pp. 106–109.

Centers for Disease Control and Prevention, 2001. Data Table of Infant Head Circumference-for-age Charts. , p.www.cdc.gov/growthcharts.

Chandler, R.F., 1975. Investigation of Inertial Properties of the Human Body. *Aerospace Medical Research Laboratory*, AMRL-TR-74.

Clauser, C.E., McConville, J.T. & Young, J.W., 1969. Weight, Volume, and Center of Mass of Segments of the Human Body. *National Technical Information Service*.

Contini, Renato, R., Drillis, J. & Bluestein, M., 1963. Determination of Body Segment Parameters. *Human Factors*, 5(5), pp.493–504.

Dempster, W.T., 1955. Space requirements of the seated operator: Geometrical, kinematic, and mechanical aspects of the body with special reference to the limbs.

Drillis, R., Contini, R. & Bluestein, M., 1963. Body Segment Parameters; A Survey of Measurement Techniques. *Artificial Limbs*, 8, pp.44–66.

Durkin, J.L., Dowling, J.J. & Andrews, D.M., 2002. The measurement of body segment inertial parameters using dual energy X-ray absorptiometry. *Journal of Biomechanics*, 35, pp.1575–1580.

Finch, C.A., 1985. Estimation of body segment parameters of college age females using a mathematical model. *University of Windsor Thesis*.

Goubel, F. & Pertuzon, E., 1973. Évaluation De L Élasticité Du Muscle in Situ Par Une Méthode De Quick-Release. *Achives Internationales de Physiologie et de Biochimie*, 81(4), pp.697–707.

Hanavan, E.P., 1964. A Mathematical Model of the Human Body. *Air Force Aerospace Medical Research Lab Wright-Patterson AFB OH*, (AFIT-GA-PHYS-64-3).

Hatze, H., 1980. A Mathematical Model for the Computational Determination of Parameter Values of Anthropomorphic Segments. *Journal of Biomechanics*, 13, pp.833–843.

Ho, W. et al., 2013. Body Segment Parameters of Young Chinese Men Determined with Magnetic Resonance Imaging. *Medicine and Science in Sports and Exercise*, 45(9), pp.1759–1766.

Huelke, D.F., 1998. An overview of anatomical considerations of infants and children in the adult world of automobile safety design. *Annual Proceedings/Association for the Advancement of Automotive Medicine*, 42, pp.93–113.

Humanetics Innovative Solutions Inc, 2017. *Hybrid-III 50th Male Dummy*, Available at: http://www.humaneticsatd.com/crash-test-dummies/frontal-impact/hiii-50m.

Jensen, R.K., 1986a. Body segment mass, radius and radius of gyration proportions of children. *Journal of Biomechanics*, 19(5), pp.359–368.

Jensen, R.K., 1989. Changes in segment inertia proportions between 4 and 20 years. *Journal of Biomechanics*, 22(617), pp.529–536.
Jensen, R.K., 1978. Estimation of the biomechanical properties of three body types using a photogrammetric method. *Journal of Biomechanics*, 11(8–9), pp.349–358.
Jensen, R.K., 1986b. The growth of children’s moment of inertia. *Medicine and Science in Sports and Exercise*, 18(4), pp.440–445.
Kudzia, P., 2015. Estimating Body Segment Inertial Parameters of the Human Body Using a Microsoft Kinect. *Queen’s University Thesis*.
Lephart, B.S.A., Bolte, J.H. & Albery, C.B., 2014. The Effect of Variable and Uniform Densities on the Inertial Properties of Cadaver Segments , a Comparison of Frozen and Thawed Densities , and Segment Densities Related to Endomorphy and Ectomorphy. *Journal of Sports*, 1(2), pp.119–135.
De Leva, P., 1996. Adjustments to Zatsiorsky-Seluyanov’s segment inertia parameters. *Journal of Biomechanics*, 29(9), pp.1223–1230.
McIllwain, J. et al., 2002. SlicerProject.
Mungiole, M. & Martin, P.E., 1990. Estimating Segment Inertial Properties: Comparison of Magnetic Resonance Imaging with Existing Methods. *Journal of Biomechanics*, 23(10), pp.1039–1046.
Ono, Y. et al., 2002. Associations of length of employment and working conditions with neck, shoulder and arm pain among nursery school teachers. *Industrial health*, 40(2), pp.149–58.
Owen, B.D., 1994. Intervention for Musculoskeletal Disorders Among Child-Care Workers. *American Academy of Pediatrics*, 94(6), pp.1077–1079.
Pearsall, D.J., Reid, J.G. & Livingston, L.A., 1996. Segmental Inertial Parameters of the Human Trunk as Determined from Computed Tomography. *Annals of Biomedical Engineering*, 24, pp.198–210.
Rao, G. et al., 2006. Influence of body segments ’ parameters estimation models on inverse dynamics solutions during gait. *Journal of Biomechanics*, 39, pp.1531–1536.
Reid, J.G., 1984. Physical properties of the human trunk as determined by computed tomography. *Archives of physical medicine and rehabilitation*, 65(5), pp.246–250.
Reid, J.G. & Jensen, R.K., 1990. Human Body Segment Inertia Parameters: A Survey and Status Report. *Exercise & Sport Sciences Reviews*, 18(1), pp.225–242.
Rodrigue, D. & Gagnon, M., 1984. Validation of Weinbach’s and Hanavan’s Models for Computation of Physical Properties of the Forearm. *Research Quarterly for Exercise and Sport*, 55(3), pp.272–277.
Sandoz, B. et al., 2010. Subject-specific body segment parameters’ estimation using biplanar X-rays: a feasibility study. *Computer Methods in Biomechanics and Biomedical Engineering*, 13(6), pp.649–654.
Smrcka, J., 2017. Dummies: Past & Present. *Humanetics Innovative Solutions*. Available at: http://www.humaneticsatd.com/about-us/dummy-history.
Snyder, R.G., 1977. Anthropometry of Infants, Children, and Youths to Age 18 for Product Safety Design. *US Government Printing Office*.
Weinbach, A., 1938. Contour Maps, Center of Gravity, Moment of Inertia and Surface Area of the Human Body. *Human Biology*, 10(3), pp.356–371.
Whitsett, C.E., 1963. Some Dynamic Response Characteristics of Weightless Man. *Air Force Inst of Tech Wright-Patterson AFB OH School of Engineering*, GAE/MECH-6(7184).
Wicke, J., Dumas, G.A. & Costigan, P.A., 2009. A comparison between a new model and current models for estimating trunk segment inertial parameters. *Journal of Biomechanics*, 42(1), pp.55–60.
Yeadon, M.R. & Morlock, M., 1989. The appropriate use of regression equations for the estimation of segmental inertia parameters. *Journal of Biomechanics*, 22(6–7), pp.683–689.

Yokoi, T., Shibukawa, K. & Ae, M., 1986. Body segment parameters of Japanese children. *Japanese Journal of Physical Eduction*, 31(1), pp.53–66.
Zatsiorsky, V. & Seluyanov, V., 1985. Estimation of the mass and inertia characteristics of the human body by means of the best predictive regression equations. *Biomechanics IX-B*, pp.233–239.
Zhu, X.P. et al., 1986. Accuracy of area measurements made from MR images compared with computed tomography. *Journal of computer assisted tomography*, 10(1), pp.96–102.

# Appendix A

# Queen's University Ethics Approval

## A.1 GREB Ethics Approval

February 08, 2016

Miss Erika Jackson
Master's Student
Department of Mechanical and Materials Engineering
Queen's University
McLaughlin Hall
Kingston, ON, K7L 3N6

**GREB Ref #: GMECH-036-16; Romeo # 6017389**
**Title: "GMECH-036-16 Toddler Automaton"**

Dear Miss Jackson:

The General Research Ethics Board (GREB), by means of a delegated board review, has cleared your proposal entitled **"GMECH-036-16 Toddler Automaton"** for ethical compliance with the Tri-Council Guidelines (TCPS 2 (2014)) and Queen's ethics policies. In accordance with the Tri-Council Guidelines (Article 6.14) and Standard Operating Procedures (405.001), your project has been cleared for one year. At the end of each year, the GREB will ask if your project has been completed and if not, what changes have occurred or will occur in the next year.

You are reminded of your obligation to advise the GREB of any adverse event(s) that occur during this one year period (access this form by signing at http://www.queensu.ca/traq/signon.html/; click on "Events"; under "Create New Event" click on "General Research Ethics Board Adverse Event Form"). An adverse event includes, but is not limited to, a complaint, a change or unexpected event that alters the level of risk for the researcher or participants or situation that requires a substantial change in approach to a participant(s). You are also advised that all adverse events must be reported to the GREB within 48 hours.

You are also reminded that all changes that might affect human participants must be cleared by the GREB. For example you must report changes to the level of risk, applicant characteristics, and implementation of new procedures. To submit an amendment form, access the application by signing at http://www.queensu.ca/traq/signon.html; click on "Events"; under "Create New Event" click on "General Research Ethics Board Request for Amendment of Approved Studies". Once submitted, these changes will automatically be sent to the Ethics Coordinator, Ms. Gail Irving, at the Office of Research Services for further review and clearance by the GREB or GREB Chair.

On behalf of the General Research Ethics Board, I wish you continued success in your research.

Sincerely,

John G. Freeman

John Freeman, Ph.D.
Chair
General Research Ethics Board

c: Dr. Genevieve Dumas, Faculty Supervisor

## A.2 Ethics Amendments

June 29, 2016

Miss Erika Jackson
Master's Student
Department of Mechanical and Materials Engineering
Queen's University
McLaughlin Hall
Kingston, ON, K7L 3N6

Dear Miss Jackson:

RE: Amendment for your study entitled**: GMECH-036-16 Toddler Automaton;** ROMEO# **6017389**

Thank you for submitting your amendment requesting the following changes:

1) to increase the scope of recruitment from Queen's daycares to the Kingston community and sending e-mails across the Queen's departments;

2) Recruitment e-mail script (v. 2016/06/29).

By this letter you have ethics clearance for these changes.

Good luck with your research.

Sincerely,

John G. Freeman

John Freeman, Ph.D.
Chair
General Research Ethics Board

c.: Dr. Genevieve Dumas, Supervisor

February 03, 2017

Miss Erika Jackson
Master's Student
Department of Mechanical and Materials Engineering
Queen's University
McLaughlin Hall
Kingston, ON, K7L 3N6

Dear Miss Jackson:

RE: Amendment for your study entitled: **GMECH-036-16 Toddler Automaton;** TRAQ # **6017389**

Thank you for submitting your amendment requesting the following change:

1) To increase your sample size from 20 to 24.

By this letter, you have ethics approval for this change.

Good luck with your research.

Sincerely,

John Freeman, Ph.D.
Chair
General Research Ethics Board

c.: Dr. Genevieve Dumas, Supervisor

### A.3 Ethics Renewal

February 03, 2017

Miss Erika Jackson
Master's Student
Department of Mechanical and Materials Engineering
Queen's University
McLaughlin Hall
Kingston, ON, K7L 3N6

**GREB TRAQ #: 6017389**
**Title: "GMECH-036-16 Toddler Automaton"**

Dear Miss Jackson:

The General Research Ethics Board (GREB) has reviewed and cleared your request for renewal of ethics clearance for the above-named study. This renewal is valid for one year from February 8, 2017. Prior to the next renewal date you will be sent a reminder memo and the link to ROMEO to renew for another year. You are reminded of your obligation to submit an Annual Renewal/Closure Form prior to the annual renewal due date (access this form at http://www.queensu.ca/traq/signon.html/; click on "Events"; under "Create New Event" click on "General Research Ethics Board Annual Renewal/Closure Form for Cleared Studies"). Please note that when your research project is completed, you need to submit an Annual Renewal/Completed Form in Romeo/traq indicating that the project is 'completed' so that the file can be closed. This should be submitted at the time of completion; there is no need to wait until the annual renewal due date.

You are reminded of your obligation to advise the GREB of any adverse event(s) that occur during this one year period. An adverse event includes, but is not limited to, a complaint, a change or unexpected event that alters the level of risk for the researcher or participants or situation that requires a substantial change in approach to a participant(s). You are also advised that all adverse events must be reported to the GREB within 48 hours. To submit an adverse event report, access the application at http://www.queensu.ca/traq/signon.html/; click on "Events"; under "Create New Event" click on "General Research Ethics Board Adverse Event Form".

You are also reminded that all changes that might affect human participants must be cleared by the GREB. For example, you must report changes in study procedures or implementation of new aspects into the study procedures. Your request for protocol changes will be forwarded to the appropriate GREB reviewers and/or the GREB Chair. To submit an amendment form, access the application at http://www.queensu.ca/traq/signon.html; click on "Events"; under "Create New Event" click on "General Research Ethics Board Request for the Amendment of Approved Studies".

On behalf of the General Research Ethics Board, I wish you continued success in your research.

Yours sincerely,

John G. Freeman

John Freeman, Ph.D.
Chair, General Research Ethics Board

c.: Dr. Genevieve Dumas, Supervisor

### A.4 Letter of Information and Consent Form

**Letter of Information**
**TODDLER DATA COLLECTION**
**For Toddler Automaton**

This research is being conducted by Erika Jackson BScE under the supervision of Geneviève Dumas PhD, in the Department of Mechanical and Material Engineering.

**Background information:** You are being invited to participate in a research study directed by Erika Jackson and overseen by Dr. Geneviève Dumas as part of Miss Jackson's Master's thesis to measure the body segment parameters in toddlers aged 18 months – 3 years to develop a toddler automaton. We will read through this consent form with you in order to describe procedures in detail and answer any questions you might have. This study is funded by the Natural Sciences and Engineering Research Council of Canada (NSERC) and reviewed by the Queen's University General Research Ethics Board. This study has been granted clearance according to the recommended principles of Canadian ethics guidelines, and Queen's policies.

**Details of the study:**

**Purpose**: Due to morphological differences between toddlers, children and adults, and the lack of data on toddlers, body segment parameters need to be obtained for that population. The aim of this study is to measure the body segment parameters of 18mo-3yr old children using a photographic method. The data collected will be used to develop a database of toddler anthropometric measurements (measurements of the human body) and in designing a toddler automaton which will be used in studies measuring low back stress in daycare workers.

**Commitment:** Your participation in the current study will consist of a one-hour session in which information regarding the morphology of your child's body will be captured. Markers (reflective tape) will be placed on bony landmarks of your child to help the researcher identify these important features in the post processing stage of the experiment. Tight clothing has been requested as a means of reducing errors associated with measurement and marker placement. The researchers will take some specific measurements such as height and total body weight. Once the markers have been placed on your child, he/she will be asked to stand in a designated area of the room with his/her palms open facing forward. When ready, the researcher will do a quick count down and ask your child to stand still for about 3 seconds. Two photographs, snapped at the exact same time, will be taken of your child. One photograph will be from the front and one from the right side. Three to five sets of photos will be taken to ensure a clear pair of images. The photographs will later be used in a software that estimate 3D volumes and body properties.

**Risks:** The parent/guardian is asked to be present to make the child more comfortable.

**Benefits:** There are no direct benefits for the subject. The data collected will expand the database of toddler anthropometrics and be used to develop a toddler automaton.

**In/Exclusions:** Toddlers aged 18 months – 3 years who are able to stand.

**Confidentiality:** All information obtained during the course of this study is strictly confidential and your child's anonymity will be protected at all times. Data will be stored in locked folders accessible only by the researchers listed above. All photos or images that are collected will be stored in encrypted files on a computer in a locked room and an encrypted hard-drive stored in a locked cabinet. The photos will be destroyed after ten years and unidentifiable information that cannot be traced to you or your child will be stored permanently. You or your child will not be identified in any publication or reports.
**Voluntary participation:** You and your child's participation is voluntary and you are free to withdraw at any time. There are no consequences for withdrawal from this study. If at any time you choose to withdraw, all data that was collected from your child previously will be destroyed.

**Payment:** Each participant will receive a token for their participation and you will be reimbursed for parking and travel expenses.

**Dissemination of findings:** Research results will be presented at a conference and/or in an open access publication relevant to the biomechanics community. The results of this study will be used to develop a database of toddler anthropometrics and to design a toddler automaton. You or your child will not be identified in any publication or reports.

**What if I have concerns?** Any questions about study participation may be directed to Erika Jackson at e.jackson@queensu.ca or at 613-533-3060 or to Professor Geneviève Dumas at genevieve.dumas@queensu.ca .. Any ethical concerns about the study may be directed to the Chair of the General Research Ethics Board at chair.GREB@queensu.ca or 613-533-6081.

Again, thank you. Your interest in participating in this research study is greatly appreciated.

**Consent Form**
**TODDLER DATA COLLECTION**
**For Toddler Automaton**

Name (please print clearly): ______________________________
Child's name: __________________________________________

1. I have read the Letter of Information and have had any questions answered to my satisfaction.

2. I understand that my child will be participating in the study called "Toddler Automaton". I understand that this means my child will be asked to have markers placed on their skin and photos taken.

3. I understand that my participation and my child's participation in this study are voluntary and I may withdraw at any time. I understand that every effort will be made to maintain the confidentiality of the data now and in the future. Only team members and the supervisor in this research project will have access to the data. The data will be in a locked office. Electronic files will be password protected. The data may also be published in professional journals or presented at scientific conferences, but any such presentations will be of general findings and will never breach individual confidentiality. All data containing personal identifiable information will be destroyed in ten years.

4. I am aware that if I have any questions about study participation they may be directed to Erika Jackson at e.jackson@queensu.ca or at 613-533-3060 or to Professor Geneviève Dumas at genevieve.dumas@queensu.ca. Any ethical concerns about the study may be directed to the Chair of the General Research Ethics Board at chair.GREB@queensu.ca or 613-533-6081.

I have read the above statements and freely consent for my child to participate in this research.

Signature: ________________________________ Date: _____________________

# Appendix B

## Marker Placement Protocol

**Anatomical Landmarks:**

The subject should be dressed in fitted clothing or in as little clothing as subject and guardian are comfortable with. For subjects requiring diapers, a fresh/dry diaper is needed to reduce extra volume in the pelvic segment.

Reflective¼ inch tape squares will be stuck on the anatomical landmarks as follows. Some locations will require the tape be stuck on a small plastic ping pong ball so that it is visible to the side camera.
The subject should be weighed prior to putting the markers on.

1. <u>C1 – side view</u> – just below the tip of the mastoid process (the bony prominence just behind the ears) and above the angle of the jaw. This region is sensitive to pressure and can be quit tender to palpation. Pin the hair out of the way.
2. <u>C1 – front view</u> – tip of nose

3. <u>C7 – back view</u> – bony prominence at the top of the back, which is most visible when the neck is in flexion (chin tucked into the chest). T1 can also be quite prominent. Place the fingers over the 2 most prominent spinous processes while the neck is flexed. Return the head to neutral position. The process that "disappears" is C6. Place a small ball with reflective marker facing the camera, on the C7.
4. <u>C7 – front view</u> –at the same level as the C7 back marker.

5. <u>Right shoulder – side view</u> – the acromion process extends like a shelf over the shoulder joint. It can be palpated at the tip of the shoulder and is often visible. Palpate along the clavicle, out to the edge of the shoulder. The marker should be 2cm below the acromion process (In the middle of the glenohumeral joint). Make sure the reflective marker is visible to the side camera.
6. <u>Right shoulder– front view</u>-place the marker at the frontal view at the same height.

7. <u>T10 – front view</u> – The xiphoid process lies at the level of T10. It is located just below the point at which the ribcage meets at the front chest. It is also known as the tip of the "breast bone". During CPR, the hands are placed just above the xiphoid process. Attach a plastic ball to this landmark and it will be visible from the side view. The reflective square should face the camera.
8. <u>T10 – back view</u> – Palpate the vertebra down from the C7 or up from the L4/L5. If the subject bends the arms and attempts to touch the elbows together in the back, the edges of the scapula can be easily palpated. T3 is found at the top edge of the scapula. T7 is at the lower edge of the scapula. The vertebra are most easily

visualized and palpated when the back is in a fully flexed position.

9. T10 – side view – visualize a line between the front and back locations of T10. Place the marker on the subject's arm at this line.

10. Right Elbow – side view - Both the lateral and medial epicondyles of the humerus are easily palpated at the elbow. When the subject bends the elbow, the lateral (outside) is more prominent. Place the marker on the lateral epicondyle.
11. Right Elbow – front view – at the level of the lateral epicondyle but facing the south camera when the hand is pronated.

12. Right wrist – side view - The ulnar styloid process is a large prominence that can be easily seen on the dorsal aspect (little finger side) of the wrist.
13. Right wrist – front view – the hands will be pronated (palms facing back) during the photo. Place the marker at the level of the ulnar styloid process.

14. Right finger – front view - place marker on the tip of the finger nail of the longest finger (the middle finger)
15. Right finger – side view – place marker on the side of the middle finger

16. Iliac crest – side view – palpate the highest points of the hipbone. The horizontal line that joins these two points is at the level of the L4 spinous process and the L4/L5 disc. The lumbar spine can be identified from this point. Place reflective tape at the level of the iliac crest, slightly to the back so that it is visible to the side camera behind the arm. This marker is used to aid in identifying the L5 markers.

17. L5 – back view – Palpate down from the L4/L5 inter space to locate the L5. Attach a small plastic ping pong ball to this landmark with double sided tape so it is visible from the side camera.
18. L5 – side view – Visualize a line from L5 to the front of the body and place a marker on the side of the body below the iliac crest marker so that it is visible from the side camera.

19. Right greater trochanter – side view – It is located approximately 10 cm. inferior to the iliac crests (highest points of the hip bones). Various methods are available to locate this landmark.

a) Place the subject's thumbs on the lateral edges of the iliac crest and extend the hand and fingers down the thigh as far as possible. The middle finger will be over the greater trochanter.
b) Another method is to ask the subject to internally and externally rotate the leg below the hip. The researcher palpates the area and can feel the ball rolling in the socket.
c) Another method is to have the subject swivel the hips from side to side while you palpate, or stick the hip out to the side.

20. Greater Trochanter – front view – at the middle of the inguinal fold at the same level as the greater trochanter side marker. Place a reflective square at this point on

the fold.

21. Crotch / Pubis – side view – this marks the lowest level of the trunk and the side marker is placed at the same level as the pubis.

22. Right knee – front view – The tibial tuberosity is an oval bony elevation that is easily palpated on the anterior aspect of the proximal end of the tibia. It is located approximately 5 cm distal to the apex of the patella.
23. Right knee – side view – at the level of the tibial tuberosity

24. Right ankle – side view – The lateral maleolus (ankle bone) is a strong process on the enlarged area at the distal end of the tibia. It is clearly visible and easily located.
25. Right ankle – front view – at the level of the lateral maleolus

26. Right toe – front view - place marker on the great toe (or the longest toe)
27. Right toe – side view – place marker on the side of the great toe (or longest toe) so that the reflective square is visible to the camera

28. Apex of the head – place the headband with the attached ball on the subject's head.

## Appendix C
## SlicerProject Overview

Upload front and side images into the Slicer software and follow the prompted instructions. Select the body model with built in segment densities and input a slice thickness of 3mm. Scale the images' vertical and horizontal axes using the reference scaling markers. Select the joint centres and outline the segment boundaries (Figure A 1).

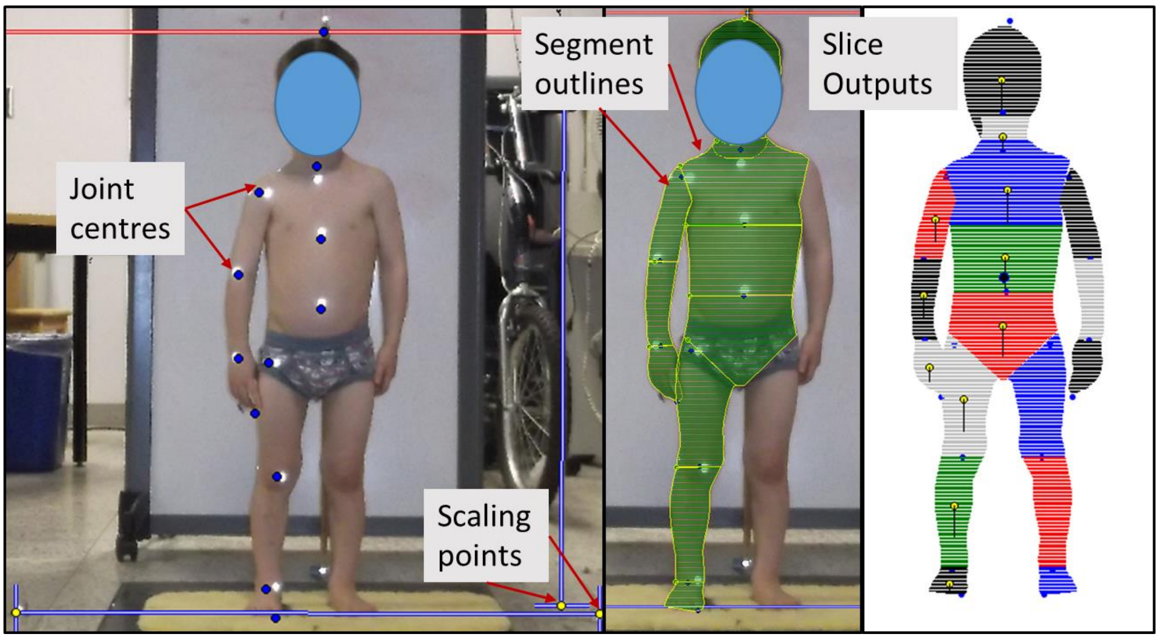


**Figure A 1: Process of digitizing photographs in SlicerProject**

The inertial data is calculated by the SlicerProject program using the process described by Jensen (1978). The output by SlicerProject includes the specific zone data: centroid, zone radii, moments of inertia of area, mass moments of inertia and transfer term for each axis and segment summary data: volume, mass, length, moments of inertia and radii of gyration.

Volume of each zone:

$$V = \pi\, r_{A/P} * r_{TVS} * r_{LON}$$

Where $r_{A/P}$ and $r_{TVS}$ are the radii of the ellipse in the anterior/posterior and transvers axes and $r_{LON}$ is the slice thickness.

Moment of inertia of area of each zone about the centroid:

$$Area\colon\ I_{A/P} = \frac{\pi}{4}\left(r_{A/P} * r_{TVS}^3\right)$$

$$Area\colon\ I_{TVS} = \frac{\pi}{4}\left(r_{TVS} * r_{A/P}^3\right)$$

$$Area\colon\ I_{LON} = I_{A/P} + I_{TVS}$$

Mass moment of inertia of each zone about the centroid:

$$Mass\colon I_{A/P} = \rho V\left(\frac{1}{4}r_{TVS}^2 + \frac{1}{12}r_{LON}^2\right)$$

$$Mass\colon I_{TVS} = \rho V\left(\frac{1}{4}r_{A/p}^2 + \frac{1}{12}r_{LON}^2\right)$$

$$Mass\colon I_{LON} = \frac{\rho V}{4}\left(r_{A/P}^2 + r_{TVS}^2\right)$$

The segment inertial data is calculated by summing across the zones. The mass moments of inertia of the segment about its centroid are found by applying the parallel axis theorem.

$$I_{segment} = \sum(I_{zone} + \ transfer\ term)$$

Where

$$Transfer\ Term_{A/P} = m_{segment}(Centre\ of\ Mass\ of\ Body_{LON} - \ Centre\ of\ Mass\ of\ Segment_{LON})^2$$

Radius of gyration of the segment:

$$k_{A/P} = \sqrt{\frac{I_{A/P}}{mass_{segment}}}$$

$$k_{TVS} = \sqrt{\frac{I_{TVS}}{mass_{segment}}}$$

$$k_{LON} = \sqrt{\frac{I_{LON}}{mass_{segment}}}$$

# Appendix D
# Subject Characteristics

**Table A 1: Individual characteristics for 12 male and 12 female subjects.**

| Subject Code | Age (years) | Height (cm) | Mass (kg) | BMI |
|---|---|---|---|---|
| B01 | 3.03 | 89.5 | 11.75 | 14.67 |
| G01 | 2.15 | 90 | 13.38 | 16.52 |
| G02 | 2.66 | 93 | 14 | 16.19 |
| B02 | 1.99 | 86.5 | 13.3 | 17.78 |
| G03 | 3.08 | 101 | 19.8 | 19.41 |
| G04 | 1.88 | 82 | 10.45 | 15.54 |
| G05 | 1.90 | 81.5 | 10.25 | 15.43 |
| B03 | 1.74 | 83 | 10.5 | 15.24 |
| G06 | 1.95 | 85 | 13.1 | 18.13 |
| G07 | 1.79 | 82 | 13 | 19.33 |
| G08 | 2.65 | 90.5 | 11.75 | 14.35 |
| B04 | 1.78 | 85.5 | 12.6 | 17.24 |
| B05 | 2.14 | 90.5 | 12.8 | 15.63 |
| B06 | 1.96 | 88.5 | 12.2 | 15.58 |
| B07 | 3.29 | 104 | 15 | 13.87 |
| G09 | 2.22 | 83.25 | 11.5 | 16.59 |
| B08 | 2.58 | 87.5 | 13.3 | 17.37 |
| B09 | 1.67 | 82 | 11.7 | 17.40 |
| B10 | 2.68 | 95 | 13.8 | 15.29 |
| G10 | 2.01 | 89.25 | 13.6 | 17.07 |
| G11 | 2.35 | 91.5 | 13.5 | 16.12 |
| B11 | 2.43 | 94 | 16.7 | 18.90 |
| B12 | 1.74 | 87 | 13.1 | 17.31 |
| G12 | 2.76 | 96 | 14.25 | 15.46 |

# Appendix E

# Subject Specific BSIPs

## E.1 Mass Proportion

**Table A 2: Segment mass proportions for males. Values are percent of total body mass.**

| Segment | B01 | B02 | B03 | B04 | B05 | B06 | B07 | B08 | B09 | B10 | B11 | B12 |
|---|---|---|---|---|---|---|---|---|---|---|---|---|
| Head | 19.4 | 17.0 | 18.6 | 18.5 | 21.0 | 20.7 | 17.7 | 16.3 | 19.6 | 16.7 | 18.0 | 19.8 |
| Neck | 1.9 | 2.0 | 1.7 | 1.4 | 1.1 | 2.1 | 1.6 | 1.8 | 1.4 | 1.7 | 1.4 | 1.9 |
| Up-Trunk | 15.6 | 14.2 | 10.9 | 13.0 | 15.1 | 15.7 | 14.5 | 14.4 | 13.6 | 14.9 | 12.8 | 12.4 |
| Abdomen | 16.2 | 14.9 | 16.9 | 20.0 | 15.9 | 13.8 | 16.5 | 18.5 | 17.5 | 18.3 | 19.1 | 19.6 |
| Pelvis | 13.9 | 16.4 | 17.8 | 14.5 | 13.2 | 14.8 | 14.4 | 16.6 | 16.6 | 14.5 | 15.1 | 15.4 |
| Trunk | 45.7 | 45.5 | 45.6 | 47.5 | 44.2 | 44.4 | 45.4 | 49.6 | 47.8 | 47.7 | 47.0 | 47.5 |
| Up Arm | 2.3 | 2.7 | 2.2 | 1.8 | 1.8 | 2.1 | 2.1 | 2.6 | 2.3 | 2.6 | 2.5 | 1.6 |
| Forearm | 1.6 | 1.7 | 2.1 | 1.6 | 1.4 | 1.7 | 1.6 | 1.7 | 1.8 | 1.7 | 1.7 | 1.5 |
| Hand | 0.7 | 1.0 | 1.1 | 0.9 | 0.1 | 0.9 | 1.1 | 0.9 | 0.9 | 1.0 | 0.7 | 0.9 |
| Thigh | 6.3 | 6.9 | 6.1 | 6.0 | 6.8 | 6.4 | 7.2 | 5.8 | 6.0 | 6.0 | 6.2 | 5.2 |
| Shank | 4.2 | 4.0 | 4.2 | 3.7 | 4.4 | 4.0 | 4.1 | 3.7 | 3.2 | 4.1 | 3.9 | 4.2 |
| Foot | 1.4 | 1.5 | 1.3 | 2.3 | 2.3 | 1.4 | 1.5 | 1.5 | 1.3 | 1.6 | 1.9 | 2.0 |

**Table A 3: Segment mass proportions for females. Values are percent of total body mass.**

| Segment | G01 | G02 | G03 | G04 | G05 | G06 | G07 | G08 | G09 | G10 | G11 | G12 |
|---|---|---|---|---|---|---|---|---|---|---|---|---|
| Head | 18.6 | 18.0 | 14.1 | 18.3 | 19.7 | 18.9 | 18.5 | 16.6 | 16.1 | 17.3 | 16.5 | 15.4 |
| Neck | 1.8 | 1.8 | 0.8 | 1.8 | 1.7 | 1.5 | 1.5 | 1.7 | 1.8 | 1.9 | 2.1 | 1.6 |
| Up-Trunk | 13.3 | 11.9 | 13.5 | 12.1 | 13.7 | 11.8 | 13.5 | 11.7 | 12.3 | 12.6 | 14.4 | 13.4 |
| Abdomen | 18.6 | 16.0 | 17.4 | 18.0 | 19.2 | 18.8 | 20.6 | 18.4 | 17.9 | 17.1 | 14.7 | 18.1 |
| Pelvis | 13.3 | 18.3 | 16.6 | 17.6 | 14.1 | 13.6 | 14.3 | 14.8 | 16.2 | 16.6 | 14.3 | 12.8 |
| Trunk | 45.3 | 46.3 | 47.5 | 47.7 | 47.1 | 44.2 | 48.5 | 44.9 | 46.4 | 46.3 | 43.4 | 44.2 |
| Up Arm | 2.8 | 2.5 | 2.4 | 2.0 | 2.0 | 2.1 | 1.6 | 2.4 | 2.2 | 2.2 | 2.8 | 2.7 |
| Forearm | 1.6 | 1.8 | 1.6 | 1.6 | 1.7 | 1.7 | 1.1 | 1.7 | 1.7 | 1.6 | 1.4 | 1.7 |
| Hand | 0.8 | 0.9 | 0.6 | 1.5 | 1.3 | 0.7 | 0.4 | 1.1 | 1.0 | 1.0 | 1.0 | 0.9 |
| Thigh | 6.9 | 6.0 | 8.4 | 5.7 | 5.6 | 7.8 | 7.4 | 6.9 | 6.9 | 6.8 | 7.9 | 8.6 |
| Shank | 3.7 | 4.1 | 4.2 | 4.2 | 3.7 | 4.0 | 3.7 | 4.1 | 4.2 | 3.9 | 4.0 | 3.9 |
| Foot | 1.3 | 1.6 | 1.6 | 1.2 | 1.4 | 1.3 | 1.6 | 2.2 | 1.8 | 1.7 | 1.8 | 1.7 |

## E.2 Centre of Mass

**Table A 4: COM location from the proximal joint centre for males. Values are percent of segment length.**

| Segment | B01 | B02 | B03 | B04 | B05 | B06 | B07 | B08 | B09 | B10 | B11 | B12 |
|---|---|---|---|---|---|---|---|---|---|---|---|---|
| Head | 67.2 | 77.1 | 74.5 | 74.5 | 68.7 | 68.1 | 65.9 | 76.3 | 73.6 | 76.7 | 69.5 | 69.7 |
| Neck | 65.9 | 80.9 | 77.3 | 75.5 | 84.1 | 72.9 | 69.4 | 71.8 | 75.3 | 79.7 | 73.9 | 72.4 |
| Up-Trunk | 52.9 | 55.6 | 54.5 | 53.5 | 54.1 | 52.3 | 52.8 | 54.9 | 54.5 | 54.0 | 51.8 | 50.5 |
| Abdomen | 50.8 | 51.0 | 51.2 | 50.6 | 51.4 | 49.6 | 49.8 | 50.1 | 51.0 | 50.4 | 55.7 | 51.2 |
| Pelvis | 44.1 | 40.4 | 38.5 | 27.0 | 35.3 | 37.5 | 37.4 | 37.0 | 32.0 | 32.7 | 45.2 | 36.0 |
| Up Arm | 50.4 | 52.5 | 52.4 | 56.8 | 54.5 | 55.0 | 51.7 | 49.8 | 45.2 | 50.4 | 52.7 | 50.6 |
| Forearm | 45.2 | 44.3 | 44.8 | 45.0 | 41.8 | 42.4 | 44.0 | 41.3 | 44.8 | 44.1 | 43.2 | 43.7 |
| Hand | 43.1 | 43.0 | 49.1 | 48.1 | 28.0 | 39.8 | 45.7 | 40.5 | 52.6 | 37.2 | 39.6 | 41.4 |
| Thigh | 49.9 | 51.1 | 49.6 | 51.6 | 50.0 | 47.3 | 49.3 | 52.6 | 52.1 | 48.5 | 53.7 | 56.8 |
| Shank | 40.5 | 45.2 | 43.9 | 46.7 | 43.9 | 44.1 | 43.9 | 41.1 | 41.3 | 45.5 | 44.5 | 42.1 |
| Foot | 22.0 | 29.4 | 28.0 | 26.5 | 32.4 | 29.1 | 25.0 | 31.1 | 19.2 | 30.2 | 27.1 | 27.1 |

**Table A 5: COM location from the proximal joint centre for females. Values are percent of segment length.**

| Segment | G01 | G02 | G03 | G04 | G05 | G06 | G07 | G08 | G09 | G10 | G11 | G12 |
|---|---|---|---|---|---|---|---|---|---|---|---|---|
| Head | 78.2 | 66.4 | 74.7 | 74.3 | 74.6 | 69.5 | 75.6 | 70.7 | 77.2 | 75.5 | 68.5 | 69.9 |
| Neck | 72.9 | 69.2 | 81.3 | 69.2 | 73.5 | 76.4 | 76.9 | 71.1 | 73.9 | 70.4 | 68.2 | 69.3 |
| Up-Trunk | 55.6 | 53.4 | 55.0 | 52.3 | 54.0 | 55.1 | 54.1 | 54.8 | 54.3 | 55.0 | 52.1 | 55.1 |
| Abdomen | 49.9 | 49.9 | 50.9 | 49.3 | 50.6 | 51.8 | 51.1 | 51.1 | 49.4 | 51.9 | 51.6 | 52.0 |
| Pelvis | 36.5 | 40.9 | 34.4 | 34.8 | 41.6 | 29.3 | 31.1 | 39.9 | 39.4 | 34.6 | 35.9 | 36.2 |
| Up Arm | 45.3 | 46.6 | 51.3 | 51.3 | 50.9 | 48.2 | 51.8 | 47.8 | 50.9 | 52.0 | 44.6 | 54.1 |
| Forearm | 42.0 | 42.3 | 42.8 | 43.3 | 43.7 | 41.3 | 42.4 | 43.6 | 44.7 | 43.7 | 42.2 | 41.8 |
| Hand | 41.4 | 40.9 | 33.0 | 43.7 | 47.7 | 42.5 | 30.0 | 44.0 | 39.6 | 41.4 | 45.1 | 37.8 |
| Thigh | 49.2 | 51.0 | 48.5 | 49.9 | 50.5 | 52.5 | 49.4 | 50.5 | 49.4 | 46.0 | 47.4 | 49.1 |
| Shank | 42.6 | 43.3 | 43.7 | 44.7 | 42.6 | 47.0 | 45.3 | 43.7 | 45.3 | 44.5 | 44.9 | 44.3 |
| Foot | 25.0 | 28.5 | 30.2 | 33.7 | 27.2 | 23.8 | 28.4 | 35.1 | 31.7 | 30.7 | 28.2 | 26.8 |

### E.3 Radius of Gyration

**Table A 6: ROG- Anterior/Posterior with respect to the COM for males. Values are percent of segment length. Red values were excluded due to subject's posture.**

| Segment | B01 | B02 | B03 | B04 | B05 | B06 | B07 | B08 | B09 | B10 | B11 | B12 |
|---|---|---|---|---|---|---|---|---|---|---|---|---|
| Head | 33.8 | 38.2 | 35.5 | 42.3 | 37.3 | 36.2 | 34.4 | 37.2 | 35.6 | 40.5 | 37.0 | 39.8 |
| Neck | 31.9 | 39.6 | 29.9 | 28.4 | 27.5 | 28.6 | 31.8 | 30.3 | 29.7 | 26.5 | 34.1 | 30.4 |
| Up-Trunk | 48.5 | 42.6 | 51.5 | 48.2 | 42.9 | 46.1 | 47.2 | 43.6 | 45.1 | 41.8 | 49.3 | 45.0 |
| Abdomen | 51.5 | 55.0 | 45.4 | 43.2 | 43.2 | 52.5 | 46.4 | 46.5 | 47.8 | 41.8 | 48.0 | 43.2 |
| Pelvis | 58.2 | 54.2 | 44.6 | 48.5 | 40.3 | 37.7 | 39.9 | 51.4 | 43.7 | 42.2 | 41.3 | 46.7 |
| Up Arm | 31.6 | 29.8 | 33.2 | 28.3 | 28.1 | 29.3 | 28.9 | 31.1 | 30.8 | 30.5 | 30.5 | 30.3 |
| Forearm | 28.1 | 28.9 | 27.9 | 28.8 | 31.3 | 28.8 | 29.0 | 28.7 | 28.4 | 29.0 | 28.7 | 29.3 |
| Hand | 26.2 | 26.2 | 19.5 | 26.1 | 19.9 | 22.4 | 27.6 | 25.1 | 26.0 | 23.9 | 25.0 | 23.7 |
| Thigh | 29.1 | 32.1 | 31.5 | 28.5 | 30.7 | 30.5 | 29.0 | 29.6 | 28.6 | 29.2 | 28.7 | 27.3 |
| Shank | 27.3 | 27.8 | 29.3 | 29.5 | 28.7 | 28.7 | 28.5 | 28.2 | 27.2 | 28.7 | 29.2 | 27.3 |
| Foot | 29.2 | 31.9 | 31.5 | 31.5 | 32.6 | 30.6 | 28.7 | 30.6 | 25.3 | 30.9 | 31.3 | 31.8 |

**Table A 7: ROG- Anterior/Posterior with respect to the COM for females. Values are percent of segment length. Red values were excluded due to subject's posture.**

| Segment | G01 | G02 | G03 | G04 | G05 | G06 | G07 | G08 | G09 | G10 | G11 | G12 |
|---|---|---|---|---|---|---|---|---|---|---|---|---|
| Head | 37.3 | 38.3 | 38.2 | 34.7 | 35.5 | 35.0 | 38.9 | 35.7 | 37.2 | 40.3 | 30.3 | 31.9 |
| Neck | 25.6 | 32.8 | 37.3 | 33.9 | 31.4 | 31.8 | 29.4 | 29.7 | 26.9 | 29.1 | 36.2 | 35.2 |
| Up-Trunk | 44.5 | 45.1 | 47.6 | 51.1 | 46.5 | 49.2 | 47.1 | 44.5 | 51.0 | 51.1 | 46.9 | 41.6 |
| Abdomen | 46.6 | 47.1 | 48.1 | 45.9 | 42.9 | 44.3 | 49.5 | 43.6 | 45.9 | 48.0 | 50.1 | 43.7 |
| Pelvis | 45.0 | 44.5 | 43.4 | 40.3 | 47.0 | 47.4 | 51.9 | 49.3 | 45.9 | 40.8 | 44.7 | 42.5 |
| Up Arm | 31.9 | 31.1 | 30.4 | 30.1 | 29.8 | 31.2 | 28.3 | 30.9 | 29.5 | 29.8 | 32.0 | 28.5 |
| Forearm | 28.1 | 27.4 | 28.2 | 27.9 | 28.6 | 26.3 | 27.3 | 28.1 | 28.2 | 28.4 | 28.0 | 29.1 |
| Hand | 26.3 | 26.3 | 19.1 | 27.5 | 27.0 | 26.3 | 16.4 | 26.4 | 27.8 | 25.5 | 25.7 | 25.6 |
| Thigh | 29.6 | 28.6 | 30.3 | 30.6 | 31.4 | 27.9 | 29.8 | 28.5 | 29.8 | 31.0 | 29.0 | 28.2 |
| Shank | 28.3 | 28.7 | 28.3 | 28.5 | 29.2 | 30.0 | 29.3 | 28.2 | 29.7 | 28.7 | 28.5 | 29.4 |
| Foot | 29.9 | 28.2 | 28.1 | 34.9 | 28.6 | 27.1 | 25.6 | 32.2 | 30.0 | 31.4 | 30.3 | 30.4 |

**Table A 8: ROG- Transverse with respect to the COM for males. Values are percent of segment length. Red values were excluded due to subject's posture.**

| Segment | B01 | B02 | B03 | B04 | B05 | B06 | B07 | B08 | B09 | B10 | B11 | B12 |
|---|---|---|---|---|---|---|---|---|---|---|---|---|
| Head | 34.8 | 40.2 | 37.0 | 44.1 | 37.1 | 37.5 | 37.3 | 39.4 | 38.3 | 43.5 | 39.5 | 42.7 |
| Neck | 30.3 | 39.5 | 32.1 | 27.7 | 25.8 | 30.0 | 29.9 | 29.4 | 28.0 | 27.9 | 31.9 | 30.2 |
| Up-Trunk | 38.7 | 36.2 | 47.0 | 42.5 | 40.9 | 38.5 | 37.4 | 40.3 | 37.5 | 37.2 | 39.2 | 43.9 |
| Abdomen | 47.1 | 52.0 | 42.3 | 41.9 | 50.7 | 48.6 | 42.4 | 44.2 | 44.0 | 40.9 | 44.7 | 43.9 |
| Pelvis | 48.7 | 48.9 | 40.3 | 41.6 | 36.5 | 42.3 | 43.9 | 46.4 | 51.2 | 41.7 | 46.2 | 53.8 |
| Up Arm | 32.5 | 30.8 | 34.0 | 29.3 | 29.2 | 30.2 | 29.3 | 32.2 | 32.1 | 31.1 | 31.8 | 31.7 |
| Forearm | 28.0 | 29.5 | 25.8 | 27.7 | 28.8 | 28.9 | 29.2 | 29.2 | 28.7 | 29.1 | 29.2 | 28.9 |
| Hand | 28.6 | 26.9 | 23.7 | 23.0 | 17.7 | 24.1 | 27.5 | 27.9 | 28.8 | 22.0 | 29.0 | 26.7 |
| Thigh | 29.9 | 33.5 | 32.8 | 29.6 | 30.4 | 30.8 | 29.3 | 30.9 | 29.6 | 29.9 | 29.3 | 28.7 |
| Shank | 27.5 | 28.1 | 29.5 | 29.6 | 29.1 | 28.9 | 28.7 | 28.4 | 27.7 | 29.0 | 29.2 | 27.7 |
| Foot | 27.8 | 29.6 | 27.1 | 26.3 | 29.9 | 26.9 | 27.7 | 28.0 | 21.2 | 30.2 | 26.7 | 27.5 |

**Table A 9: ROG- Transverse with respect to the COM for females. Values are percent of segment length. Red values were excluded due to subject's posture.**

| Segment | G01 | G02 | G03 | G04 | G05 | G06 | G07 | G08 | G09 | G10 | G11 | G12 |
|---|---|---|---|---|---|---|---|---|---|---|---|---|
| Head | 40.7 | 39.2 | 38.8 | 39.0 | 36.4 | 36.3 | 39.4 | 35.9 | 40.3 | 42.8 | 32.5 | 34.1 |
| Neck | 24.3 | 30.8 | 34.2 | 31.9 | 30.7 | 31.0 | 28.8 | 29.8 | 27.5 | 25.4 | 33.2 | 34.5 |
| Up-Trunk | 36.7 | 38.5 | 41.4 | 41.1 | 40.2 | 41.2 | 43.2 | 41.6 | 42.2 | 39.5 | 38.4 | 36.2 |
| Abdomen | 42.8 | 45.7 | 44.3 | 41.6 | 38.8 | 39.4 | 47.2 | 41.6 | 44.0 | 43.9 | 45.8 | 42.7 |
| Pelvis | 51.6 | 38.7 | 52.8 | 44.5 | 40.2 | 54.2 | 42.5 | 43.9 | 47.5 | 46.8 | 53.3 | 48.8 |
| Up Arm | 32.6 | 31.5 | 31.2 | 31.1 | 30.4 | 32.8 | 30.1 | 31.8 | 30.9 | 30.8 | 32.9 | 28.7 |
| Forearm | 28.5 | 27.7 | 28.9 | 28.3 | 28.3 | 26.9 | 29.1 | 28.2 | 28.9 | 29.0 | 28.5 | 29.0 |
| Hand | 25.9 | 25.0 | 21.6 | 26.9 | 27.4 | 28.2 | 27.1 | 27.1 | 26.7 | 26.4 | 26.9 | 25.2 |
| Thigh | 30.6 | 29.1 | 31.2 | 31.5 | 32.9 | 28.6 | 30.1 | 29.4 | 30.5 | 31.4 | 30.1 | 28.8 |
| Shank | 28.6 | 28.9 | 28.8 | 28.6 | 29.6 | 30.5 | 29.5 | 28.5 | 30.1 | 28.8 | 28.7 | 29.6 |
| Foot | 26.6 | 25.7 | 25.8 | 34.2 | 26.8 | 21.9 | 30.7 | 28.2 | 28.1 | 27.9 | 27.2 | 29.4 |

**Table A 10: ROG- Longitudinal with respect to the COM for males. Values are percent of segment length. Red values were excluded due to subject's posture.**

| Segment | B01 | B02 | B03 | B04 | B05 | B06 | B07 | B08 | B09 | B10 | B11 | B12 |
|---|---|---|---|---|---|---|---|---|---|---|---|---|
| Head | 30.6 | 34.7 | 29.6 | 37.2 | 33.0 | 32.2 | 30.5 | 34.8 | 32.9 | 36.7 | 34.1 | 37.8 |
| Neck | 35.8 | 52.3 | 39.2 | 34.8 | 34.7 | 35.6 | 37.3 | 35.5 | 36.2 | 34.4 | 41.8 | 35.8 |
| Up-Trunk | 45.3 | 41.2 | 59.5 | 54.0 | 46.3 | 42.4 | 44.1 | 46.1 | 42.8 | 39.8 | 46.1 | 51.7 |
| Abdomen | 55.9 | 64.8 | 48.5 | 45.5 | 59.9 | 59.3 | 50.5 | 51.0 | 51.8 | 42.9 | 49.5 | 48.2 |
| Pelvis | 49.9 | 57.5 | 36.1 | 42.3 | 43.9 | 36.6 | 38.9 | 46.2 | 45.3 | 48.2 | 40.4 | 48.4 |
| Up Arm | 11.8 | 16.8 | 14.2 | 13.9 | 15.1 | 13.4 | 12.3 | 14.5 | 14.9 | 13.2 | 16.1 | 12.7 |
| Forearm | 11.9 | 16.2 | 16.5 | 14.9 | 19.2 | 13.8 | 11.4 | 14.2 | 13.7 | 12.5 | 14.1 | 14.1 |
| Hand | 22.2 | 17.8 | 19.9 | 20.0 | 11.2 | 15.9 | 16.2 | 18.8 | 20.1 | 17.7 | 20.0 | 17.9 |
| Thigh | 17.1 | 22.0 | 21.4 | 18.1 | 18.3 | 18.8 | 15.1 | 19.4 | 18.8 | 17.5 | 17.5 | 17.3 |
| Shank | 10.5 | 14.6 | 14.0 | 13.5 | 15.0 | 12.5 | 11.6 | 12.8 | 14.3 | 11.8 | 15.1 | 12.9 |
| Foot | 14.3 | 17.9 | 19.7 | 20.9 | 18.3 | 18.3 | 15.1 | 16.3 | 17.0 | 16.1 | 20.8 | 20.1 |

**Table A 11: ROG- Longitudinal with respect to the COM for females. Values are percent of segment length. Red values were excluded due to subject's posture.**

| Segment | G01 | G02 | G03 | G04 | G05 | G06 | G07 | G08 | G09 | G10 | G11 | G12 |
|---|---|---|---|---|---|---|---|---|---|---|---|---|
| Head | 39.2 | 34.3 | 33.9 | 37.0 | 32.7 | 30.4 | 34.3 | 32.3 | 35.1 | 38.3 | 27.4 | 29.2 |
| Neck | 28.0 | 36.3 | 47.5 | 35.1 | 38.3 | 37.0 | 36.2 | 33.3 | 31.6 | 32.1 | 41.9 | 39.9 |
| Up-Trunk | 40.5 | 40.7 | 52.6 | 53.0 | 49.1 | 52.5 | 51.4 | 48.2 | 54.7 | 47.2 | 43.6 | 40.1 |
| Abdomen | 50.0 | 55.2 | 52.3 | 47.7 | 41.2 | 41.8 | 55.6 | 48.3 | 50.8 | 52.1 | 54.7 | 49.9 |
| Pelvis | 40.2 | 39.3 | 43.0 | 40.8 | 42.7 | 45.1 | 42.8 | 41.4 | 53.2 | 40.4 | 45.3 | 41.6 |
| Up Arm | 13.8 | 13.7 | 13.1 | 14.1 | 13.8 | 15.4 | 13.8 | 13.3 | 15.0 | 15.0 | 14.1 | 12.3 |
| Forearm | 12.8 | 12.2 | 14.6 | 13.8 | 12.2 | 13.8 | 13.2 | 12.6 | 15.4 | 14.0 | 13.5 | 12.2 |
| Hand | 20.1 | 19.0 | 15.0 | 20.4 | 19.8 | 22.2 | 22.1 | 21.7 | 21.0 | 17.6 | 18.6 | 22.0 |
| Thigh | 19.0 | 17.2 | 17.2 | 19.2 | 20.4 | 17.6 | 20.0 | 15.7 | 18.4 | 19.1 | 16.9 | 14.9 |
| Shank | 13.2 | 12.0 | 12.4 | 12.9 | 13.7 | 13.9 | 15.6 | 12.5 | 15.2 | 13.4 | 12.5 | 11.2 |
| Foot | 17.3 | 15.5 | 14.9 | 15.0 | 14.4 | 18.4 | 20.8 | 18.6 | 15.2 | 18.6 | 17.1 | 15.2 |

# Appendix F

## Sex Specific Regression Equations

**Table A 12: Mass proportion and age linear regression coefficients for males and females.**

**%mass = age (a) + b**

| | Males | | | | Females | | | |
|---|---|---|---|---|---|---|---|---|
| **Segment** | **a** | **b** | **$R^2$** | **Correlation** | **a** | **b** | **$R^2$** | **Correlation** |
| Head | -1.1001 | 21.085 | 0.15 | -0.39 | -3.2055 | 24.645 | 0.66 | -0.81 |
| Neck | 0.0509 | 1.5629 | 0.01 | 0.09 | -0.3381 | 2.4299 | 0.19 | -0.44 |
| Up Trunk | 1.3599 | 10.872 | 0.29 | 0.52 | 0.0619 | 12.713 | 0.001 | 0.03 |
| Abdomen | -1.3233 | 18.004 | 0.01 | -0.09 | -1.6365 | 21.646 | 0.20 | -0.45 |
| Pelvis | -1.102 | 17.762 | 0.20 | -0.45 | 0.5975 | 13.854 | 0.02 | 0.14 |
| Trunk | -0.0655 | 46.638 | 0.001 | -0.02 | -0.9771 | 48.213 | 0.07 | -0.26 |
| Up Arm | 0.2124 | 1.7385 | 0.11 | 0.33 | 0.5576 | 1.0418 | 0.42 | 0.65 |
| Forearm | -0.0538 | 1.8001 | 0.03 | -0.17 | 0.1398 | 1.2922 | 0.09 | 0.31 |
| Hand | -0.0275 | 0.9026 | 0.003 | -0.06 | -0.1435 | 1.2678 | 0.04 | -0.20 |
| Thigh | 0.4203 | 5.2952 | 0.18 | 0.45 | 1.1491 | 4.456 | 0.23 | 0.48 |
| Shank | 0.1542 | 3.6218 | 0.07 | 0.27 | 0.2323 | 3.4553 | 0.25 | 0.50 |
| Foot | -0.1482 | 1.9991 | 0.05 | -0.22 | 0.325 | 0.8429 | 0.22 | 0.47 |

**Table A 13: Mass proportion and BMI linear regression coefficients for males and females.**

**%mass = BMI (a) + b**

| | Males | | | | Females | | | |
|---|---|---|---|---|---|---|---|---|
| **Segment** | **a** | **b** | **$R^2$** | **Correlation** | **a** | **b** | **$R^2$** | **Correlation** |
| Head | -0.2551 | 22.73 | 0.06 | -0.03 | -0.1236 | 19.387 | 0.01 | -0.12 |
| Neck | -0.0454 | 2.4116 | 0.06 | -0.23 | -0.1257 | 3.7542 | 0.37 | -0.61 |
| Up Trunk | -0.2287 | 17.632 | 0.06 | -0.24 | 0.1176 | 10.893 | 0.04 | 0.21 |
| Abdomen | 0.3571 | 11.502 | 0.08 | 0.28 | 0.2352 | 13.988 | 0.06 | 0.24 |
| Pelvis | 0.3066 | 10.324 | 0.12 | 0.35 | 0.0472 | 14.431 | 0.002 | 0.04 |
| Trunk | 0.435 | 39.458 | 0.17 | 0.41 | 0.4 | 39.312 | 0.16 | 0.40 |
| Up Arm | 0.0906 | 0.7529 | 0.15 | 0.39 | -0.0726 | 3.5252 | 0.10 | -0.32 |
| Forearm | 0.0046 | 1.6062 | 0.001 | 0.04 | -0.0608 | 2.6255 | 0.25 | -0.50 |
| Hand | -0.0137 | 1.0626 | 0.01 | -0.08 | -0.1444 | 3.3493 | 0.58 | -0.76 |
| Thigh | -0.0589 | 7.1945 | 0.03 | -0.17 | 0.2755 | 2.4857 | 0.19 | 0.44 |
| Shank | -0.1291 | 6.0556 | 0.39 | -0.63 | -0.0157 | 4.2482 | 0.02 | -0.13 |
| Foot | 0.0394 | 1.0284 | 0.03 | 0.16 | -0.0573 | 2.5399 | 0.10 | -0.31 |

# Appendix G

# Total Body Mass Error and Subject Difficulties

**Table A 14: Difference in estimated and measured mass of specific subjects with descriptions of possible causes of error**

| | Age | Measured Mass | Estimated Mass | % Diff | Off centre (camera) | Approx distance off | Diaper | Clothes | Comments |
|---|---|---|---|---|---|---|---|---|---|
| B01 | 3.03 | 11.75 | 11.76 | 0.07 | Side | 2.5 | 1 | | |
| B02 | 1.99 | 13.3 | 13.35 | 0.37 | | 0 | 1 | | Leaning forward slightly |
| B03 | 1.74 | 10.5 | 10.73 | 2.23 | Front | 7.5 | 1 | | Photos are from two different moments |
| B04 | 1.78 | 12.6 | 12.44 | -1.28 | Side | -6 | 1 | 1 | Subject slightly rotated and arm bent |
| B05 | 2.14 | 12.8 | 12.85 | 0.41 | Front | 5 | 1 | 1 | Arms bent and movement between photos |
| B06 | 1.96 | 12.2 | 12.34 | 1.19 | Side | 2 | 1 | | Arm hides back contour |
| B07 | 3.29 | 15 | 15.2 | 1.35 | | 0 | | | |
| B08 | 2.58 | 13.3 | 13.66 | 2.68 | | 0 | 1 | | Arm minimally hides back contour |
| B09 | 1.67 | 11.7 | 11.81 | 0.9 | Front | -2.5 | 1 | | Photos are from two different moments |
| B10 | 2.68 | 13.8 | 14.33 | 3.85 | | 0 | | 1 | |
| B11 | 2.43 | 16.7 | 17.57 | 5.24 | | 0 | 1 | 1 | |
| B12 | 1.74 | 13.1 | 13.1 | -0.01 | | 0 | 1 | | Slight body twist |
| G01 | 2.15 | 13.4 | 14.07 | 4.97 | | 0 | 1 | 1 | |
| G02 | 2.66 | 14 | 13.84 | -1.17 | Front | -2.5 | | | |
| G03 | 3.08 | 19.8 | 19.61 | -0.94 | | 0 | | | Neck is hidden |
| G04 | 1.88 | 10.45 | 11 | 5.22 | | 0 | 1 | | Head and arm movement between photos |
| G05 | 1.9 | 10.3 | 10.89 | 5.73 | | 0 | 1 | | Photos are from two different moments |
| G06 | 1.95 | 13.1 | 13.7 | 4.57 | Side | 7.5 | 1 | | Arm hides back contour |
| G07 | 1.79 | 13 | 13.45 | 3.5 | | 0 | 1 | | Arm hides back contour |
| G08 | 2.65 | 11.75 | 11.88 | 1.1 | | 0 | 1 | | |
| G09 | 2.22 | 11.5 | 11.74 | 2.06 | | 0 | 1 | 1 | |
| G10 | 2.01 | 13.6 | 13.56 | -0.28 | | 0 | 1 | 1 | |
| G11 | 2.35 | 13.5 | 13.49 | -0.1 | Back | 5 | 1 | | |
| G12 | 2.76 | 14.25 | 14.36 | 0.75 | | 0 | | | Body twist |

# Appendix H

## Subject Photos

**Figure A 2: Front and side male subject photos with subject code**

**Figure A 3: Front and side female subject photos with subject code**


* G12 was the pilot subject. The only difference in protocol was the use of the subject placement mat. The pilot subject was included in the analysis as the subject was able to stand in the correct placement without the mat.